



UNIVERSITÀ DI PISA

Facoltà di Ingegneria
Corso di Laurea in Ingegneria Aerospaziale

Tesi di Laurea

Multibody Analysis of Solar Array Deployment using Flexible Bodies

Anno Accademico 2006-2007

Relatori

Prof. G. Mengali

Prof. A. Salvetti

Dr. B. Specht

Candidato:

Luca Bagnoli

*„man muss noch Chaos in sich haben,
um einen tanzenden Stern gebären zu können“*

Friedrich Nietzsche

Abstract

The solar panels represent the main device for collecting and converting solar energy into electrical energy and they are widely used in space missions supplying the energy necessary for both spacecrafts and payloads. To optimize the sun exposed surface the panels are usually organized in wings configurations, that, stored during the launch, deploy in the space at the beginning of the operative phase of the satellite.

This work of thesis focus on this deployment phase and on the associated dynamic loads. The need of this investigation is connected to the strict requirements on the deployment. Since we want to be sure of the complete deployment in every condition with high margin of safety, the energy stored in the deployment mechanism is quite oversized. This leads to the dynamic loads that we want to estimate.

The key topic of the thesis consists in the generation of a flexible multi-body model for solar arrays deployment studies and analysis. The main aim of this model is the verification and validation of a usually pre-existing rigid model used for the conceptual studies of the deployment.

In this rigid model, generated directly in ADAMS environment, all the structural stiffness is condensed in a small number of DOF (rotational springs located on the hinge lines). It's clear that this way of modelling does not cover higher frequency or side dynamics effects. By the introduction of a flexible model we want to investigate these effects and check the right working of the mechanism also in presence of deformation. Optionally, using the flexible model, we can also have a first estimation of stresses and strains due to the dynamics of the deployment.

The two main requirements for a flexible model are to be easy to generate and to be compatible with the related rigid model. These two aspects are important to avoid significant impact on the project budget. The flexible bodies are generated using the user friendly interface of PATRAN (avoiding or minimizing manual inputs in NASTRAN) and then importing this flexible bodies in an ADAMS adapted rigid model (avoiding to re-built the flexible model from the beginning).

The first chapter of the thesis will show the theoretical background of the NASTRAN-ADAMS interface for the generation of flexible bodies. This theoretical part, even if not strictly necessary for the final-user, is anyway important for the full comprehension of some of the choices that will be adopted.

The second chapter will introduce and explain the main characteristics of a solar array rigid model using BEPI COLOMBO MPO solar array and AMOS 3 solar array as examples. The third chapter will focus on the generation of the flexible model using the same two formers examples.

In chapter four the results of the two models will be compared and in the fifth chapter the consequent conclusions will be drawn. In last chapter six will be shown other possible fields of application of the flexible body modelling with ADAMS.

I pannelli solari rappresentano il principale sistema per raccogliere e convertire energia solare in energia elettrica e sono largamente utilizzati in missioni spaziali per fornire l'energia necessaria sia al satellite che al suo payload. Per ottimizzare la superficie esposta al sole i pannelli sono spesso organizzati in configurazioni alari che, raccolte durante la fase di lancio, vengono dispiegate nello spazio all'inizio della fase operativa del satellite.

Questo lavoro di tesi è focalizzato su questa fase di dispiegamento e sui carichi dinamici ad essa associati. Il bisogno di questa indagine è connesso ai severi requisiti imposti sul dispiegamento. Dato che vogliamo essere sicuri del completo dispiegamento in qualsiasi condizione operativa con un alto margine di sicurezza, l'energia immagazzinata nel sistema di apertura è sovradimensionata.

Questo produce i carichi dinamici nella struttura che vogliamo stimare.

Il principale obiettivo del presente lavoro di tesi consiste nella generazione di un modello multi-body a corpi flessibili per lo studio e l'analisi del dispiegamento dei pannelli solari. Lo scopo di questo modello sarà quello di verificare e convalidare i risultati di un modello rigido preesistente utilizzato nei primi studi concettuali di dispiegamento.

In questo modello rigido, generato direttamente in ambiente ADAMS, la rigidità strutturale è condensata in un ridotto numero di g.d.l. (molle rotazionali collocate lungo le linee di cerniera). E' chiaro che questa modellazione non comprende quindi effetti di alta frequenza o di dinamiche trasversali. Con l'introduzione del modello flessibile vogliamo investigare questi effetti, controllare il corretto funzionamento del meccanismo anche in presenza di deformazioni ed eventualmente avere una prima stima delle tensioni dovute alla dinamica del dispiegamento.

I principali due requisiti del modello flessibile sono la facilità di generazione e la compatibilità con il relativo modello rigido. Questi due aspetti sono di fondamentale importanza per evitare impatti significativi sul budget del progetto.

Per ottenere il modello flessibile, i vari corpi che lo compongono sono generati utilizzando l'interfaccia grafica di PATRAN (cercando di evitare e minimizzare gli input diretti nel codice NASTRAN) e quindi importati in un modello rigido adattato in ADAMS (evitando in questo modo di costruire un modello flessibile dall'inizio).

Il primo capitolo della tesi riporta la teoria matematica su cui si basa l'interfaccia NASTRAN-ADAMS per la generazione dei corpi flessibili. Questa parte teorica, anche se non strettamente necessaria all'utente finale del modello, è importante per la piena comprensione di alcune delle scelte che verranno adottate.

Il secondo capitolo introduce e spiega le principali caratteristiche del modello rigido utilizzando due diverse configurazioni di pannelli solari come esempi, quella del MPO (Mercury Polar Orbiter) di BEPI COLOMBO e quella del satellite di telecomunicazioni AMOS 3. Il terzo capitolo riguarda la generazione del modello flessibile e vengono utilizzate a scopo esplicativo le solite due configurazioni del capitolo precedente.

Il capitolo quarto contiene una comparazione tra i due modelli e il quinto le conclusioni che ne emergono. L'ultimo capitolo riporta altre possibili applicazioni per l'utilizzo di modelli flessibili in ADAMS.

Acknowledgement

This work of thesis is the result of a six months stage in EADS Astrium GmbH, Mechanical and Thermal analysis & test department, Friedrichshafen, Germany.

For this extraordinary and formative experience I'm grateful first of all to my Professor Giovanni Mengali and to Stefano Lucarelli. They made this experience possible and enlarged my horizons, always ready to support and encourage me.

For his trust and the opportunity to be part of his team my sincere gratitude goes to Dr. Werner Konrad.

This work has not been possible without the patient, the advices and the teachings of my advisor Dr. Bernhard Specht. My warm gratefulness goes to him. His suggestions and his critics were precious for my personal growth and for the right development of this thesis.

A particular thanks to Danilo, Domenico, Guenther and Stephen. With them I shared more than a working experience and they represent the piece of Germany I miss more.

Many people passed through these university years and all of them contributed in some way to this result. Mentioning them here doesn't want to be a reward but just a way to make them understand how important they are and how strongly influenced me.

My first thought goes to my parents, to my brother and to my whole family. For their support and for supporting me, for their blind trust and their proudness of me that has always made me feel special. It's rhetorical to say that I would not be here without them... it is not the gratitude and my true love that I owe them but too many times I forgot to express.

To Francesca. For all the countless beautiful moments spent together and all the dreams we shared during these years. For being and always having been close.

To Gabriele. For his brotherly friendship, his precious support and his contagious order.

To my historical friends Adalberto, Andrea, Emanuele, Gabriele, Gigi and Simone. Inseparable adventures and everyday life companions, always present, always ready to remind me not to take myself and life too seriously.

To all the other friends that, even if their names can't be present in these few rows, will always have their place in my thoughts and my memories.

Thank you all. I'm sure my happiness is your happiness today, and this my greatest triumph.

Questo lavoro di tesi è il risultato di uno stage di sei mesi presso EADS Astrium GmbH, dipartimento di analisi Termica e Meccanica, Friedrichshafen, Germania.

Per questa straordinaria e formativa esperienza sono grato prima di tutto al mio Professore Giovanni Mengali e a Stefano Lucarelli. Loro hanno reso possibile questa esperienza e allargato i miei orizzonti, sempre pronti ad aiutarmi e incoraggiarmi.

Per la sua fiducia e l'opportunità di far parte del suo team la mia sincera gratitudine va al Dr. Werner Konrad.

Questo lavoro non sarebbe stato possibile senza la pazienza, i consigli e gli insegnamenti del mio advisor Dr. Bernhard Specht. Devo a lui calorosi ringraziamenti. I suoi suggerimenti e le sue critiche sono stati preziosi per la mia crescita personale e per la buona riuscita di questa tesi.

Un grazie particolare a Danilo, Domenico, Guenther e Stephen. Con loro ho condiviso più che una esperienza di lavoro e rappresentano la parte della Germania di cui sento maggiormente la mancanza.

Molte persone hanno attraversato questi anni universitari e tutte loro hanno contribuito in qualche modo a questo risultato. Menzionarle qui non vuole essere un premo ma solo un modo per far loro capire quanto siano state importanti per me e quanto fortemente mi abbiano influenzato.

Il primo pensiero va ai miei genitori, a mio fratello e a tutta la mia famiglia. Per il loro supporto e per l'avermi sopportato, per la loro fiducia e l'orgoglio nei miei confronti che mi ha fatto sempre sentire speciale. E' retorico dire che non sarei qui senza di loro...non lo è il sincero affetto e la gratitudine che devo loro ma troppe volte ho dimenticato di esprimere.

A Francesca. Per gli innumerevoli stupendi momenti passati insieme e per tutti i sogni che abbiamo condiviso in questi anni. Per essere ed essere sempre stata vicina.

A Gabriele. Per la sua fraterna amicizia, il suo prezioso supporto e il suo ordine contagioso.

Ai mie amici storici Adalberto, Andrea, Emanuele, Gabriele, Gigi e Simone. Inseparabili compagni di avventure e della vita di tutti i giorni, sempre presenti, sempre pronti a ricordarmi di non prendere la vita o me stesso troppo sul serio.

A tutti gli altri amici che non possono trovare spazio tra queste poche righe, ma che avranno sempre un posto particolare nei miei ricordi e pensieri.

Grazie a tutti voi. Sono sicuro che la mia felicità e anche la vostra oggi, e questa è la mia vittoria più grande.

Luca Bagnoli
Pisa, 17 Ottobre 2007

Contents

Abstract.....	i
Aknowledgement.....	iii
Contents	v
List of Figures.....	ix
List of Tables	xiii
Acronyms.....	xiv
1 Theoretical Background.....	1
1.1 The base of the flexible model.....	1
1.2 Modal superposition	2
1.2.1 Component mode synthesis — The Craig-Bampton method.....	3
1.2.2 Mode shape orthonormalization	6
1.3 Modal flexibility in ADAMS.....	10
1.3.1 Flexible marker kinematics.....	10
1.3.1.1 Position	10
1.3.1.2 Velocity.....	12
1.3.1.3 Orientation	13
1.3.1.4 Angular velocity	15
1.3.2 Applied loads	15
1.3.2.1 Point forces and torques.....	15
1.3.3 Flexible body equations of motion	17
1.3.3.1 Kinetic energy and the mass matrix.....	18
1.3.3.2 Potential energy and the stiffness matrix.....	21
1.3.3.3 Dissipation and the damping matrix	22
1.3.3.4 Constraints	22
1.3.3.5 Governing differential equation of motion — final form	22

2 The Rigid Model.....	24
2.1 The rigid model objective	24
2.2 The ADAMS rigid model	25
2.2.1 Inertia of bodies	26
2.2.2 Motorization Spring Torque	27
2.2.3 Friction.....	27
2.2.4 Harness Torque effects	28
2.2.5 Closed Cable Loop (CCL) synchronization mechanism	29
2.2.6 Dampers or engine holding torque.....	31
2.2.7 Latch up of deployment hinges.....	31
2.2.8 Bending Stiffness of solar array structure collocated in the HLs	32
2.3 Applied Examples.....	34
2.3.1 BEPI COLOMBO MPO solar array – Rigid model	35
2.3.2 AMOS-3 solar array – Rigid model.....	38
2.3.2.1 In orbit model.....	38
2.3.2.2 On ground model	42
3 The Flexible Model	43
3.1 Introduction to the flexible model	43
3.1.1 Full-Flexible model.....	44
3.1.2 Semi-flexible model.....	45
3.2 Generation of Flexible bodies.....	46
3.2.1 Definition of Attachment Points and of their DOF.....	48
3.2.2 Fix-interface normal modes	50
3.2.3 PLOTEL element.....	55
3.3 ADAMS flexible model.....	58
3.3.1 Splitting forces and relocating them in their real application points	58
3.3.2 Introducing auxiliary point	59
3.3.3 Redefining markers dependencies	60
3.3.4 Modifying the kinds of hinges and friction	61
3.3.5 Introducing kinematical locking	63
3.3.6 Modifying the ADAMS/solver script	65
3.4 Applied Exemples.....	67
3.4.1 BEPI COLOMBO MPO solar array – semi-flexible model	67
3.4.1.1 Splitting and repositioning of forces.....	68
3.4.1.2 Modifying the kinds of hinges and friction	68
3.4.1.3 Locking devices	70
3.4.1.4 Flexible panels	70
3.4.1.5 ADAMS solver script	72
3.4.2 AMOS-3 solar array Full-flexible model – in orbit model.....	73
3.4.2.1 Splitting and repositioning forces	73
3.4.2.2 Modifying the kinds of hinges and friction	75
3.4.2.3 Locking devices	75
3.4.2.4 Flexible bodies.....	76

3.4.2.5 ADAMS solver script	77
3.4.3 AMOS-3 solar array Full-flexible model – On ground model	78
3.4.3.1 Aerodynamic load applied on simple nodes	78
3.4.3.2 Support brackets represented as different bodies	79
3.4.3.3 Coexistence in same model of rigid and flexible parts(hybrid-model)	80
4 Analysis of Results	82
4.1 BEPI COLOMBO MPO S/A – Semi-flex vs Rigid Model	82
4.1.1 Solar array Deployment	82
4.1.2 Latch-up torque	84
4.1.3 Loads on SADM I/F	87
4.1.3.1 SADM I/F forces	87
4.1.3.2 SADM I/F torques	88
4.2 AMOS-3 S/A in orbit – Full-flex vs Rigid Model	90
4.2.1 Solar array Deployment	90
4.2.2 Latch-up torque	91
4.2.2.1 HL3 latch-up	92
4.2.2.2 HL2 latch-up	92
4.2.2.3 HL1 latch-up	93
4.2.3 CCL forces	94
4.2.4 Eddy current dumper	95
4.2.5 Torque on SADM I/F	96
4.3 AMOS-3 S/A on ground – Hybrid vs Rigid	98
4.3.1 Latch-up torque	98
5 Summary and Outlook	99
5.1 Rigid vs Flexible – Pro & Con of the two models	99
5.2 Developments of Hybrid model	102
6 Alternative Fields of Application	104
6.1 Alternative application of the flexible approach	104
6.1.1 Stress & Strain in ADAMS environment	104
6.1.2 Flexible model impact analysis	106
6.1.3 Vibration Analysis in ADAMS	108
Appendixes	111
A Latch-up spring Tuning	112
A.1 Getting data from NASTRAN	112
A.1.1 Constraining the PATRAN model	114
A.1.2 Flexible mode frequency	116
A.2 ADAMS model	116
A.2.1 Constraining the ADAMS model	117
A.2.2 Spring Manual Tuning	118

A.2.3 Spring Automatic Tuning	118
B Flexible Body Generation	123
B.1 Adapt the FEM model	123
B.1.1 Rigid hinges and mass splitting.....	124
B.1.2 Attachment Points definition.....	127
B.1.3 PLOTTEL grid definition	128
B.2 Definition of Load Cases	132
B.3 Analysis.....	132
B.4 Editing the BDF file	137
C Flexible Body with Strees & Strain	139
C.1 Full mesh S&S	139
C.2 Spot mesh S&S + PLOTTEL	145
C.3 Checking the results in ADAMS environment	150
D Flexible Bodies in Adams	152
D.1 Importing a flexible body.....	152
D.1.1 Alignment	153
D.1.2 Connections.....	156
D.1.2.1 Load on simple nodes	158
D.1.2.2 Loads with an offset respect to the AP	160
D.1.2.3 Loads on Attachment Points	160
D.2 Flexible body properties	161
D.2.1 Damping ratio	162
D.2.2 Modes Control	163
Bibliography	164

List of Figures

Figure 1.1.1-1: Example of modal superposition	2
Figure 1.2.1-1: Constraint Modes of a 2D beam	4
Figure 1.2.1-2: First two fixed-boundary modes of a 2D beam	4
Figure 1.2.2-1: Craig-Bampton modal basis and Craig-Bampton orthogonalized basis ..	7
Figure 1.2.2-2: Constraint mode and relative boundary eigenvector on a plate	8
Figure 1.3.1-1: Flexible body reference system in ADAMS	10
Figure 2.2.1-1: Five bodies solar array	26
Figure 2.2.2-1: Deployment spring system.....	27
Figure 2.2.3-1: ADAMS Friction model	28
Figure 2.2.4-1: ADAMS harness torque model.....	28
Figure 2.2.5-1: CCL synchronization example.....	29
Figure 2.2.5-2: Principle of CCL Synchronization.....	29
Figure 2.2.5-3: Torques and Forces generated by CCL.....	30
Figure 2.2.5-4: Torque on Yoke due to guided CCL cables.....	30
Figure 2.2.7-1: Latch-up principle	31
Figure 2.2.7-2: Example of latch-up obtained by a latching spring	32
Figure 2.2.8-1: Latch-up spring tuning	32
Figure 2.2.8-2: Latching spring contributions	33
Figure 2.3.1-1: BEPI COLOMBO MPO solar array	35
Figure 2.3.1-2: ADAMS rigid model elements	36
Figure 2.3.1-3: BEPI COLOMBO MPO s/a deployment sequence	37
Figure 2.3.2-1: AMOS-3 solar array (in-orbit).....	38
Figure 2.3.2-2: ADAMS rigid model.....	39
Figure 2.3.2-3: AMOS-3 CCL mechanism.....	39
Figure 2.3.2-4: AMOS-3 deployment sequence	41
Figure 2.3.2-5: AMOS-3 on-ground model	42
Figure 2.3.2-6: AMOS-3 on ground deployment	42
Figure 3.1.2-1: Latch-up spring obtained from data test	45
Figure 3.2.1-1: Example of load applied on a simple node	49
Figure 3.2.1-2: Attachment point definition	49
Figure 3.2.1-3: Attachment point in a rigid structure	49
Figure 3.2.2-1: Latch-up torque workbench	50
Figure 3.2.2-2: Latch-up reaction torque	51
Figure 3.2.2-3: Latch-up torque maximum close-up	51

Figure 3.2.2-4: Latching torque for a semi-flexible model.....	54
Figure 3.2.3-1: Mesh grid use for visualization purpose in ADAMS.....	55
Figure 3.2.3-2: PLOTTEL elements grid used for visualization in ADAMS	56
Figure 3.2.3-3: Correct use of PLOTTEL	56
Figure 3.2.3-4: File size reduction due to the use of PLOTTEL elements	57
Figure 3.3.1-1: Example of force splitting in BEPI COLOMBO MPO rigid model.....	59
Figure 3.3.2-1: Generation of auxiliary reference points in the model.....	59
Figure 3.3.4-1: Modified joints in flexible model	61
Figure 3.3.4-2: Loss of coplanarity in a flexible model with spherical hinges.....	61
Figure 3.3.4-3: Equivalent friction properties for different kinds of joints	62
Figure 3.3.5-1: Latch-up mechanism in Semi-flexible and full-flexible model	63
Figure 3.3.5-2: Different ways to fix the rotational DOF.....	64
Figure 3.3.6-1: HMAX sensitiveness for full-flexible and semi-flexible model.....	66
Figure 3.3.6-2: Effect of different output-step on the plot of results.....	66
Figure 3.4.1-1: BEPI COLOMBO MPO rigid and semi-flexible model.....	67
Figure 3.4.1-2: Forces splitting.....	68
Figure 3.4.1-3: Joints modification.....	68
Figure 3.4.1-4: Measured Latch-up torque spline.....	70
Figure 3.4.1-5: BEPI COLOMBO MPO Flexible model characteristics	71
Figure 3.4.1-6: Rigid hinges obtained by RBE2 superimposition.....	71
Figure 3.4.1-7: Main differences between Rigid and Semi-flexible solver scripts	72
Figure 3.4.2-1: AMOS-3 rigid and full-flexible model	73
Figure 3.4.2-2: Offset of CCL loads	74
Figure 3.4.2-3: AMOS-3 full-flexible model.....	74
Figure 3.4.2-4: New set of hinges.....	75
Figure 3.4.2-5: Rotation DOF suppression by fixing the rotational speed.....	75
Figure 3.4.2-6: AMOS-3 full-flexible model characteristic	76
Figure 3.4.2-7: Full-flexible model script example	77
Figure 3.4.3-1: AMOS-3 on-ground hybrid model.....	78
Figure 3.4.3-2: Aerodynamic loads on the panles	79
Figure 3.4.3-3: Supporting brackets interfaces.....	79
Figure 3.4.3-4: Rigid and flexible parts in the same model.....	80
Figure 3.4.3-5: Latch-up spring tuning procedure.....	81
Figure 4.1.1-1: Rigid vs Semi-flexible deploment	83
Figure 4.1.2-1: Latch-up torque on HL2.....	84
Figure 4.1.2-2: Close up on the maximum latch-up torque	85
Figure 4.1.2-3: Comparison between Rigid and Semi-flex model latch-up torque.....	85
Figure 4.1.3-1: SADM forces comparison.....	87
Figure 4.1.3-2: SADM torques comparison.....	88
Figure 4.2.1-1: Rigid vs Full-flexible deployment	90
Figure 4.2.2-1: Full-flexible model latch-up torque on the 3 HLs	91
Figure 4.2.2-2: Comparison between Rigid and Full-flexible latch-up torque on HL3 .	92
Figure 4.2.2-3: Comparison between Rigid and Full-flexible latch-up torque on HL2 .	92
Figure 4.2.2-4: Comparison between Rigid and Full-flexible latch-up torque on HL1 .	93
Figure 4.2.3-1: Comparison between Rigid and Full-flexible yoke CCL forces.....	94
Figure 4.2.3-2: Comparison between Rigid and Full-flexible panel CCL forces.....	94
Figure 4.2.4-1: Comparison between Rigid and Full-flexible eddy current damper torque	95
Figure 4.2.5-1: Effect on the lack of preload on Yoke Ty torque.....	96
Figure 4.2.5-2: Yoke Ty torque considering the preload.....	97

Figure 4.2.5-3: Yoke Tx torque	97
Figure 4.3.1-1: Amos-3 on-ground model Latch-up torque on HL3	98
Figure 5-1: Deployment and transversal planes	100
Figure 5-2: ARABSAT deployed configuration.....	102
Figure 5-3: ARABSAT first phase deployment	102
Figure 5-4: ARABSAT second phase deployment.....	103
Figure 5-5: ARABSAT hybrid model	103
Figure 6.1-1: Stress visualization in a loaded rod with three different approaches.....	104
Figure 6.1-2: BEPI COLOMBO MPO panel 1 FEM model for the impact analysis ...	105
Figure 6.1-3: Impact and hot spot stress analysis	106
Figure 6.1-4: Spacecraft model ready for vibration analysis.....	107
Figure 6.1-5: Generation of an ADAMS model using different flexible sub-groups...	108
Figure 6.1-6: Response analysis of GAIA s/a ADAMS flexible model.....	109
Figure A.1-1: Full-flexible model in PATRAN.....	112
Figure A.1-2: Semi-flexible model in PATRAN.....	112
Figure A.1-3: Flexible mode in ADAMS rigid model.....	113
Figure A.1-4: First two flexible modes in NASTRAN obtained from a f-f analysis ...	113
Figure A.1-5: Constraints on HL2	114
Figure A.1-6: First NASTRAN constrained model flexible mode.....	114
Figure A.1-7: NASTRAN first flexible mode frequencies.....	115
Figure A.2-1: ADAMS model obtained from the spacecraft model.....	115
Figure A.2-2: Constraints in the ADAMS model	116
Figure A.2-3: Latch-up spring tuning pattern.....	117
Figure A.2-4: ADAMS rigid model.....	117
Figure A.2-5: <i>Modify Design Variable Window</i>	118
Figure A.2-6: <i>Modify Torsion Design Window</i>	118
Figure A.2-7: <i>Perform Vibration Analysis Window</i>	119
Figure A.2-8: <i>Create Design Variable Window</i>	119
Figure A.2-9: <i>Create Vibration Design Objective Macro Window</i>	119
Figure A.2-10: <i>Create Design Objective Window</i>	120
Figure A.2-11: <i>Perform Vibration Analysis Window</i>	120
Figure A.2-12: <i>Design Evaluation Tools Window</i>	120
Figure A.2-13: <i>Information Window</i>	121
Figure B.1-1: AMOS-3 FEM model.....	123
Figure B.1-2: Hinges masses split between the two panels	124
Figure B.1-3: RBE2 elements superposition on the panels	125
Figure B.1-4: RBE2 rigid elements superposition in the yoke	125
Figure B.1-5: APs definition on rigid parts	127
Figure B.1-6: Visualization of a saddle deformation using plotel.....	129
Figure B.1-7: Fine mesh + PLOTEL mesh on panel 2	129
Figure B.1-8: PLOTEL mesh grid	130
Figure B.3-1: <i>Analysis Window</i>	132
Figure B.3-2: <i>Aset/Qset Doflist Window</i>	132
Figure B.3-3: <i>Solution Parameters Window</i>	133
Figure B.3-4: <i>MSC.Adams Input Parameters Window</i>	133
Figure B.3-5: <i>Adams Output Units Window</i>	134
Figure B.3-6: <i>MSC.Adams Input Parameters Window</i>	134

Figure B.3-7: <i>Subcases Window</i>	135
Figure B.3-8: <i>Subcase select Window</i>	135
Figure B.4-1: <i>MSC.Adams Input Parameters Window</i>	136
Figure B.4-2: Modification to apply to the BDF file.....	137
Figure B.4-3: Sizes differences using or not the PLOTEL.....	137
Figure C.1-1: BEPI COLOMBO MPO panel 1 FEM model.....	139
Figure C.1-2: Analysis Window	140
Figure C.1-3: Aset/Qset Window	140
Figure C.1-4: Solution Parameter Window	141
Figure C.1-5: MSC.Adams Input Parameters Window	141
Figure C.1-6: Subcases Window	142
Figure C.1-7: Output Request Window	143
Figure C.1-8: Subcases Select Window.....	143
Figure C.2-1: Groups needed for generate a spot mesh stress model.....	144
Figure C.2-2: FEM groups for graphical and stress visualization in ADAMs	144
Figure C.2-3: Group containing the whole set of element.....	145
Figure C.2-4: MSC.Adams Input Parameters Window	146
Figure C.2-5: Output Request Window	147
Figure C.2-6: Modification to apply to the BDF file.....	148
Figure C.3-1: Stresses in a Full-mesh model.....	149
Figure C.3-2: Stresses in a Spot-mesh model.....	149
Figure C.3-3: ADAMS model used to compare the stress with NASTRAN	150
Figure C.3-4: Comparison of stress between full mesh model and PLOTEL model ...	150
Figure C.3-5: Comparison of stress between ADAMS and NASTRAN models	150
Figure D.1-1: ADAMS starting rigid model.....	152
Figure D.1-2: Entrance Menu Window	153
Figure D.1-3: Swap a rigid body for a flexible body – Aligment Window	153
Figure D.1-4: First positioning of bodies (CM aligned).....	154
Figure D.1-5: Main Toolbox Window	154
Figure D.1-6: Select Window	155
Figure D.1-7: Flexible and rigid bodies aligned.....	156
Figure D.1-8: Swap a rigid body for a flexible body – Connections Window	157
Figure D.1-9: node_finder Window.....	158
Figure D.1-10: Swap a rigid body for a flexible body – Connections Window	158
Figure D.1-11: Swap a rigid body for a flexible body – Connections Window	159
Figure D.2-1: Information Window	160
Figure D.2-2: Flexible body modify Window	161

List of Tables

Table 1-1: Discrete form of inertia invariants	20
Table 3-1: Panels used in the comparison	50
Table 3-2: Free body modes comparison.....	52
Table 3-3: Fix-interface modes comparison.....	53
Table 3-4: Differences between rigid and flexible model friction properties.....	69
Table B-1: Group for the analysis and related PLOTEL mesh group	131
Table D-1: Keyboard shortcuts to move the model.....	155
Table D-2: General rules for connections.....	160

Acronyms

DOF	Degree of Freedom
FEM	Finite Element Model
MBS	Multi-Body System
HL	Hinge Line
SA	Solar Array
YO	Yoke
S/C	Space Craft
CCL	Close Cable Loop
MPO	Mars Polar Orbiter
SADM	Solar Array Drive Mechanism
MNF	Modal Neutral File
AP	Attachment Point
CB	Craig-Bampton
ECSS	European Cooperation on Space Standardization

Chapter 1

Theoretical background

1.1 The base of the flexible model

This chapter introduces the mathematical background behind the generation of the solar array flexible model. This part is not strictly necessary to the final user but is important to understand some choices that will be shown in next chapters as, for example, the choice of attachment points and their DOF. We will consider a pre-existing FEM model and we will show how ADAMS deal with it to create a new entity with a reduced number of DOF.

1.1.1 Flexible bodies in ADAMS

ADAMS is a Multiple Body System package of software that allow the user to create a multi-body system, generate its related mathematical model using a user friendly interface (ADAMS/View) and solve the system of non-linear coupled differential and algebraic equations associated (ADAMS/solver).

Beside that, ADAMS has the capability to interface with FEM (Finite Element Method) Software. Consequently it has the possibility to deal with flexible bodies generated by

the FEM model using particular reduction method to condense the entire set of FEM degrees of freedom (DOF).

The current approach to the flexible body description with a product called ADAMS/Flex was introduced in 1996. The bodies are represented by a new element called FLEX_BODY.

1.2 Modal superposition

The most important assumption behind the FLEX_BODY is that we consider only small, linear body deformations relative to a local reference frame, while that reference frame is undergoing large and non-linear global motion.

The discretization of a flexible component in a finite element model approximates the infinite number of DOF by a finite, but very large number of finite element DOF. The linear deformations of the nodes of this finite element mode, \mathbf{u} , can be expressed as a linear combination of a smaller number of shape vectors (or mode shapes), ϕ .

$$\mathbf{u} = \sum_{i=1}^M \phi_i q_i \quad (1.1)$$

where M is the number of mode shape. The scale factors or amplitudes, q , are the modal coordinates. As a simple example of how a complex shape is built as a linear combination of simple shapes, observe Figure 1.1.1-1.

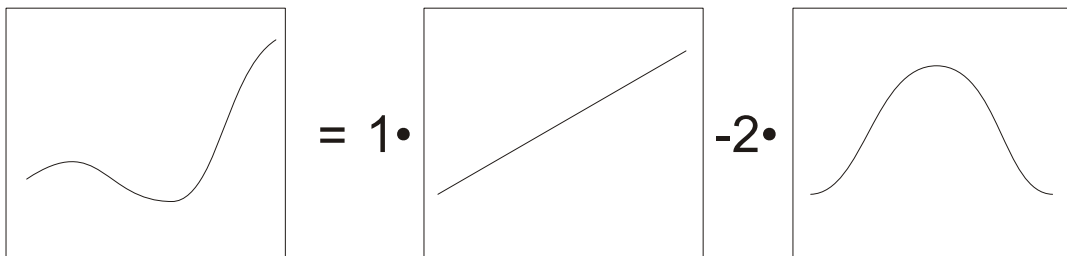


Figure 1.1.1-1: Example of modal superposition

The basic premise of modal superposition is that the deformation behaviour of a component with a very large number of nodal DOF can be captured with a much smaller number of modal DOF. We refer to this reduction in DOF as *modal truncation*.

Equation 1.1 is frequently presented in a matrix form

$$\mathbf{u} = \Phi \mathbf{q} \quad (1.2)$$

where \mathbf{q} is the vector of modal coordinates and the modes ϕ_i have been deposited in the columns of the modal matrix Φ . After modal truncation Φ becomes a rectangular matrix and represent the transformation from the small set of modal coordinates \mathbf{q} , to larger set of physical coordinates, \mathbf{u} .

The next step will be the understanding of how optimize our modal basis, selecting a minimal amount of modal coordinates to capture the maximum amount of interesting deformations.

1.2.1 Component mode synthesis — The Craig-Bampton method

In an early release of ADAMS/Flex it was assumed that eigenvectors would provide a useful modal basis. To prevent spurious constraints in the system, it was recommended to use the eigenvectors of an unconstrained system.

In general it is not easy with this basis to capture the effects of attachments on flexible body. To achieve good results it is necessary to include an excessive number of modes and for this reason this approach was set aside.

The better solution is to use Component Mode Synthesis (CMS) techniques, in particular the Craig-Bampton method.

The Craig-Bampton method allows the user to exclude a subset of DOF from modal superposition. These DOF, which we refer to as boundary DOF (or attachment DOF or interface DOF), are preserved exactly in the Craig-Bampton modal basis. There is no loss in resolution of these DOF when higher order modes are truncated.

The Craig-Bampton method achieves this with a very simple scheme. The system DOF are partitioned into boundary DOF, \mathbf{u}_B , and interior DOF, \mathbf{u}_I .

Two sets of mode shapes are defined, as follows:

Constraint modes: These modes are static shapes obtained by giving each boundary DOF a unit displacement while holding all other boundary DOF fixed. The basis of constraint modes completely spans all possible motions of the boundary DOFs, with a one-to-one correspondence between the modal coordinates of the constraint modes and the displacement in the corresponding boundary DOF, $\mathbf{q}_C = \mathbf{u}_B$.

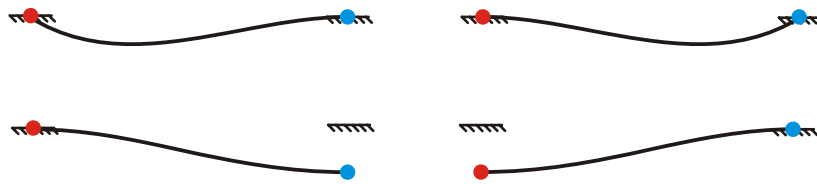


Figure 1.2.1-1: Constraint Modes of a 2D beam

Figure 1.2.1-1 shows four constraint modes for a beam that has attachment points at the two ends. The figures on the top show the constraint mode corresponding to a unit rotation while the figures below correspond to a unit translation.

Fixed-boundary normal modes: These modes are obtained by fixing the boundary DOF and computing an eigensolution. There are as many fixed-boundary normal modes as the user desires. These modes define the modal expansion of the interior DOF. The quality of this modal expansion is proportional to the number of modes retained by the user.



Figure 1.2.1-2: First two fixed-boundary modes of a 2D beam

Figure 1.2.1-2 shows two fixed-boundary normal modes for a beam that has attachment points at the two ends.

The relationship between the physical DOF and the Craig-Bampton modes and their modal coordinates is expressed by the following equation.

$$\mathbf{u} = \begin{Bmatrix} \mathbf{u}_B \\ \mathbf{u}_I \end{Bmatrix} = \begin{bmatrix} \mathbf{I} & \mathbf{0} \\ \Phi_{IC} & \Phi_{IN} \end{bmatrix} \begin{Bmatrix} \mathbf{q}_C \\ \mathbf{q}_N \end{Bmatrix} \quad (1.3)$$

Where

\mathbf{u}_B are the boundary DOF

\mathbf{u}_I are the interior DOF

$\mathbf{I}, \mathbf{0}$ are identity and zero matrices, respectively

Φ_{IC} are the physical displacements of the interior DOF in the constraint modes

Φ_{IN} are the physical displacements of the interior DOF in the normal modes

\mathbf{q}_C the modal coordinates of the constraint modes

\mathbf{q}_N the modal coordinates of the fixed-boundary normal modes

The generalized stiffness and mass matrices corresponding to the Craig-Bampton modal basis are obtained via a modal transformation. The stiffness transformation is

$$\hat{\mathbf{K}} = \Phi^T \mathbf{K} \Phi = \begin{bmatrix} \mathbf{I} & \mathbf{0} \\ \Phi_{IC} & \Phi_{IN} \end{bmatrix}^T \begin{bmatrix} \mathbf{K}_{BB} & \mathbf{K}_{BI} \\ \mathbf{K}_{IB} & \mathbf{K}_{II} \end{bmatrix} \begin{bmatrix} \mathbf{I} & \mathbf{0} \\ \Phi_{IC} & \Phi_{IN} \end{bmatrix} = \begin{bmatrix} \hat{\mathbf{K}}_{CC} & \mathbf{0} \\ \mathbf{0} & \hat{\mathbf{K}}_{NN} \end{bmatrix} \quad (1.4)$$

while the mass transformation is

$$\hat{\mathbf{M}} = \Phi^T \mathbf{M} \Phi = \begin{bmatrix} \mathbf{I} & \mathbf{0} \\ \Phi_{IC} & \Phi_{IN} \end{bmatrix}^T \begin{bmatrix} \mathbf{M}_{BB} & \mathbf{M}_{BI} \\ \mathbf{M}_{IB} & \mathbf{M}_{II} \end{bmatrix} \begin{bmatrix} \mathbf{I} & \mathbf{0} \\ \Phi_{IC} & \Phi_{IN} \end{bmatrix} = \begin{bmatrix} \hat{\mathbf{M}}_{CC} & \hat{\mathbf{M}}_{NC} \\ \hat{\mathbf{M}}_{CN} & \hat{\mathbf{M}}_{NN} \end{bmatrix} \quad (1.5)$$

where the subscripts **I**, **B**, **N** and **C** denote internal DOF, boundary DOF, normal mode and constraint mode, respectively. The caret on $\hat{\mathbf{M}}$ and $\hat{\mathbf{K}}$ denotes that this is the generalized mass and stiffness matrix.

Equations 1.4 and 1.5 have a few noteworthy properties:

- $\hat{\mathbf{M}}_{NN}$ and $\hat{\mathbf{K}}_{NN}$ are diagonal matrices because they are associated with eigenvectors.
- $\hat{\mathbf{K}}$ is block diagonal. There is no stiffness coupling between the constraint modes and fixed-boundary normal modes.
- $\hat{\mathbf{M}}$ is not block diagonal because there is inertia coupling between the constraint modes and the fixed-boundary normal modes.

1.2.2 Mode shape orthonormalization

The Craig-Bampton method is a powerful method for tailoring the modal basis to capture both the desired attachment effects and the desired level of dynamic content. However, the raw Craig-Bampton modal basis has certain deficiencies that make it unsuitable for direct use in a dynamic system simulation. These are:

1. Embedded in the Craig-Bampton constraint modes are 6 rigid body DOF which must be eliminated before the ADAMS analysis because ADAMS provides its own large-motion rigid body DOF.
2. The Craig-Bampton constraint modes are the result of a static condensation. Consequently, these modes do not advertise the dynamic frequency content that they contribute to the flexible system.
3. Craig-Bampton constraint modes cannot be disabled because to do so would be equivalent to applying a constraint on the system.

These problems with the raw Craig-Bampton modal basis are resolved by applying a simple mathematical operation on the Craig-Bampton modes.

The Craig-Bampton modes are not an orthogonal set of modes, as evidenced by the fact that their generalized mass and stiffness matrices $\hat{\mathbf{K}}$ and $\hat{\mathbf{M}}$, encountered in equations 1.4 and 1.5, are not diagonal.

By solving an eigenvalue problem

$$\hat{\mathbf{K}}\mathbf{q} = \lambda\hat{\mathbf{M}}\mathbf{q} \quad (1.6)$$

we obtain eigenvectors that we arrange in a transformation matrix \mathbf{N} , which transforms the Craig-Bampton modal basis to an equivalent, orthogonal basis with modal coordinates

$$\mathbf{N}\mathbf{q}^* = \mathbf{q} \quad (1.7)$$

The effect on the superposition formula is

$$\mathbf{u} = \sum_{i=1}^M \phi_i q_i = \sum_{i=1}^M \phi_i \mathbf{N}\mathbf{q}^* = \sum_{i=1}^M \phi_i^* \mathbf{q}^* \quad (1.8)$$

Where ϕ_i^* are the orthogonalized Craig-Bampton modes.

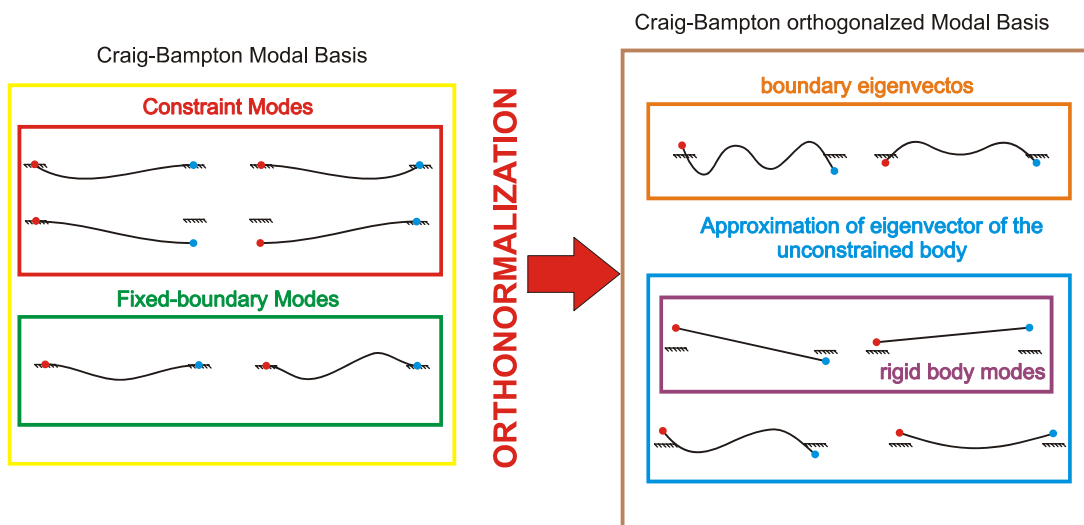


Figure 1.2.2-1: Craig-Bampton modal basis and Craig-Bampton orthogonalized basis

The orthogonalized Craig-Bampton modes are not eigenvectors of the original system. They are eigenvectors of the Craig-Bampton representation of the system and as such have a natural frequency associated with them. Figure 1.2.2-1 shows the effect of the orthonormalization for the beam example. A physical description of these modes is difficult, but in general the following is observed:

- Fixed-boundary normal modes are replaced with an approximation of the eigenvectors of the unconstrained body. This is an approximation because it is based only on the Craig-Bampton modes. Out of these modes, 6 modes are the rigid body modes.
- Constraint modes are replaced with boundary eigenvector, a concept best illustrated by comparing the modes before and after orthogonalization of a rectangular plate which has Craig-Bampton attachment points along one of its long edges as shown in Figure 1.2.2-2. The Craig-Bampton constraint mode is a unit displacement of one of its edge nodes with all the other nodes along that edge fixed. After orthonormalization we see modes like the one depicted on the right of the figure, which has a sinusoidal curve along the boundary edge.

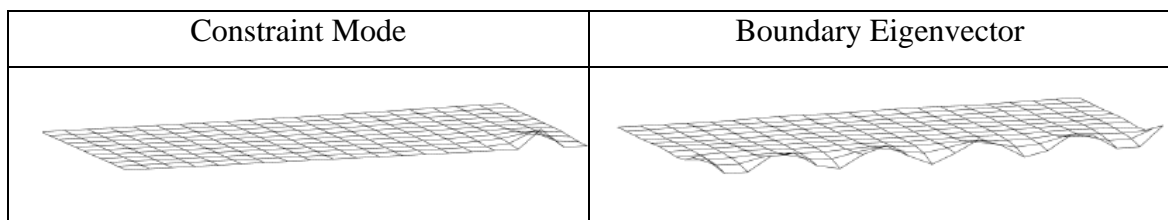


Figure 1.2.2-2: Constraint mode and relative boundary eigenvector on a plate

We conclude that the orthonormalization of the Craig-Bampton modes addresses the problems identified earlier, because:

1. Orthonormalization yields the modes of the unconstrained system, 6 of which are rigid body modes, which can now be disabled.
2. Following the second eigensolution, all modes have an associated natural frequency. Problems arising from modes contributing high-frequency content can now be anticipated.

3. Although the removal of any mode constrains the body from adopting that particular shape, the removal of a high-frequency such as the boundary eigenvector of Figure 1.2.2-2 is clearly more benign than removing the relative constraint mode. The removal of the latter mode prevents the associated boundary node from moving relative to its neighbors. Meanwhile, the removal of the former mode only prevents boundary edge from reaching this degree of “waviness”.

1.3 Modal flexibility in ADAMS

In this section we show how ADAMS capitalizes on modal superposition in the two key areas of the ADAMS formulation:

- Flexible marker kinematics
- Flexible body equations of motion

1.3.1 Flexible marker kinematics

Marker kinematics refers to the position, orientation, velocity, and acceleration of markers. ADAMS uses the kinematics of markers in three key areas:

- Marker position and orientation must be known in order to satisfy constraints like those imposed in JOINT and JPRIM elements.
- To project point forces applied at markers on generalized coordinates of the flexible body.
- The marker measures, (for example DX, WZ, PHI, ACCX, and so on) that appear in expressions and user-written subroutines require information about position, orientation, velocity, and acceleration of markers

1.3.1.1 Position

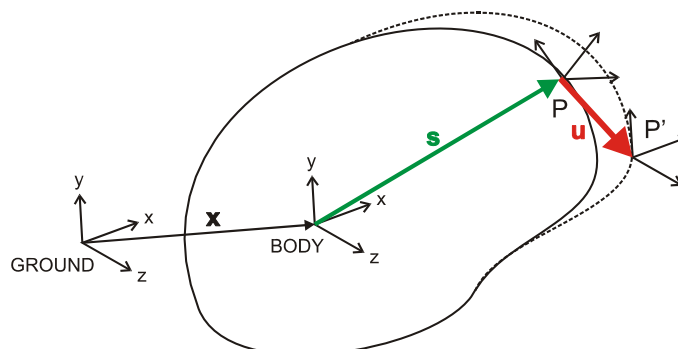


Figure 1.3.1-1: Flexible body reference system in ADAMS

The instantaneous location of a marker that is attached to a node, P, on a flexible body, B, is the sum of three vectors (see).

$$\vec{r}_p = \vec{x} + \vec{s}_p + \vec{u}_p \quad (1.9)$$

Where

\vec{x} is the position vector from the origin of the ground reference frame to the origin of the local body reference frame, B, of the flexible body.

\vec{s}_p is the position vector of the undeformed position of point P with respect to the local body reference frame of body B.

\vec{u}_p is the translational deformation vector of point P, the position vector from the point's undeformed position to its deformed position.

We rewrite Eq. 1.9 in a matrix form, expressed in the ground coordinate system

$$\mathbf{r}_p = \mathbf{x} + {}^G\mathbf{A}^B (\mathbf{s}_p + \mathbf{u}_p) \quad (1.10)$$

Where

\mathbf{x} is the position vector from the ground origin to the origin of the local body reference frame, B, of the flexible body, expressed in the ground coordinate system. The elements of the \mathbf{x} vector, x , y and z , are generalized coordinates of the flexible body.

\mathbf{s}_p is the position vector from the local body reference frame of B to the point P, expressed in the local body coordinate system. This is a constant.

${}^G\mathbf{A}^B$ is the transformation matrix from the local body reference frame of B to ground. This matrix is also known as the direction cosines of the local body reference frame with respect to ground. In ADAMS, orientation is captured using a body fixed 3-1-3 set of Euler angles ψ , θ and ϕ . The Euler angles are generalized coordinates of the flexible body.

\mathbf{u}_p is the translational deformation vector of point P, also expressed in the local body coordinate system. The deformation vector is a modal superposition

$$\mathbf{u}_p = \mathbf{\Phi}_p \mathbf{q} \quad (1.11)$$

Where $\mathbf{\Phi}_p$ is the slice from the modal matrix that corresponds to the translational DOF of node P. The dimension of the $\mathbf{\Phi}_p$ matrix is $3 \times M$ where M is the number of modes. The modal coordinates q_i , ($i = 1, \dots, M$) are also generalized coordinates of the flexible body.

Therefore, the total set of generalized coordinates of the flexible body is

$$\xi = \left\{ \begin{array}{c} x \\ y \\ z \\ \psi \\ \theta \\ \phi \\ q_i, (i=1..M) \end{array} \right\} = \left\{ \begin{array}{c} \mathbf{x} \\ \boldsymbol{\psi} \\ \mathbf{q} \end{array} \right\} \quad (1.12)$$

1.3.1.2 Velocity

For the purpose of computing kinetic energy, we compute the instantaneous translational velocity of P relative to ground which is obtained by differentiating Eq. 1.10 with respect to time

$$\mathbf{v}_p = \dot{\mathbf{x}} + {}^G \dot{\mathbf{A}}^B (\mathbf{s}_p + \mathbf{u}_p) + {}^G \mathbf{A}^B \dot{\mathbf{u}}_p \quad (1.13)$$

Taking advantage of the relationship

$${}^G \dot{\mathbf{A}}^B \mathbf{s} = {}^G \mathbf{A}^B \left({}^G \boldsymbol{\omega}_B^B \times \mathbf{s} \right) = {}^G \mathbf{A}^B {}^G \tilde{\boldsymbol{\omega}}_B^B \times \mathbf{s} = -{}^G \mathbf{A}^B \tilde{\mathbf{s}}^G \boldsymbol{\omega}_B^B \quad (1.14)$$

where ${}^G \boldsymbol{\omega}_B^B$ is the angular velocity of the body relative to ground expressed in body coordinates with the tilde denoting the following skew product

$$\mathbf{a} \times \mathbf{b} = \begin{bmatrix} 0 & -a_z & a_y \\ a_z & 0 & -a_x \\ -a_y & a_x & 0 \end{bmatrix} \mathbf{b} = \tilde{\mathbf{a}} \mathbf{b} = -\tilde{\mathbf{b}} \mathbf{a} \quad (1.15)$$

we can write

$$\mathbf{v}_p = \dot{\mathbf{x}} - {}^G \mathbf{A}^B \left(\widetilde{\mathbf{s}_p + \mathbf{u}_p} \right) \mathbf{B} \dot{\boldsymbol{\psi}} + {}^G \mathbf{A}^B \boldsymbol{\Phi}_p^* \dot{\mathbf{q}} \quad (1.16)$$

We have introduced the relationship:

$${}^G \boldsymbol{\omega}_B^B = \mathbf{B} \dot{\boldsymbol{\psi}} \quad (1.17)$$

relating the angular velocity to the time derivative of the orientation states.

1.3.1.3 Orientation

To satisfy angular constraints, ADAMS must instantaneously evaluate the orientation of a marker on a flexible body, as the body deforms. As the body deforms, the marker rotates through small angles relative to its reference frame. Much like translational deformations, these angles are obtained using a modal superposition, similar to Eq. 1.11:

$$\boldsymbol{\theta}_p = \boldsymbol{\Phi}_p^* \mathbf{q} \quad (1.18)$$

Where Φ_p^* is the slice from the modal matrix that corresponds to the rotational DOF of node P. The dimension of the Φ_p^* matrix is $3 \times M$ where M is the number of modes.

The orientation of marker J relative to ground is represented by the Euler transformation matrix, ${}^G \mathbf{A}^J$. This matrix is the product of three transformation matrices:

$${}^G \mathbf{A}^J = {}^G \mathbf{A}^B {}^B \mathbf{A}^P {}^P \mathbf{A}^J \quad (1.19)$$

Where

${}^G \mathbf{A}^B$ is the transformation matrix from the local body reference frame of B to ground.

${}^B \mathbf{A}^P$ is the transformation matrix due to the orientation change due to the deformation of node P.

${}^P \mathbf{A}^J$ is the constant transformation matrix that was defined by the user when the marker was placed on the flexible body.

The matrix ${}^B \mathbf{A}^P$ requires more attention. The direction cosines for a vector of small angles, θ_p , are

$${}^B \mathbf{A}^P = \begin{bmatrix} 1 & -\theta_{pz} & \theta_{py} \\ \theta_{pz} & 1 & -\theta_{px} \\ -\theta_{py} & \theta_{px} & 1 \end{bmatrix} = \mathbf{I} + \tilde{\boldsymbol{\theta}}_p \quad (1.20)$$

where the tilde denotes the skew operator (Eq. 1.15).

1.3.1.4 Angular velocity

The angular velocity of a marker, J, on a flexible body is the sum of the angular velocity of the body and the angular velocity due to deformation

$${}^G\boldsymbol{\omega}_B^J = {}^G\boldsymbol{\omega}_B^P = {}^G\boldsymbol{\omega}_B^B + {}^B\boldsymbol{\omega}_B^P = {}^G\boldsymbol{\omega}_B^B + \boldsymbol{\Phi}_p^* \dot{\mathbf{q}} \quad (1.21)$$

1.3.2 Applied loads

The treatment of forces in ADAMS distinguishes between point loads and distributed loads. This section will focus only on the point forces and torque since they are the only of interest for the models that will be developed in further chapters.

1.3.2.1 Point forces and torques

A point force \vec{F} and a point torque \vec{T} that are applied to a marker on a flexible body must be projected on the generalized coordinates of the system.

The force and torque are written in matrix form, and expressed in the coordinate system of marker K.

$$\mathbf{F}_K = \begin{bmatrix} f_x \\ f_y \\ f_z \end{bmatrix} \quad \mathbf{T}_K = \begin{bmatrix} t_x \\ t_y \\ t_z \end{bmatrix} \quad (1.22)$$

The generalized force Q consists of a generalized translational force, a generalized torque (a generalized force on the Euler angles) and a generalized modal force, thus:

$$\mathbf{Q} = \begin{bmatrix} \mathbf{Q}_T \\ \mathbf{Q}_R \\ \mathbf{Q}_M \end{bmatrix} \quad (1.23)$$

Generalized Translational Force: Since the governing equations of motion, Eq. 1.42, are written in the global reference frame, the generalized force on the translational coordinates is obtained by transforming \mathbf{F}_K to global coordinates.

$$\mathbf{Q}_T = {}^G \mathbf{A}^K \mathbf{F}_K \quad (1.24)$$

where ${}^G \mathbf{A}^K$ is given in Eq. 1.19. The generalized translational force is independent of the point of force application.

An applied torque does not contribute to \mathbf{Q}_T .

Generalized Torque: The total torque on a flexible body, due to \vec{F} and \vec{T} is $\vec{T}_{TOT} = \vec{T} + \vec{p} \times \vec{F}$, where \vec{p} is the position vector from the origin of the local body reference frame of the body to the point of force application. The total torque, can be written in matrix form, with respect to the ground coordinate system as:

$$\mathbf{T}_{TOT} = {}^G \mathbf{A}^K \mathbf{T}_K + \mathbf{p} \times {}^G \mathbf{A}^K \mathbf{F}_K \quad (1.25)$$

Where \mathbf{p} is expressed in the ground coordinates. Using the tilde notation of Eq. 1.20 this can be written as

$$\mathbf{T}_{TOT} = {}^G \mathbf{A}^K \mathbf{T}_K + \tilde{\mathbf{p}} {}^G \mathbf{A}^K \mathbf{F}_K \quad (1.26)$$

The transformation from torque in physical coordinates to the generalized torque on the body Euler angles is provided by the B matrix in Eq. 1.16

$$\mathbf{Q}_R = [{}^G \mathbf{A}^K \mathbf{B}]^T \mathbf{T}_{TOT} = [{}^G \mathbf{A}^K \mathbf{B}]^T [{}^G \mathbf{A}^K \mathbf{T}_K + \tilde{\mathbf{p}} {}^G \mathbf{A}^K \mathbf{F}_K] \quad (1.27)$$

Generalized Modal Force: The generalized modal force on a body due to applied point forces or point torques at P is obtained by projecting the load on the mode shapes.

As the applied force \mathbf{F}_K and torque \mathbf{T}_K are given with respect to marker K, they must first be transformed to the reference frame of the flexible body

$$\mathbf{F}_I = \left[{}^G \mathbf{A}^B \right]^T {}^G \mathbf{A}^K \mathbf{F}_K \quad (1.28)$$

$$\mathbf{T}_I = \left[{}^G \mathbf{A}^B \right]^T {}^G \mathbf{A}^K \mathbf{T}_K \quad (1.29)$$

and then projected on the mode shapes. The force is projected on the translational mode shapes and the torque is projected on the angular mode shapes

$$\mathbf{Q}_F = \Phi_p^T \mathbf{F}_I + \Phi_p^{*T} \mathbf{T}_I \quad (1.30)$$

Where Φ_p and Φ_p^* slices of the modal matrix corresponding to the translational and angular DOF of point P, as discussed in section 1.3.1.

Note that since the modal matrix Φ is only defined at nodes, point forces and point torques can only be applied at nodes.

1.3.3 Flexible body equations of motion

The governing equations for a general multi body system are derived from Lagrange's equations of the form

$$\begin{cases} \frac{d}{dt} \left(\frac{\partial L}{\partial \dot{\xi}} \right) - \frac{\partial L}{\partial \xi} + \frac{\partial \mathcal{F}}{\partial \dot{\xi}} + \left[\frac{\partial \Psi}{\partial \xi} \right]^T \lambda - \mathbf{Q} = 0 \\ \Psi = 0 \end{cases} \quad (1.31)$$

Where

L is the Lagrangian, defined below

\mathcal{F} is an energy dissipation function, defined below

Ψ are the constraint equations

λ are the Lagrange multipliers for the constraints

ξ are the generalized coordinates as defined in Eq. 1.12

\mathbf{Q} are the generalized applied forces (the applied forces projected on)

The Lagrangian is defined as

$$L = T - V$$

where T and V denote kinetic and potential energy respectively.

The remainder of this section is devoted to the derivation of the contributions to Eq. 1.41, in the following order:

- Kinetic energy and the mass matrix
- Potential energy and the stiffness matrix
- Dissipation and the damping matrix
- Constraints

1.3.3.1 Kinetic energy and the mass matrix

The velocity from Eq. 1.16 can be expressed in terms of the time derivative of the state vector

$$\mathbf{v}_p = \left[\begin{bmatrix} \mathbf{I} & -{}^G\mathbf{A}^B \left(\widetilde{\mathbf{s}_p + \mathbf{u}_p} \right) \mathbf{B} \\ \mathbf{0} & {}^G\mathbf{A}^B \Phi_p \end{bmatrix} \right] \cdot \dot{\xi} \quad (1.32)$$

We can now compute the kinetic energy. The kinetic energy for a flexible body is given as

$$T = \frac{1}{2} \int_V \rho \mathbf{v}^T \mathbf{v} dV \approx \frac{1}{2} \sum_p m_p \mathbf{v}_p^T \mathbf{v}_p + {}^G \boldsymbol{\omega}_p^{BT} \mathbf{I}_p {}^G \boldsymbol{\omega}_p^B \quad (1.33)$$

where m_p and \mathbf{I}_p are the nodal mass and nodal inertia tensor of node P , respectively. Note that \mathbf{I}_p is often a negligible quantity which arises when reduced continuum descriptions, i.e. bars, beams, or shells, are employed in your flexible component model. Lumped masses and inertia may also contribute to this term.

Substituting for \mathbf{v} and $\boldsymbol{\omega}$ and simplifying yields an equation for the kinetic energy in ADAMS' generalized mass matrix and generalized coordinates.

$$T = \frac{1}{2} \dot{\boldsymbol{\xi}}^T \mathbf{M}(\boldsymbol{\xi}) \dot{\boldsymbol{\xi}} \quad (1.34)$$

For clarity of presentation we partition the mass matrix, $\mathbf{M}(\boldsymbol{\xi})$, into a 3×3 block matrix

$$\mathbf{M}(\boldsymbol{\xi}) = \begin{bmatrix} \mathbf{M}_{tt} & \mathbf{M}_{tr} & \mathbf{M}_{tm} \\ \mathbf{M}_{tr}^T & \mathbf{M}_{rr} & \mathbf{M}_{rm} \\ \mathbf{M}_{tm}^T & \mathbf{M}_{rm}^T & \mathbf{M}_{mm} \end{bmatrix} \quad (1.35)$$

where the subscripts t , r and m denote translational, rotational, and modal DOF respectively.

The expression for the mass matrix $\mathbf{M}(\boldsymbol{\xi})$ simplifies to an expression in nine inertia invariants.

$$\left\{ \begin{array}{l} \mathbf{M}_{tt} = \mathcal{I}^1 \mathbf{I} \\ \mathbf{M}_{tr} = -\mathbf{A} [\mathcal{I}^2 + \mathcal{I}_j^3 q_j] \mathbf{B} \\ \mathbf{M}_{tm} = \mathbf{A} \mathcal{I}^3 \\ \mathbf{M}_{rr} = \mathbf{B}^T [\mathcal{I}^7 - [\mathcal{I}_j^8 + \mathcal{I}_j^{8T}] q_j - \mathcal{I}_{ij}^9 q_i q_j] \mathbf{B} \\ \mathbf{M}_{rm} = \mathbf{B}^T [\mathcal{I}^4 - \mathcal{I}_j^5 q_j] \\ \mathbf{M}_{mm} = \mathcal{I}^6 \end{array} \right. \quad (1.36)$$

The explicit dependence of the mass matrix on the modal coordinates is evident. The dependence on orientation coordinates of the system comes about because of the transformation matrices **A** and **B**.

The inertia invariants are computed from the N nodes of the finite element model based on information about each node's mass, m_p , its undeformed location \mathbf{s}_p , and its participation in the component modes Φ_p . The discrete form of the inertia invariants are provided in Table 1.1.

$\mathcal{I}^1 = \sum_{p=1}^N m_p$		Scalar
$\mathcal{I}^2 = \sum_{p=1}^N m_p \mathbf{s}_p$		(3×1)
$\mathcal{I}_j^3 = \sum_{p=1}^N m_p \Phi_p$	$j = 1, \dots, M$	$(3 \times M)$
$\mathcal{I}^4 = \sum_{p=1}^N m_p \tilde{\mathbf{s}}_p \Phi_p + \mathbf{I}_p \Phi_p'$		$(3 \times M)$
$\mathcal{I}_j^5 = \sum_{p=1}^N m_p \tilde{\phi}_{pj} \Phi_p$	$j = 1, \dots, M$	$(3 \times M)$
$\mathcal{I}^6 = \sum_{p=1}^N m_p \Phi_p^T \Phi_p + \Phi_p'^T \mathbf{I}_p \Phi_p'$		$(M \times M)$
$\mathcal{I}^7 = \sum_{p=1}^N m_p \tilde{\mathbf{s}}_p^T \tilde{\mathbf{s}}_p + \mathbf{I}_p$		(3×3)
$\mathcal{I}_j^8 = \sum_{p=1}^N m_p \tilde{\mathbf{s}}_p \tilde{\phi}_{pj}$	$j = 1, \dots, M$	(3×3)
$\mathcal{I}_{jk}^9 = \sum_{p=1}^N m_p \tilde{\phi}_{pj} \tilde{\phi}_{pk}$	$j, k = 1, \dots, M$	(3×3)

Table 1-1: Discrete form of inertia invariants

1.3.3.2 Potential energy and the stiffness matrix

Frequently, the potential energy consists of contributions from gravity and elasticity in the quadratic form.

$$V = V_g(\xi) + \frac{1}{2} \xi^T \mathbf{K} \xi \quad (1.37)$$

In the elastic energy term, \mathbf{K} is the generalized stiffness matrix which is, in general, constant. Only the modal coordinates, \mathbf{q} , contribute to the elastic energy. Therefore, the form of \mathbf{K} is

$$\mathbf{K} = \begin{bmatrix} \mathbf{K}_{tt} & \mathbf{K}_{tr} & \mathbf{K}_{tm} \\ \mathbf{K}_{tr}^T & \mathbf{K}_{rr} & \mathbf{K}_{rm} \\ \mathbf{K}_{tm}^T & \mathbf{K}_{rm}^T & \mathbf{K}_{mm} \end{bmatrix} = \begin{bmatrix} 0 & 0 & 0 \\ 0 & 0 & 0 \\ 0 & 0 & \mathbf{K}_{mm} \end{bmatrix} \quad (1.38)$$

where \mathbf{K}_{mm} is the generalized stiffness matrix of the structural component with respect to the modal coordinates, \mathbf{q} . It is not the full structural stiffness matrix of the component.

V_g is the gravitational potential energy,

$$V_g = \int_V \rho \mathbf{r}_p \cdot \mathbf{g} dV = \int_V \rho \left[\mathbf{x} + \mathbf{A}(\mathbf{s}_p + \Phi(P)\mathbf{q}) \right]^T \mathbf{g} dV \quad (1.39)$$

where \mathbf{g} denotes the gravitational acceleration vector. The resulting gravitational force is

$$\mathbf{f}_g = \frac{\partial V_g}{\partial \xi} = \begin{bmatrix} \left[\int_V \rho dV \right] \mathbf{g} \\ \left[\int_V \rho (\mathbf{s}_p + \Phi(P)\mathbf{q})^T dV \right] \frac{\partial \mathbf{A}^T}{\partial \psi} \mathbf{g} \\ \left[\int_V \rho \Phi^T(P) dV \right] \mathbf{A}^T \mathbf{g} \end{bmatrix} \quad (1.40)$$

1.3.3.3 Dissipation and the damping matrix

The damping forces depend on the generalized modal velocities and are assumed to be derivable from the quadratic form

$$\mathcal{F} = \frac{1}{2} \dot{\mathbf{q}}^T \mathbf{D} \dot{\mathbf{q}} \quad (1.41)$$

which is known as Rayleigh's dissipation function. The matrix \mathbf{D} contains the damping coefficients, d_{ij} , and is generally constant and symmetric. In the case of orthogonal mode shapes, the damping matrix can be effectively defined using a diagonal matrix of modal damping ratios, c_i . This damping ratio could be different for each of the orthogonal modes and can be conveniently defined as a ratio of the critical damping for the mode, c_i^{cr} (where the critical damping ratio is defined as the level of damping that eliminates harmonic response).

1.3.3.4 Constraints

ADAMS satisfies position and orientation constraints for flexible body markers by using the marker kinematics properties presented in section 1.3.1.

1.3.3.5 Governing differential equation of motion — final form

The final form of the governing differential equation of motion, in terms of the generalized coordinates is

$$\mathbf{M} \ddot{\boldsymbol{\xi}} + \dot{\mathbf{M}} \dot{\boldsymbol{\xi}} - \frac{1}{2} \left[\frac{\partial \mathbf{M}}{\partial \boldsymbol{\xi}} \dot{\boldsymbol{\xi}} \right]^T \dot{\boldsymbol{\xi}} + \mathbf{K} \boldsymbol{\xi} + \mathbf{f}_g + \mathbf{D} \dot{\boldsymbol{\xi}} + \left[\frac{\partial \Psi}{\partial \boldsymbol{\xi}} \right]^T \boldsymbol{\lambda} - \mathbf{Q} = 0 \quad (1.42)$$

The entries in Eq. 1.42 are:

$\xi, \dot{\xi}, \ddot{\xi}$ the flexible body generalized coordinates and their time derivatives

\mathbf{M} the flexible body mass matrix in Eq. 1.34

$\dot{\mathbf{M}}$ the time derivative of the flexible body mass matrix

$\frac{\partial \mathbf{M}}{\partial \xi}$ the partial derivative of the mass matrix with respect to the flexible body generalized coordinates. This is a $(M + 6) \times (M + 6) \times (M + 6)$ tensor, where M is the number of modes

\mathbf{K} the generalized stiffness matrix

\mathbf{f}_g the generalized gravitational force

\mathbf{D} the modal damping matrix

Ψ the algebraic constraint equations

λ Lagrange multipliers for the constraints

\mathbf{Q} generalized applied force

Chapter 2

The Rigid Model

2.1 The rigid model objective

The objective of a rigid analysis is to simulate and assess the operational quality of the deployment function of a solar array.

The rigid model focus mainly on two aspects

- ***Torque Margin Analysis***

A quasi static analysis that has to demonstrate the motorization margin of safety for a deployment worst case approach (cold case). The worst case approach comprises the highest resistive forces and torques occurring at a cold temperature extreme condition (higher frictions). The solar array has to keep deploying and reach the deployed configuration even if it is stopped in a partial-deployed configuration.

- ***Dynamic Load Analysis***

A dynamic analysis that has to determinate the maximum reaction loads onto the structure of the solar array. This aspect reflects in general lowest resistive magnitude and highest motorization magnitudes of related components.

Usually the first analysis fixes the motorization items of the deployment mechanism. If, for example, the deployment is obtained using deployment springs this analysis will settle their stiffness and their wind-up angles.

The requirements on the torque margin, according to ESA ECSS rule, impose a margin of 2:1 between the driving torque versus resistive torque with uncertainty factors included.

The success criteria for torque margin are defined, at each Hinge Line (HL) through the following formula.

$$TM_j = \frac{\Sigma D_j}{\Sigma R_j} \geq 2 \quad \text{for } j = 1, 2, 3 \quad (2.1)$$

ΣD_j = sum of driving torque at HL #j

ΣR_j = sum of resistive torque at HL #j with UFs included

Due to the strict requirements the potential energy that at the end will be stored in the mechanism will be quite high and for this reason we need to calculate the dynamic loads. In fact all this surplus of energy could generate high shock loads at the latch-ups.

It's clear that with the flexible model investigation we will be interested in a better comprehension of all the dynamic effects of this second analysis.

2.2 The ADAMS rigid model

A solar array wing is modelled as a mechanical Multiple Body System (MBS). The equation of motion consist of a system of non-linear coupled differential and algebraic equations due to large displacements and rotations during the deployment process. The related mathematical model is set up with the MBS software package ADAMS.

Using this software we can create a 3D model of our solar array and analyse the kinematical and dynamic behaviour for in-orbit or on-ground deployment.

The rigid model usually takes into account the following physical effects:

- Inertia of bodies
- Motorization spring torque
- Friction : *Bearing friction in the hinges*
Friction between cam and latch-up pin
- Harness torque effects
- Optional Closed Cable Loop (CCL) synchronization mechanism
- Optional dampers or engine holding torque
- Latch up of deployment hinges
- Bending Stiffness of solar array structure collocated in the HLs
- Aerodynamic loads (on-ground test simulation)

2.2.1 Inertia of bodies

All the bodies that compose a rigid model of a SA are usually drawn directly in ADAMS environment. ADAMS automatically assigns inertia properties to each body according to their geometry. There is also the option to enter the inertia properties with a manual input.

Figure 2.2.1-1 shows an example of a 5 bodies solar array model: 3 panels, the yoke (YO) and the space craft (S/C).

For what concerns the space craft we can leave the default value assigned by ADAMS because during the deployment analysis is considered fixed to the ground.

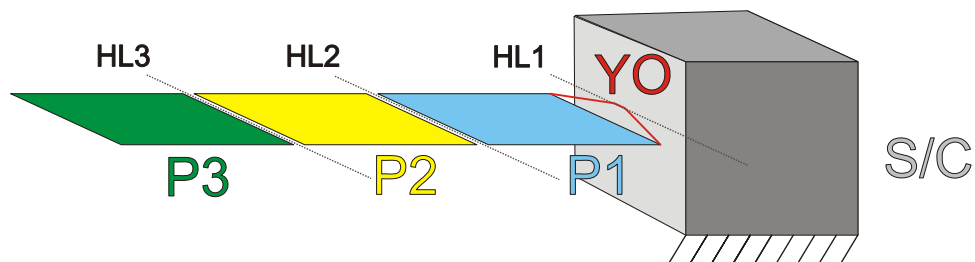


Figure 2.2.1-1: Five bodies solar array

2.2.2 Motorization Spring Torque

This torque is the element that drives out the SA deployment. In a solar array this torque is obtained using rotational springs integrated in the hinges locations as indicated in Figure 2.2.2-1 (broken line). The wind-up angle (and so the preload) of the springs is adjusted according to the torque margin requirement.

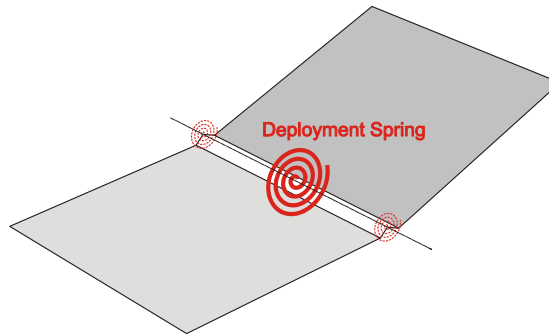


Figure 2.2.2-1: Deployment spring system

In a rigid model however there is no need to consider the real position and number of these springs since we can easily represent their resulting torque (a global torque sum of the others since they work as parallel spring) located in one generic point of the HL axis as shown in Figure 2.2.2-1 (solid line).

2.2.3 Friction

The friction modelling is based on Coulomb's law. Friction torque due to hinge reaction forces and due to the latch-up pin contact with the cam is taken into account. The following expression describes the sliding friction torque which depends on the friction coefficient μ_h , hinge pin radius r_p and the radial hinge reaction force F_r .

$$T_{fric} = \mu_h \cdot r_p \cdot F_r + T_{pret} \quad (2.2)$$

The quantity T_{pret} includes all constant friction torque contributions, which includes the cam friction effect for all hinges.

Figure 2.2.3-1 shows the ADAMS friction dialogue box and on the right we can see that in a rigid model usually spherical joints are used instead of revolutes ones. This choice has been made to keep the level of over constraints in the model as lower as possible.

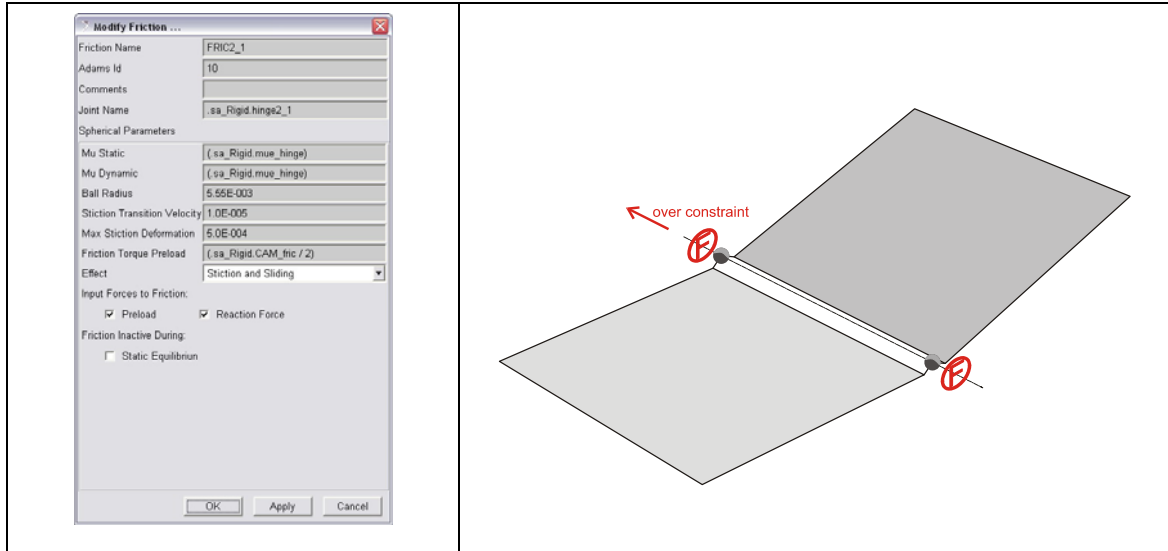


Figure 2.2.3-1: ADAMS Friction model

2.2.4 Harness Torque effects

This torque wants to take into account the effect of the cable harness of the SA. It depends on the deployment angle of each HL and can be a resistive or a motorization torque according to the behaviour of bended cables that can tend to keep the bended shape (resistive) or try to assume the straight position (motorization) as outlined in Figure 2.2.4-1.

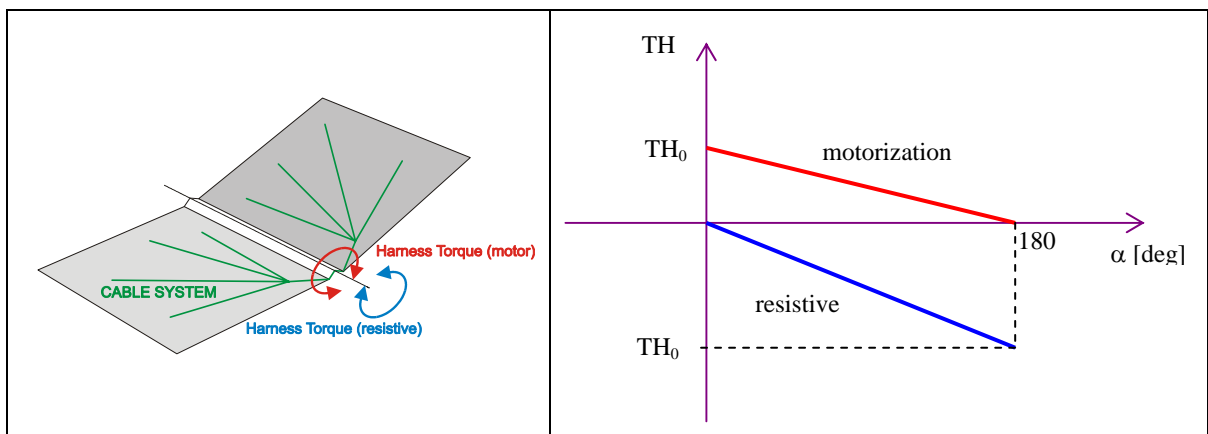


Figure 2.2.4-1: ADAMS harness torque model

2.2.5 Closed Cable Loop (CCL) synchronization mechanism

The principle of the Closed Cable Loop (CCL) synchronisation is a coupling of the rotation of one body with the rotation of the body following the next. This synchronization is obtained with a system of pulleys as shown in Figure 2.2.5-1.

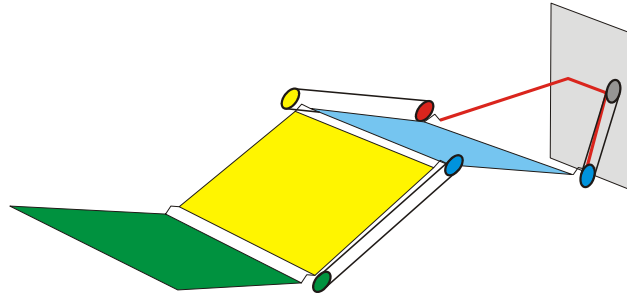


Figure 2.2.5-1: CCL synchronization example

If there are 3 subsequent bodies connected by hinges, the CCL couples the rotation of body 1 and 3 as outlined in Figure 2.2.5-2. The CCL cables are fixed to pulleys; the first pulley is attached to body 1 and the second one to body 3. The values of the pulley radius r_1 and r_2 determine the kinematical transmission ratio of the CCL.

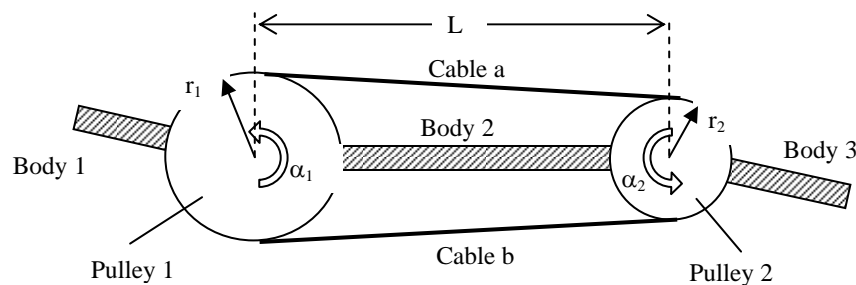


Figure 2.2.5-2: Principle of CCL Synchronization

The cable tension forces F_a and F_b generate a torque T_1 on body 1, a torque T_2 on body 3, a resulting force between the two hinge points F_{ax} and a pair of lateral forces F_{lat} according to the following expressions.

$$T_1 = r_1 \cdot (F_b - F_a) \tag{2.3}$$

$$T_2 = r_2 \cdot (F_a - F_b) \tag{2.4}$$

$$F_{ax} = (F_a + F_b) \cdot \frac{L}{\sqrt{(r_1 - r_2)^2 + L^2}} \tag{2.5}$$

$$F_{lat} = (F_a - F_b) \cdot \frac{r_1 - r_2}{\sqrt{(r_1 - r_2)^2 + L^2}} \tag{2.6}$$

The torques and forces on body 1 and body 3 generated by the CCL are outlined in Figure 2.2.5-3. The lateral force only occurs if the two pulleys have a different radius.

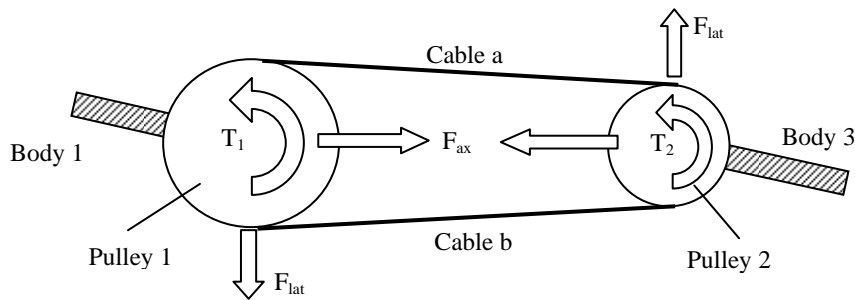


Figure 2.2.5-3: Torques and Forces generated by CCL

The resulting torque on the yoke due to the guided CCL cables is outlined in Figure 2.2.5-4.

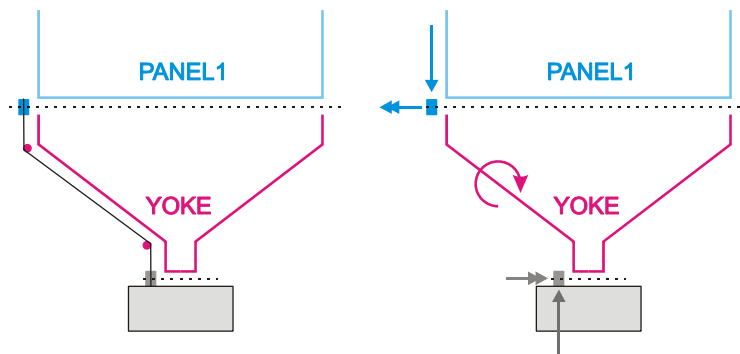


Figure 2.2.5-4: Torque on Yoke due to guided CCL cables

2.2.6 Dampers or engine holding torque

These elements are represented in ADAMS as torques. Their function is to dissipate kinetic energy out of the mechanism in order to attenuate the resulting dynamic loads.

2.2.7 Latch up of deployment hinges

The latch up of the hinges is necessary to fix the relative position of two consecutive bodies when they reach their deployed configuration. In the most cases this blocking has to be permanent and so there is no need of unlocking mechanisms. Usually a simple cam mechanism is used for the latching; when the angle between the two bodies reach the desired value the cam reach is seat and the mechanism is locked as shown in Figure 2.2.7-1.

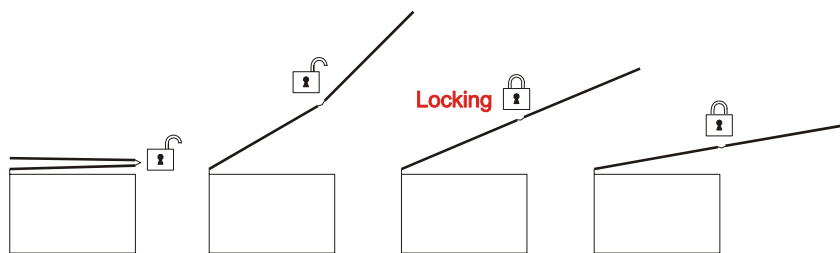


Figure 2.2.7-1: Latch-up principle

In ADAMS the locking can be obtained using for example a MOTION element (we can for example impose a zero rotational velocity on the HL when the two bodies reach the desired angle) but such an approach is not suitable for a rigid body model.

The latching is in fact obtained thanks to a latching spring located on the HL we want to lock as reported in Figure 2.2.7-2. The spring is deactivated during the first phase of deployment and activated at the latch-up (in the case of Figure 2.2.7-2 when the two panels reach 180°). The reason of this choice will be explained in the next paragraph.

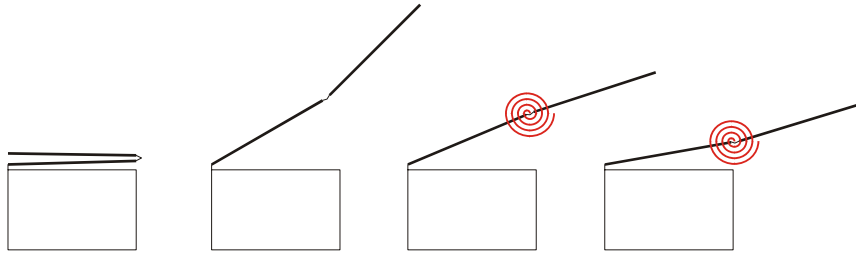


Figure 2.2.7-2: Example of latch-up obtained by a latching spring

2.2.8 Bending Stiffness of solar array structure collocated in the HLs

The problem that emerges with a full rigid model is that this model is not suitable for dynamic analysis. For example the stresses on panels generated by the latching shock would reach extremely high value (theoretically infinite) because of the infinite stiffness of the structure involved in the latch-up. It's clear that such an output would be completely useless for our dynamic analysis.

This problem can be avoided introducing a concentrated stiffness on the hinge line as shown in Figure 2.2.7-2. The structural stiffness of the two latched bodies will be condensed in just one rotational DOF (one spring for each latched-up HL).

To tune these springs we will use a linear modes analysis and we will try to match the frequency of the lower flexible mode of the FEM model with the adjusted stiffness of the latch-up spring.

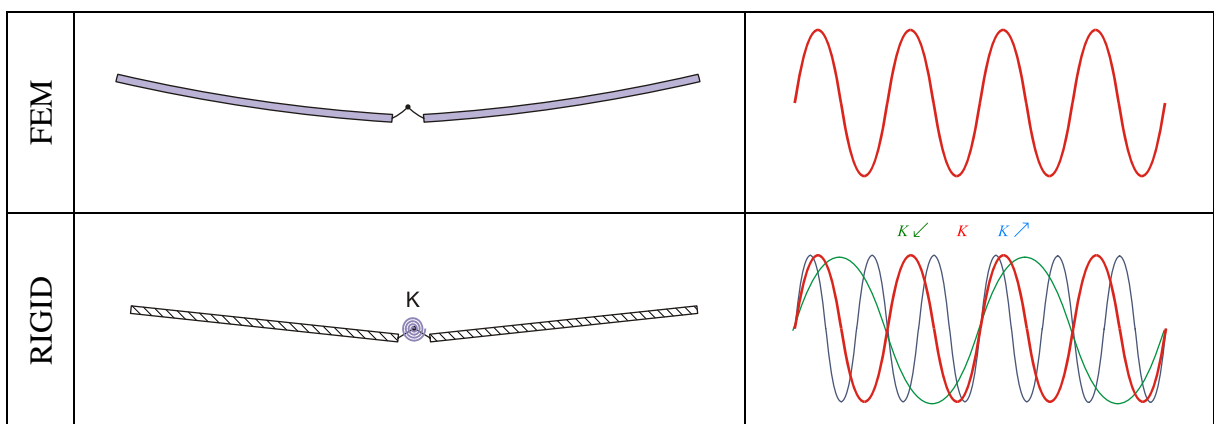


Figure 2.2.8-1: Latch-up spring tuning

The strong approximation behind this method is evident. We simplify a structure with a very high number of DOF (FEM model) by one with only one DOF. Anyway, as we will show in further chapters comparing the results of the rigid model with the flexible ones, this approximation is really good for estimating the latch-up torque.

Beside this, the use of the spring let us also to introduce experimental data on the hinge stiffness in our model as outlined in Figure 2.2.8-2.

We can in fact obtain the stiffness of structure (no hinges) by the same tuning process with the only difference of substituting the BEAM elements that represent the hinges arms in the FEM model by rigid elements (RBE2). In such a way in fact the hinges will not contribute to the structural stiffness.

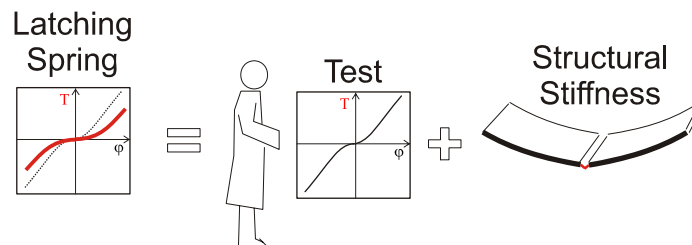


Figure 2.2.8-2: Latching spring contributions

The equation below is then used to calculate the total stiffness and introduce the experimental law inside the model. The resulting stiffness yields an augmented rotation in the latching spring as shown in Figure 2.2.8-2 (the red line of the T vs φ chart).

$$K_{TOT} \cong \left(\frac{1}{K_{STRUCT}} + \frac{1}{K_{HINGES}} \right)^{-1} \quad (2.7)$$

For a better comprehension of the tuning process please refer to Appendix A.

2.3 Applied Examples

In the following paragraph we will show two examples of rigid modelling.

- BEPI COLOMBO Mercury Polar Orbiter (MPO) solar array
- AMOS-3 solar array
 - In orbit model
 - On ground model

We have chosen these two examples because they cover the major part of applied solutions. More complex solar arrays (with more panels) can be easily obtained from this two models (see Chapter 5). The results of the rigid dynamic analysis will be reported in Chapter 4 and directly compared with the relative results obtained from the flexible analysis.

2.3.1 BEPI COLOMBO MPO solar array – Rigid model

The model consist of 3 rigid bodies, the space craft, the yoke with integrated inboard panel and the out-board panel. The in-board and out-board panel are connected by hinges like a double hinged door. The hinge (one revolute joint) between the SC and in-board panel represent the Solar Array Drive Mechanism (SADM).

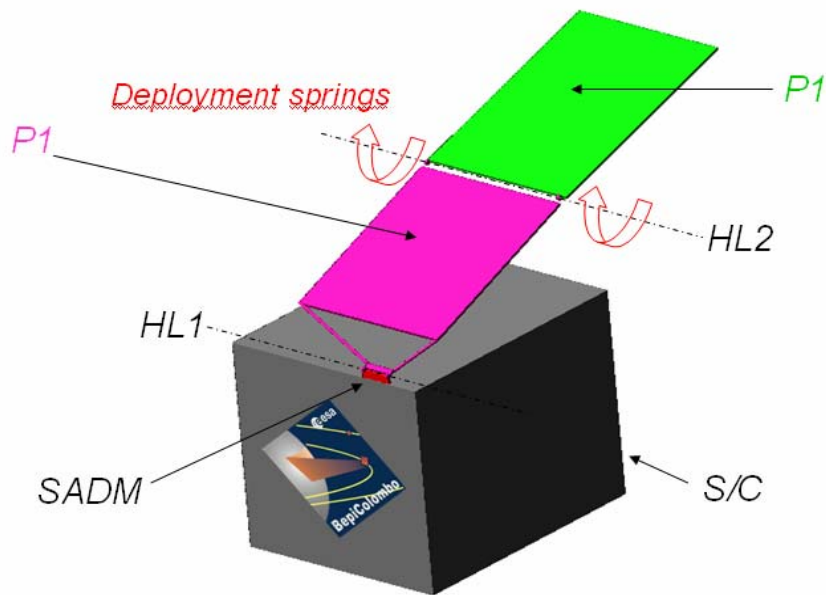


Figure 2.3.1-1: BEPI COLOMBO MPO solar array

The deployment motion is driven by deployment spring elements in HL2. There are two further rotational springs in HL2, one represents the harness torque and the second one represents the latch-up stiffness. The latter spring is deactivated during the deployment process and is activated when the latch-up occurs.

After release of the hold-down mechanisms the out-board panel jumps out and starts with the spring driven deployment. The latch-up occurs at a deployment angle of 180° .

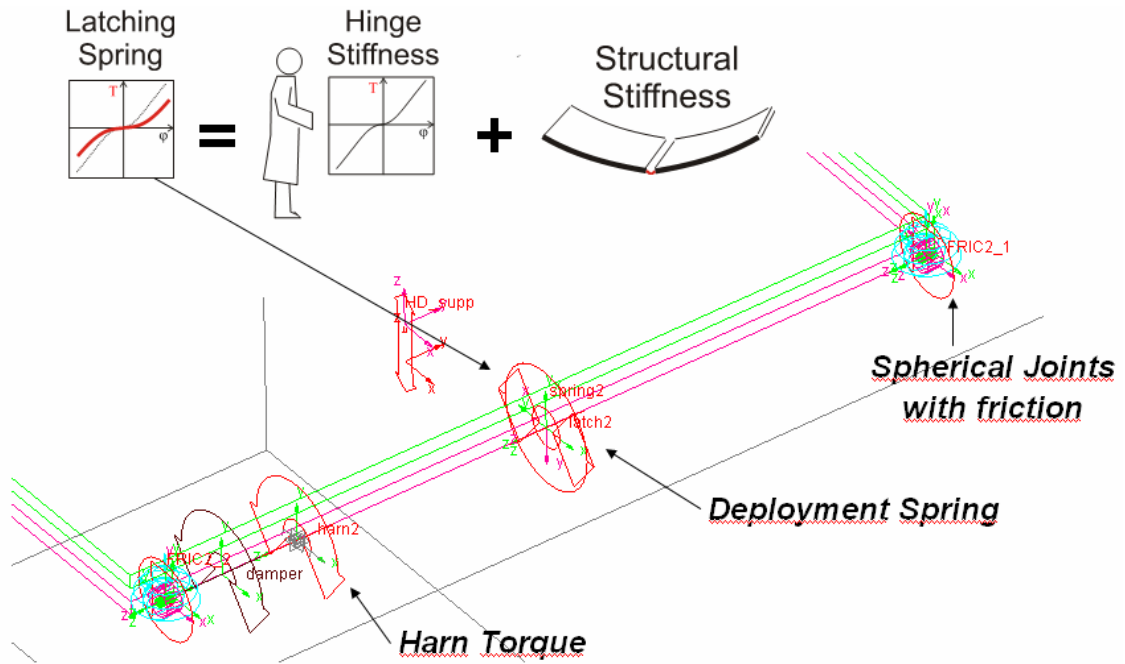


Figure 2.3.1-2: ADAMS rigid model elements

As outlined in Figure 2.3.1-2, in the case of BEPI COLOMBO MPO we have experimental data for hinges on HL2 to be included in the latching spring stiffness. The same picture shows also a damper that is used only in the torque margin analysis to dissipate kinetic energy and to establish a quasi-static deployment.

The SADM will be not powered during the spring driven deployment of the SA. It is assumed that the motor-gear unit produces a constant holding torque in the non powered mode that is modelled as a friction preload torque on the revolute joint between in-board panel and the S/C. An increase of this resistive torque (generated for example by an activated SADM during the deployment) would cause an impact between the in-board panel and the S/C. This case will be treated in Chapter 6.

The sequence of pictures in Figure 2.3.1-3 shows the deployment of the solar array for the dynamic analysis (hot-case condition).

After time 6.24 s the deployment phase is terminated and the SADM will set the array in the working position. This motorized phase is quite slow and has not interest from a dynamic point of view.

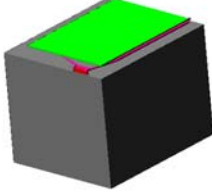
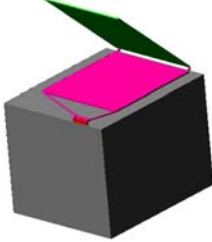
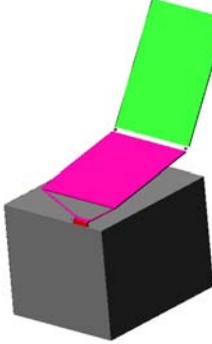
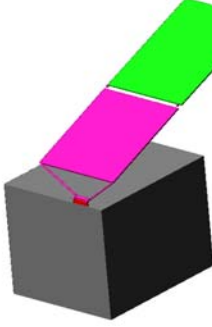
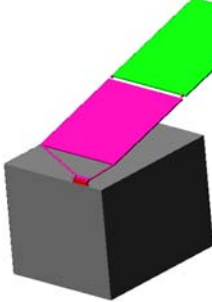
<p>Stowed Configuration (t = 0.0 s)</p>	
<p>After Release – Free Deployment (t = 2.8 s)</p>	
<p>Free Deployment Continue (t = 4.0 s)</p>	
<p>Latch-up HL2 (t = 4.24 s)</p>	
<p>Free Deployment end (t = 6.24 s)</p>	

Figure 2.3.1-3: BEPI COLOMBO MPO s/a deployment sequence

2.3.2 AMOS-3 solar array – Rigid model

2.3.2.1 In orbit model

The total model consists of 4 rigid bodies, one for the SADM, one for the yoke and one for each panel. The SADM body is fixed to the S/C, which represents the ground of the simulation model. SADM, yoke and the two panels are connected by hinges like a double hinged door.

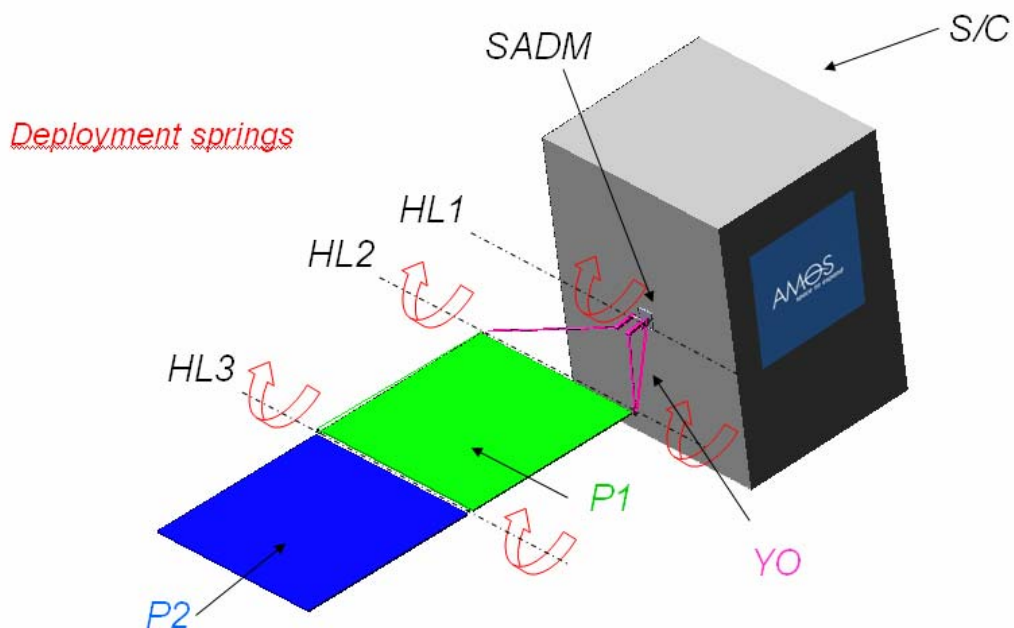


Figure 2.3.2-1: AMOS-3 solar array (in-orbit)

The deployment motion is driven by deployment spring elements in HL1, 2 and 3. The rotation in HL1 is damped by an Eddy Current damper element.

There are two further springs in each hinge-line, one represents the harness torque and the second one represents the latch-up device with a representative locking stiffness.

The latter spring is deactivated during the deployment process and is activated when the latch-up occurs in the related hinge-line.

Non-linear torque / force elements apply the synchronization torque at the bodies, and account for the forces resulting from the CCL cables.

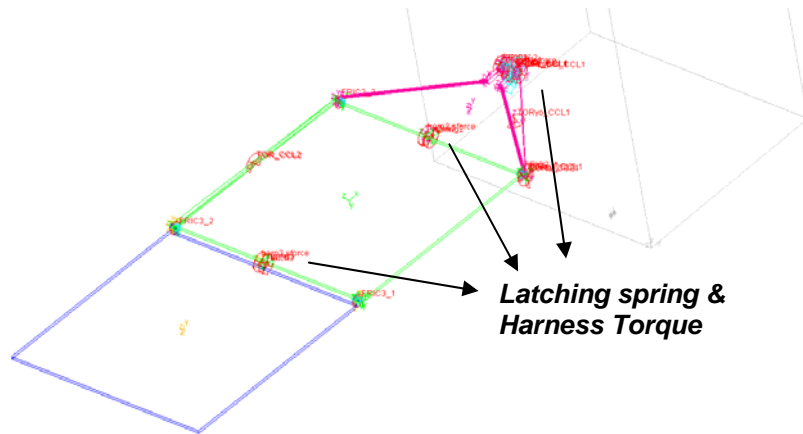


Figure 2.3.2-2: ADAMS rigid model

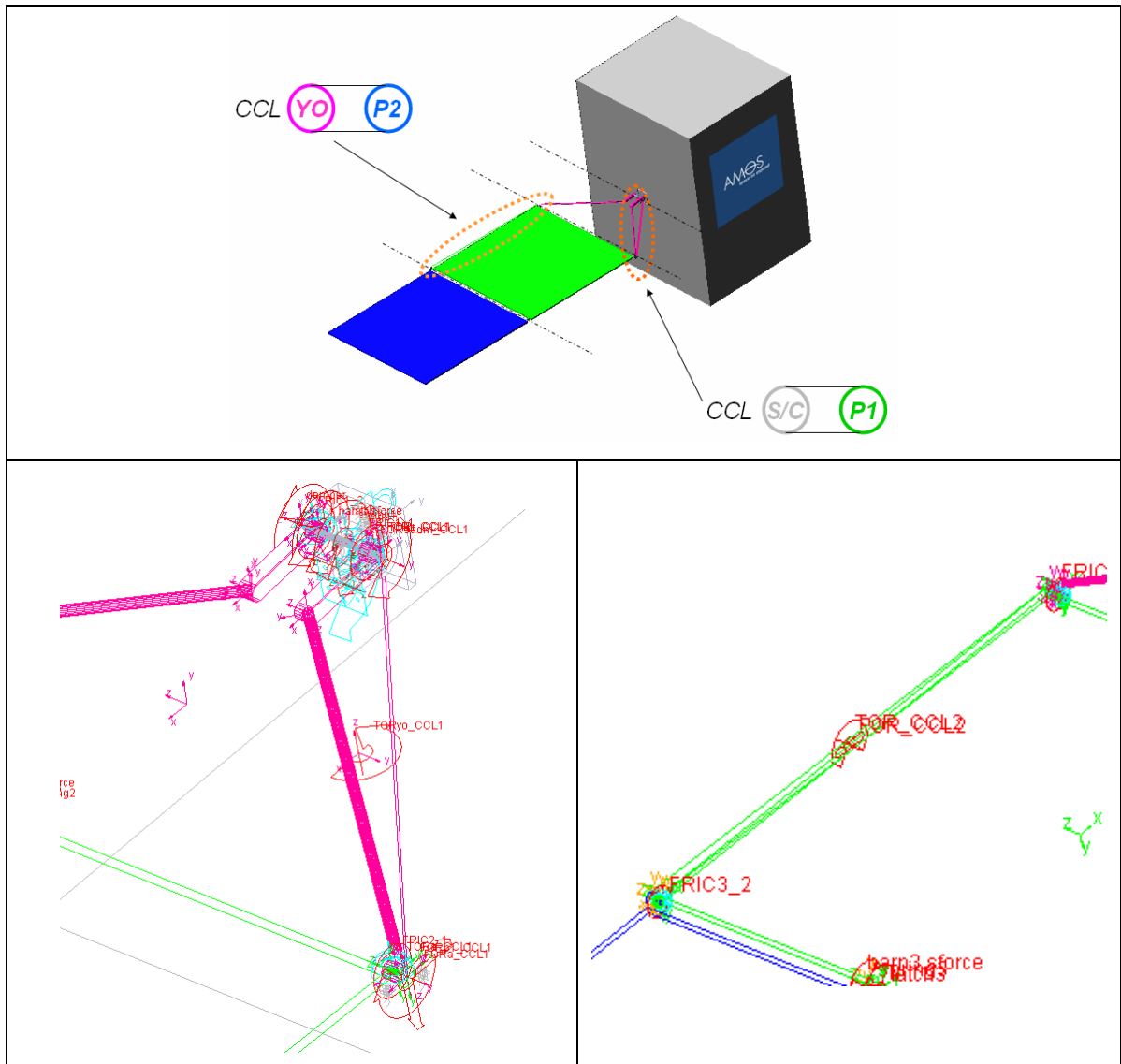


Figure 2.3.2-3: AMOS-3 CCL mechanism

Figure 2.3.2-3 shows the CCL system in AMOS-3 solar array. The lines that appear in the ADAMS rigid model are just geometrical lines used to graphically represent the two CCL's ; as we have seen in Figure 2.2.5-4 the CCL's are represented in the model using the resulting forces and torques. The inertial properties of pulleys are included in the body to which they are linked to.

For what concern the latch-up stiffness in AMOS-3 case we have no experimental data. That means that this time for the tuning of the latching spring we will use the FEM mesh without substituting any rigid element. In other word the stiffness of the hinges arms will coincide with the stiffness of the BEAM elements used to model them inside the FEM model (see paragraph 2.2.8).

Figure 2.3.2-4 shows a sequence of the deployment. Notice the effect of the CCL system in the rotation synchronization of the three bodies.

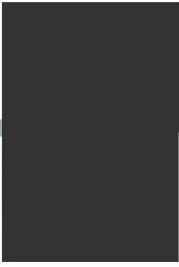
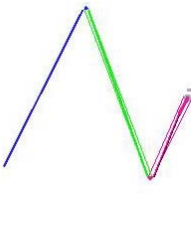
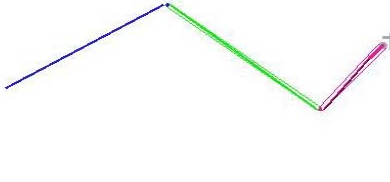
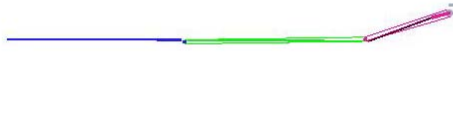
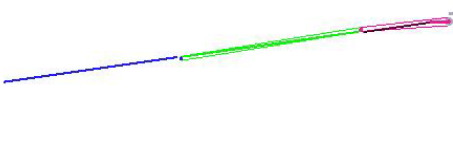
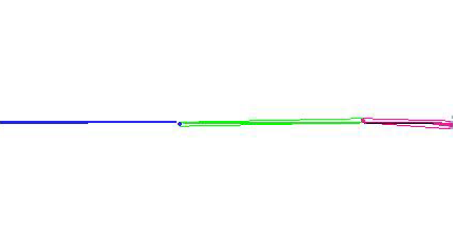
<p>Stowed Configuration (t = 0.0s)</p>	
<p>After Release – Free Deployment (t = 4.0 s)</p>	
<p>Free Deployment Continue (t = 6.0 s)</p>	
<p>Latch-up HL3 (t = 7.4 s)</p>	
<p>Latch-up HL2 (t = 8.5 s)</p>	
<p>Latch-up HL1 (t = 11.6s) Fully Deployed Configuration</p>	

Figure 2.3.2-4: AMOS-3 deployment sequence

2.3.2.2 On ground model

The following model describes the solar array with the on-ground test rig.

The model as shown in Figure 2.3.2-5 is the same used for the in orbit model with the addition of the supporting structure which is necessary to support the solar array on ground and unload the hinges from the 1g effect.

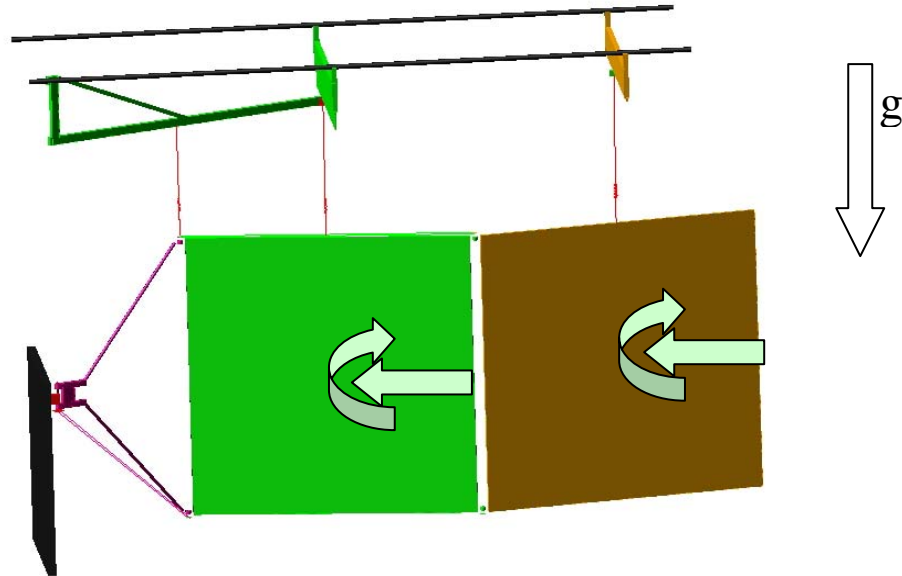


Figure 2.3.2-5: AMOS-3 on-ground model

The other difference introduced in the on-ground model is the presence of aerodynamic forces and torques for considering the air resistive effect as shown in Figure 2.3.2-5.

The inertia properties of the brackets that connect the panels to the supporting springs are included in the panels.

The reasons that justify the study of this model beyond the in orbit one will be clarify in next chapter.

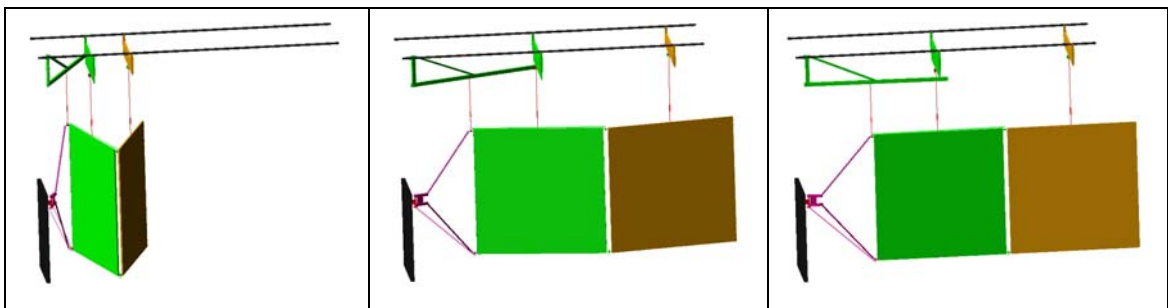


Figure 2.3.2-6: AMOS-3 on ground deployment

Chapter 3

The Flexible Model

3.1 Introduction to the flexible model

As we have seen in Chapter 2 the rigid model is the first step to study and understand the dynamics of a solar array deployment. Using this model one can easily monitor the behaviour of all the different variables and minimize the potential energy stored in the deployment springs in order to guarantee that the deployment springs are able to overcome the resistive torque with sufficient margin of safety.

Anyway a rigid model can be just a first step for the analysis of the solar array because of its conservativeness. When in fact we are interested in the dynamic loads a rigid approach can bring us to overestimate forces and torques and consequently to design structures stronger more than necessary.

The typical dynamic load is the torque due to the latch-up of two adjacent panels. If one neglects in this case the flexibility of the two panels, the latch-up torque would be overestimated. The shock to which the panel is subjected in reality will be less.

The introduction of the condensed stiffness allows us to use the rigid model also for a reliable estimation of the latch-up torque. Anyway this method was based on strong approximations; we took in consideration only the first bending mode of the structure to calculate its relative stiffness neglecting all the other higher frequency modes. The legitimacy of this choice will be proven in this chapter.

Another important difference that the flexible model will introduce is the deformation of the parts that form the mechanism. However, this deficiency does not cause a great problem for a classical solar array structure. The stiffness of the structure and the magnitude of the loads involved usually make the deformations small and not able to compromise the right working of the mechanism.

In this chapter all the rigid parts of the structure will be substituted by corresponding flexible ones and the resulting flexible model will be compared with the previous one. Two kinds of flexible models will be discussed. One is a *full-flexible* model, the other is a *semi-flexible* model.

The rigid model had two scenarios to investigate, one when the dynamic behaviour is critical (hot case) and the other when the resistive torque is critical (cold case).

The principal interest of the flexible approach will be to get a better description of the dynamics, and therefore this chapter focuses on the dynamic load aspect also in the two application examples at the end.

The results of the analyses will be shown and compared with those obtained by the rigid model in Chapter 4.

3.1.1 Full-Flexible model

This model is composed by completely flexible bodies (hinges arms and panels). The advantages of such a solution is that the user has just to substitute the rigid parts by the corresponding flexible elements without taking care of the latching torque springs. In fact, in this model we don't need these springs anymore since we can assume that all the flexible properties of the hinges are already stored in the flexible bodies. The latching springs in the rigid ADAMS model have to be substituted by fix joints (or equivalently we can fix the rotational DOF of the revolute joints by ADAMS MOTION elements,

see § 3.3.5) and the latching torque is represented by the reaction torque in the hinge joints.

The negative aspect of this solution is that usually the stiffness of the hinges is not the same of the beam elements that are used to represent them in the FEM model.

If we know the hinges stiffness from, for example, experimental data, we need another approach to insert this stiffness inside the model.

3.1.2 Semi-flexible model

This model is derived from a modified FEM with rigid members instead of the beam elements representing the hinges. In practice this model allows to insert the stiffness of the hinges as a rotational spring with an external function as we saw in Chapter 2 for the augmented rotation (§ 2.2.8).

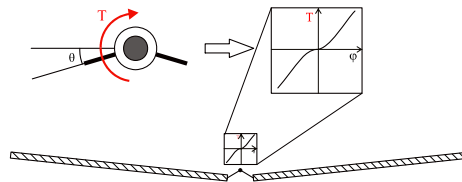


Figure 3.1.2-1: Latch-up spring obtained from data test

The only thing that we have to do is modify the latching torque using the function obtained by experimental tests. We don't have this time to correct its value because the stiffness of the panels are inside the model (the panels are flexible).

3.2 Generation of Flexible bodies

The flexible parts will be generated using the NASTRAN – ADAMS interface of NASTRAN.

All the information (model stiffness, mass and loads matrixes, nodes location, mass invariants) are stored in one single file for each flexible body created, a Modal Neutral File (MNF). For the theory behind this interface one can refer to Chapter 1.

For what concern the generation of the MNF file and how to import them in ADAMS please refer to the Appendixes 2 and 4.

The three fundamental aspects that have to be taken in consideration during the generation of a flexible body are

1. The definition of the Attachment Points and their DOF
2. The choice of the number of dynamic modes (fix-interface normal modes)
3. Generation of PLOTEL elements grid

While the meaning of the first two points is clear from Chapter 1 point 3 introduces a new aspect that will be further explained in paragraph 3.2.3.

It is clear that the bigger the number of fix-interface modes and of APs' DOF is the better is the approximation of the behaviour of the flexible body.

On the other hand, if we increase the number of modes that describe the body, we increase the dimensions of the several matrixes involved in the solution of the problem and so the complexity of the numerical resolution.

From there, we look for a method that lets us to catch the essence of the flexible body using a minimum number of modes.

The number of modes will depend on the objective of our analysis. If we are interested in a frequency-response analysis or in a latching torque evaluation it's clear that we will have to consider different numbers of modes.

The default number of fix-interface modes to pass to ADAMS in the NASTRAN-ADAMS interface is 26 while, regarding the DOF of the APs, the MSC advice is to consider all the 6 DOFs in a 3D problem.

$$N_{\text{modes}} = N_{\text{fix-interface}} + \sum_i n_{\text{DOF}_i} \cdot AP_i \longrightarrow N_{\text{modes}} = 26 + \sum_i 6 \cdot AP_i$$

This number of modes doesn't rise a problem when we deal with a single flexible body in a rigid environment; but when we have to deal with a bigger number of flexible bodies interacting each other, this yields a heavy numerical burden with a high number of DOF, many of which are useless for a dynamic analysis.

3.2.1 Definition of Attachment Points and of their DOF

As we have seen in the first chapter the definition of the Attachment Points (AP) is of essential importance for capturing the effect of attachments on the flexible body. Their definition is quite intuitive; one has to define an AP in every node of the body that is in contact with other bodies, subjected to forces or displacements (for this reason an AP is also called *interface* or *boundary* node) and for each AP selected the whole set of relative DOF should be used. If we not consider all these 6 DOF, and so all the constraint modes related to an AP, it has the effect of additional constraints in the model and consequently, this may lead to converge and locking problems in the dynamic analysis.

In our model this rule has always to be applied for the hinge nodes. However, an exception can be made for the forces when we are not interested in their local effects. If we don't need a good resolution of the zone where the load is applied and if we are interested only to its global effect we can avoid to define an AP and apply the load directly on the simple node.

The aerodynamic loads on AMOS-3 on-ground models are an example of such a case; we are interested only in the global effects of these loads and we can apply them in the node closest to the centre of mass. Another example is shown in Figure 3.2.1-1. This time too we don't need to know the local effect of the concentrated torque on the yoke (also because in reality is generated by two forces from the pulleys that bend the cable) but we want to take into account its global effect (on the frictions for example) by applying the torque to a simple node of the yoke.

On the other hand, in case of an impact analysis (see Chapter 6) we are interested in a better local description and so we will define the node located on the impact point as an AP.

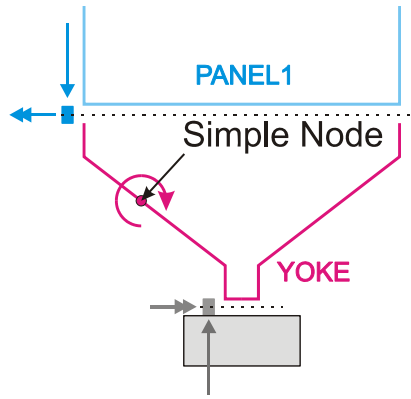


Figure 3.2.1-1: Example of load applied on a simple node

When we define the APs for a semi-flexible model we have to pay attention to how we define the RBE2 elements that make the hinges rigid. As shown in second part of Figure 3.2.1-2 the AP node has always to be the independent node of an RBE2 element otherwise we get an error during the generation of the MNF file.

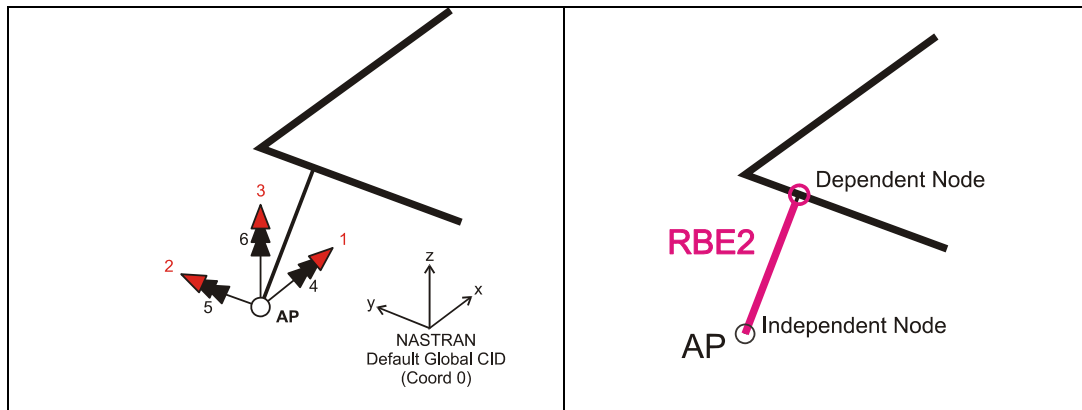


Figure 3.2.1-2: Attachment point definition

For the same reason we can't put more than one AP on the rigid part of a structure. Figure 3.2.1-3 shows the rigid part of a yoke. Only the AP shown in the figure is possible, the other nodes are dependent.

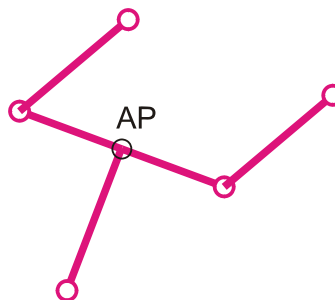


Figure 3.2.1-3: Attachment point in a rigid structure

3.2.2 Fix-interface normal modes

To show the influence of the number of modes on the latching torque we can create a simple workbench in ADAMS to test the response of different panels characterized by different numbers of fix-interface normal modes.

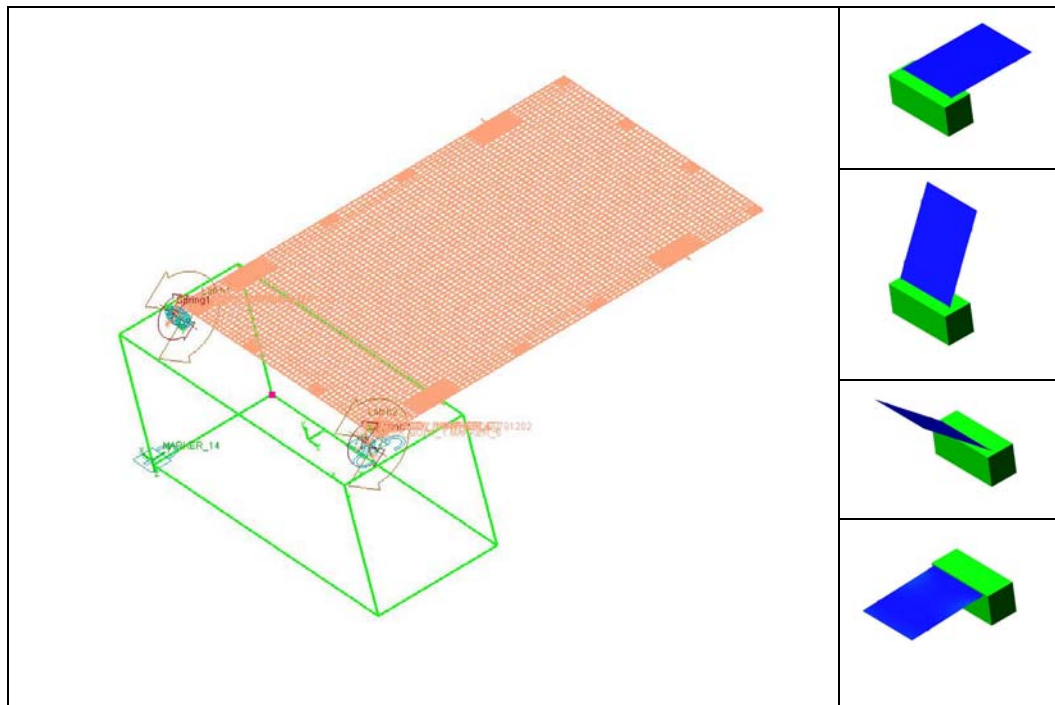


Figure 3.2.2-1: Latch-up torque workbench

The model shown in Figure 3.2.2-1 represents the deployment of 180° of a simple panel. The deployment springs used are comparable with the ones commonly used in a solar array. We have used for this analysis 7 different panels as shown in Table 3-1.

FLEX PANEL MODEL	Number of Modes
2 AP (all DOF) + 2 Fix-interface modes	8 flex modes + 6 rigid modes
2 AP (all DOF) + 3 Fix-interface modes	9 flex modes + 6 rigid modes
2 AP (all DOF) + 4 Fix-interface modes	10 flex modes + 6 rigid modes
2 AP (all DOF) + 5 Fix-interface modes	11 flex modes + 6 rigid modes
2 AP (all DOF) + 10 Fix-interface modes	16 flex modes + 6 rigid modes
2 AP (all DOF) + 20 Fix-interface modes	26 flex modes + 6 rigid modes
2 AP (all DOF) + 30 Fix-interface modes	36 flex modes + 6 rigid modes

Table 3-1: Panels used in the comparison

The latching torque is retrieved from the reaction torque of the fix hinge that takes the place of the revolution joint after the latching.

If we plot the different results obtained for this joint reaction using different panels we obtain the chart of Figure 3.2.2-2

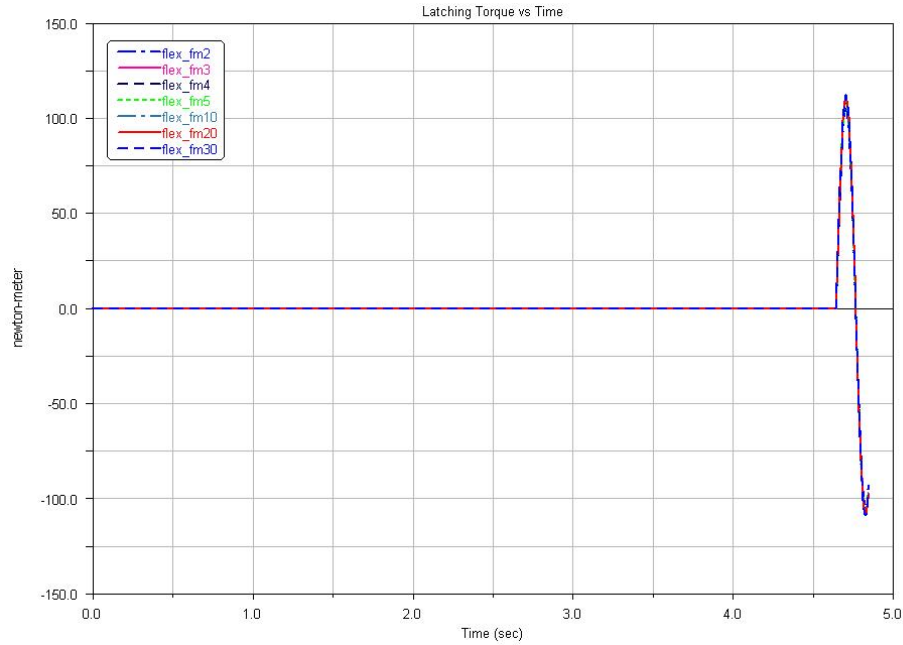


Figure 3.2.2-2: Latch-up reaction torque

All the solutions are very close together. This clearly means that the latching torque is mainly covered by the first flexible modes of the flexible bodies. If we zoom in the zone of the maximum we obtain the chart shown in Figure 3.2.2-3.

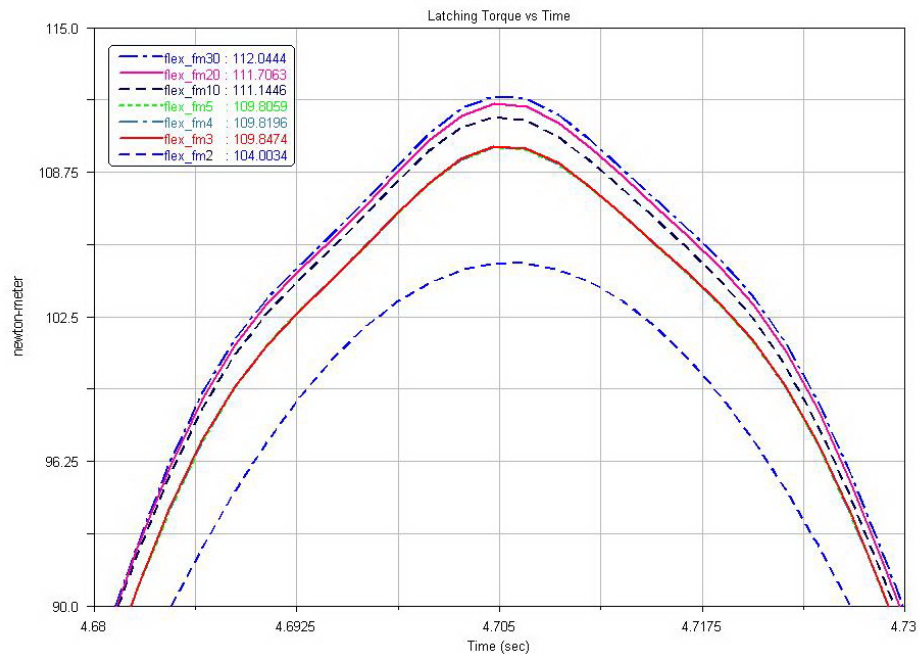


Figure 3.2.2-3: Latch-up torque maximum close-up

The chart of Figure 3.2.2-3 shows that using only 2 fix-interface modes we obtain a solution with an error of about the 6% of the 30 fix-interface modes solution and that this error decreases under the 1% using 10 fix-interface modes. Another interesting analysis has been done with this set of panels by comparing a linear modal analysis in NASTRAN (no modal reduction – Lanczos extraction method) with an equivalent one in ADAMS (with modal reduction – CB modified method). Table 3-2 shows the comparison between *free-free* modal analyses.

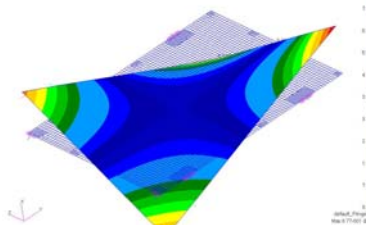
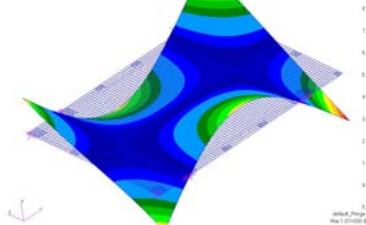
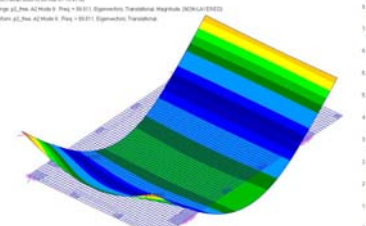
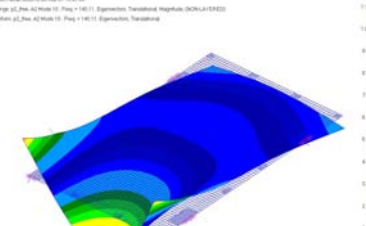
	NASTRAN 50 modes	2 fix-int modes	3 fix-int modes	4 fix-int modes	5 fix-int modes	10 fix-int modes	20 fix-int modes	30 fix-int modes
1	-	-	-	-	-	-	-	-
2	R	I	G	I	D	-	-	-
3	-	-	-	-	-	-	-	-
4	-	-	-	M	O	D	E	S
5	-	-	-	-	-	-	-	-
6	-	-	-	-	-	-	-	-
7	12.91139	12.98702	12.98702	12.91614	12.91577	12.91187	12.91143	12.91141
8	89.67096	261.2859	99.03446	92.81318	91.71484	89.85175	89.68369	89.67787
9	89.81052	262.8423	262.8423	99.03446	99.03446	89.93391	89.83246	89.81470
10	140.1103	487.9353	425.2162	425.2162	397.1317	140.6669	140.1983	140.1274
11	158.4317	1021.951	626.5447	626.5447	425.2162	158.4347	158.4319	158.4318
12	193.6772	1758.566	1021.951	652.3099	626.5447	194.8922	193.8207	193.7030
13	217.7992	3376.774	1774.167	1074.211	705.7159	222.2132	217.9624	217.8985
14	241.6165	5160.212	3376.774	1774.167	1124.669	249.2651	241.7493	241.6384
15	291.7085		5174.918	3863.741	1774.167	416.0325	291.9003	291.7401
16	334.2977			5174.918	3910.721	831.8419	342.5514	335.0040
17	343.5419				5174.918	1086.953	354.8986	343.7928
18	378.0834					1232.466	378.6522	378.1548
19	394.9094					1234.342	395.6719	395.0163
20	418.1989					3917.713	418.4501	418.2947
21	433.5092					4943.677	498.3786	434.7848
22	502.4376					6214.290	502.5256	502.4433
23	502.5098	7					506.5185	502.5122
24	520.9161						709.1509	520.9482
25	567.3090						710.0027	567.7160
26	575.9814						879.4793	577.6417
27	612.0406						1533.661	612.1559
28	653.6310						1707.959	660.8406
29	670.3247						1935.823	670.9120
30	741.9323						6474.952	742.2226
31	774.0734						8759.484	774.1385
32	788.4421						10511.58	788.5526
33	819.2414							845.8192
34	849.7916	9						894.5002
35	874.9873							1107.723
36	884.2588							1319.852
37	912.0236							2164.983
38	943.7952							2321.385
39	964.1910							2855.979
40	966.8573							6665.197
41	1002.112							13572.50
42	1073.715							13728.60
43	1085.869							
44	1094.571							

Table 3-2: Free body modes comparison

The second analysis, Table 3-3, shows the results obtained if we fix the two hinges of the panel (the 2 APs). Because of the fact that we fix the APs the results that we obtain in ADAMS are the same that we observe in NASTRAN (the fix-interface modes are in fact obtained fixing the DOF of the APs).

	NASTRAN 50 modes	2 fix-int modes	3 fix-int modes	4 fix-int modes	5 fix-int modes	10 fix-int modes	20 fix-int modes	30 fix-int modes
1	4.103071	4.103071	4.103071	4.103071	4.103070	4.103070	4.103071	4.103071
2	9.523196	9.523195	9.523196	9.523197	9.523195	9.523195	9.523195	9.523197
3	54.19069		54.19068	54.19068	54.19068	54.19070	54.19070	54.19070
4	69.25148			69.25147	69.25147	69.25148	69.25146	69.25147
5	97.80708				97.80714	97.80715	97.80714	97.80715
6	121.5842					121.5842	121.5842	121.5842
7	158.4196					158.4196	158.4196	158.4196
8	182.4240					182.4240	182.4240	182.4240
9	185.9918					185.9918	185.9918	185.9918
10	234.9154					234.9154	234.9154	234.9154
11	266.3860						266.3862	266.3862
12	287.8708						287.8716	287.8717
13	289.5280						289.5281	289.5281
14	322.2658						322.2658	322.2658
15	370.9318	1					370.9318	370.9318
16	396.3294	2					396.3294	396.3294
17	414.6130						414.6130	414.6130
18	502.5464						502.5466	502.5466
19	503.0186						503.0186	503.0186
20	513.7064						513.7104	5137.105
21	525.2734							525.2762
22	534.3716							534.3735
23	565.7713							565.7714
24	612.5683							612.5686
25	671.0543							671.0544
26	739.8488	3						739.8636
27	754.5557	4						754.5690
28	771.8421							771.8623
29	777.1147							777.1183
30	798.4374							798.4492
31	850.3492							
32	899.0864							
33	944.2161							
34	963.4950							
35	964.4594							
36	973.8625							

Table 3-3: Fix-interface modes comparison

One can conclude from the comparisons that for a good representation of the flexible properties 10 fix-interface modes are a good compromise between results (latching torque) and computational costs.

The same analysis can also be applied to the semi-flexible model. For the entity of the latching spring stiffness we can use a tuned value to get similar torque magnitude as with the pure flexible case.

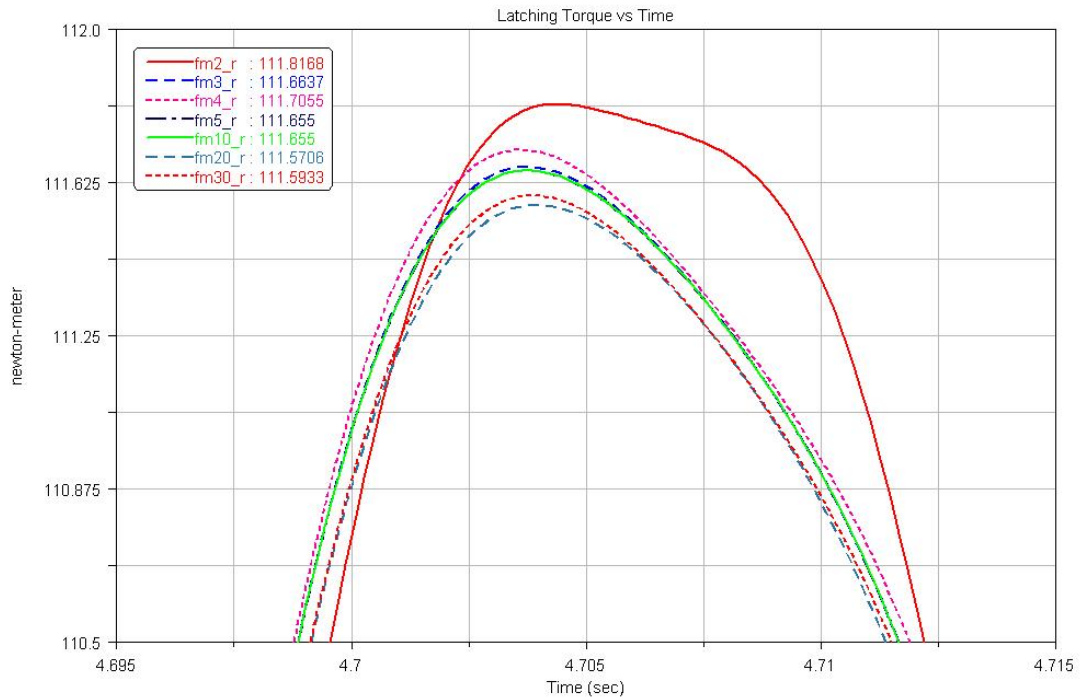


Figure 3.2.2-4: Latching torque for a semi-flexible model

In the case of the semi-flexible model we see that the dependency of the latching torque with the number of fix-internal modes decreases significantly (Figure 3.2.2-4).

A number of 5 fix-interface modes are sufficient for the semi-flexible model.

At the end we can summarize all the choices to take in the following table

	PURE – FLEXIBLE MODEL	SEMI – FLEXIBLE MODEL
APs & their DOF	All the interface nodes of the flexible bodies with all the DOF of the nodes	All the interface nodes of the flexible bodies with all the DOF of the nodes
Fix-interface modes	From 10 on	From 5 on

3.2.3 PLOTEL element

The MNF file contains all the data related to mass and stiffness matrices but all the information about the elements of the model are lost during the translation. ADAMS need only the nodes and the properties connected to their DOF but not the elements.

The only thing that ADAMS uses is the mesh grid to visualize the flexible body as shown in Figure 3.2.3-1.

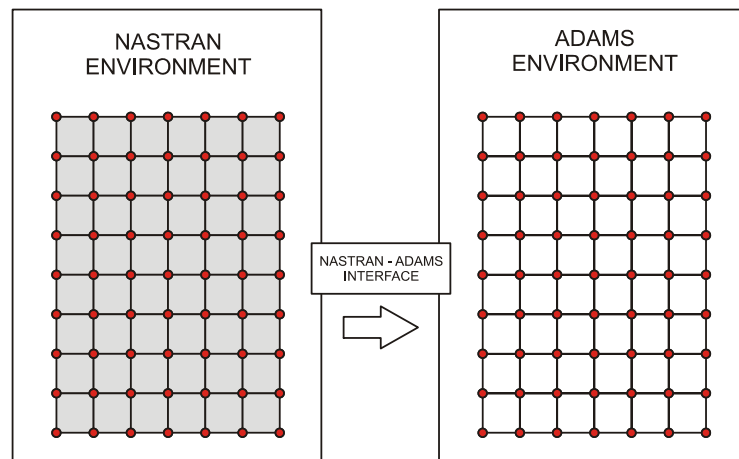


Figure 3.2.3-1: Mesh grid use for visualization purpose in ADAMS

For a flexible panel usually the mesh used in the FEM model is quite fine; this will be translated in a lot of faces for the graphical representation of the MNF file in ADAMS making at the same time the file heavy and difficult to handle by the software.

We can optimize the MNF file reducing the number of faces used for visualization defining a new grid in the FEM model using PLOTEL elements. A PLOTEL element is a dummy element and its only purpose is to visualize a node to node line.

Figure 3.2.3-2 shows what happens when we define a PLOTEL elements grid and we pass it to ADAMS.

Using 12 PLOTEL elements we are able to reduce the number of graphical faces in ADAMS from the original 48 to 4. As shown in the picture only 9 nodes will be visible in ADAMS environment but does not mean that the others are not considered. All the nodes with all their properties will be used for generating the MNF file but only the ones linked by PLOTEL elements will be visible. For this reason we have to take care to include all the nodes we need in the ADAMS model inside this grid.

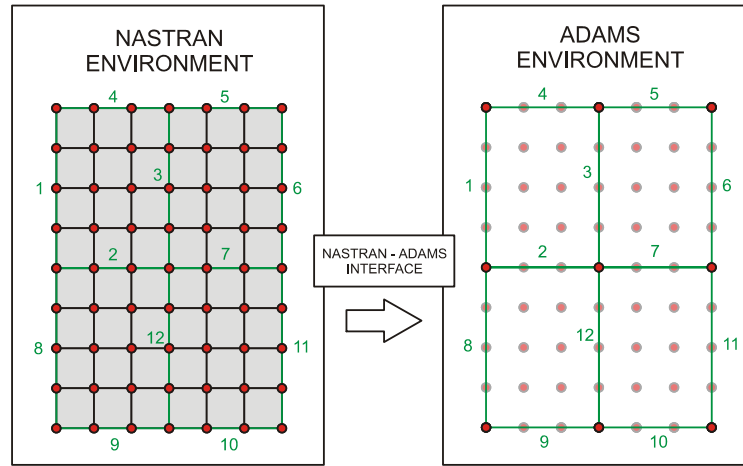


Figure 3.2.3-2: PLOTTEL elements grid used for visualization in ADAMS

There is not a particular strategy for creating the PLOTTEL elements mesh. It is clear that if we create a fine mesh we will have a better graphical result and a better comprehension of the deformation shapes but we will pay this in terms of file size and computational time.

When defining the PLOTTEL lines one has to avoid the intersection between two or more PLOTTEL elements because this could generate misunderstanding. This situation is well explained in the example of Figure 3.2.3-3 about a saddle deformation.



<p>A square plane undergoes a saddle deformation.</p>		
<p> The intersection between two PLOTTEL elements generates a bad deformation shape. The saddle geometry is lost.</p>		
<p> If we avoid the intersection we obtain a better approximation of the deformation shape.</p>		

Figure 3.2.3-3: Correct use of PLOTTEL

It is clear that if we reduce the numbers of faces too much we will have a difficult visualization in ADAMS; for example if we exaggerate the reduction this could make modal shapes be difficult to understand and so on.

Even if the definition of the PLOTEL elements grid is possible in the PATRAN pre-processor environment for the right working of the interface we have to modify few strings of the BDF file generated before running NASTRAN. We have in fact to impose manually that the PLOTEL elements grid has to be used for visualization purpose in ADAMS.

For a more detailed tutorial about the PLOTEL elements generation please refer to Appendix B.

Figure 3.2.3-4 shows the mesh reduction adopted for the MNF file of AMOS-3 solar array panel 2. The reduced MNF file size is around 35 times smaller than the original one!

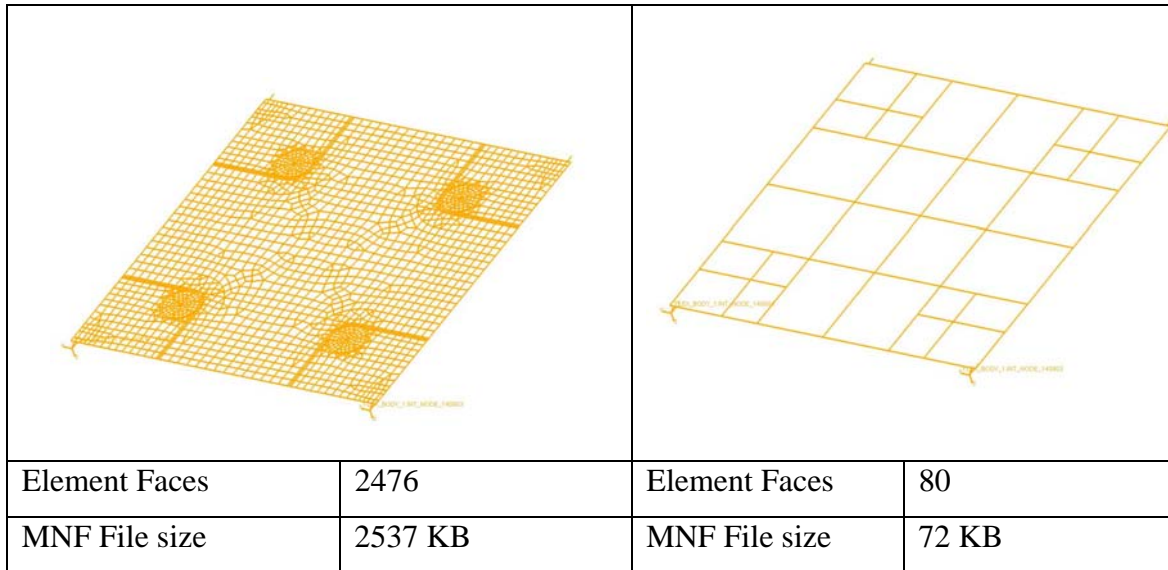


Figure 3.2.3-4: File size reduction due to the use of PLOTEL elements

3.3 ADAMS flexible model

Once we have run the NASTRAN-ADAMS interface we obtain a MNF file for every flexible bodies of our FEM model.

The next step at this point is to create a flexible dynamic model of the solar array deployment.

Since the first step in the design of a solar array deployment model is an ADAMS rigid model we can avoid to build a new model from the beginning and try to modify the rigid one such that the flexible bodies can be imported easily. For this purpose we can use a function in ADAMS/View that enables the user to replace a rigid body with is flexible representation (refer to Appendix D).

The principal changes to apply to the ADAMS rigid model are reported in the following list

- Split the forces and relocate them in their real application points
- Introducing auxiliary points
- Redefine markers dependencies
- Modify the kinds of hinges and friction
- Change from spring locking to kinematical locking (full-flexible only)
- Modify the ADAMS/solver script

3.3.1 Splitting forces and relocating them in their real application points

In a rigid model there is no need to place the forces in their real application points along the hinge line. One can simple put the global force due to the two deployment spring in just one torque applied along the hinge line.

In the case of a flexible model instead we have to ensure that all the forces act in their application points.

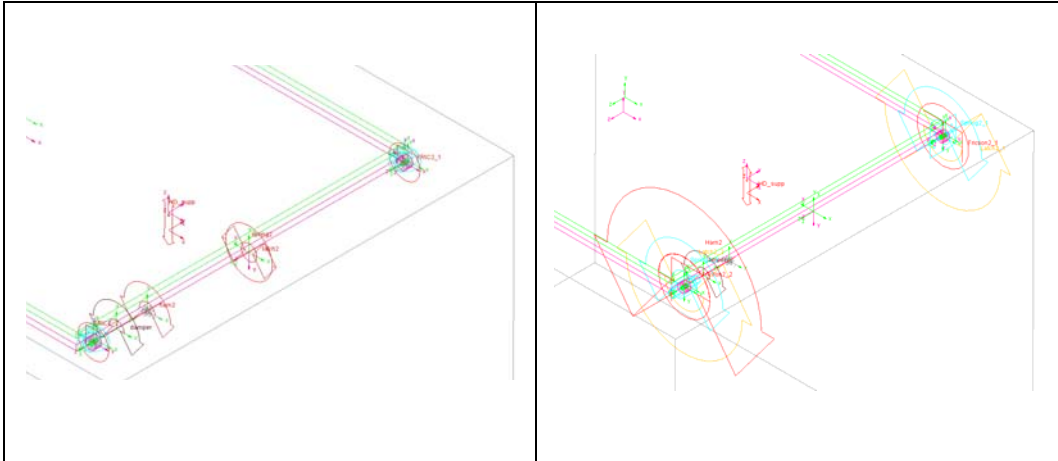


Figure 3.3.1-1: Example of force splitting in BEPI COLOMBO MPO rigid model

In Figure 3.3.1-1 shows hinge line 2 of BEPI COLOMBO MPO solar array before and after the splitting and relocation of the loads. Also the appearance of the forces is changed for a better comprehension and an easy selection.

3.3.2 Introducing auxiliary points

For the correct positioning of the flexible bodies during the import it is sometimes necessary to define some auxiliary points. As shown in Appendix D the rigid bodies are usually positioned using a three points method; we have always to ensure that each rigid and its equivalent flexible body have three points in common.

Figure 3.3.2-1 shows the case of a generic end panel of a solar array. In this case we have to create the reference marker 3 to allow the exact position of the flexible representation of the panel (in red).

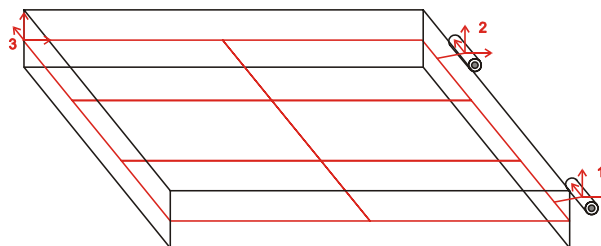


Figure 3.3.2-1: Generation of auxiliary reference points in the model

As will be remarked in Appendix D the right positioning of the flexible body is mandatory for the right end of the simulation. For this reason we have to guarantee that the rigid panel and the flexible one have exact the same reference points and especially the hinges points.

3.3.3 Redefining markers dependencies

Another important aspect to take into account is the dependency of some elements of the model with markers.

An example of these elements could be the sensor that feels the 180° deployment angle. In a rigid model such a sensor can be referred to each couple of markers on the hinge line. In a flexible model instead the sensor has to be referred to a couple of markers located on the hinge location. There are two reasons for this change:

1. Different points of the HL reach the 180° at different times
2. Only two markers located in a hinge keep their exact relative orientation during the deployment.

While the second reason represents really a problem (if the marker that define the sensor are not parallel the ADAMS simulation can failure) the former is not so important; in fact the difference of time in which usually two hinges reach the 180° is very small.

This fact allows an important simplification of the model.

We can impose a contemporary locking of the two hinges using only one sensor that feels just one of them.

An analogous check has to be made for force functions. We have to be sure that force functions refer to markers that are located on their application points. An easy way to do that is to refer always the force functions to the marker associated to the related forces (when a force is defined ADAMS creates automatically two associated markers, one on the action body and the other on the reaction one).

3.3.4 Modifying the kinds of hinges and friction

Spherical joints are used for hinges in the rigid body modelling. The reason of this approach was to reduce the number of redundant constraints of the model. In a flexible approach we can replace these joints with revolute and cylindrical joints obtaining a model closer to the reality.

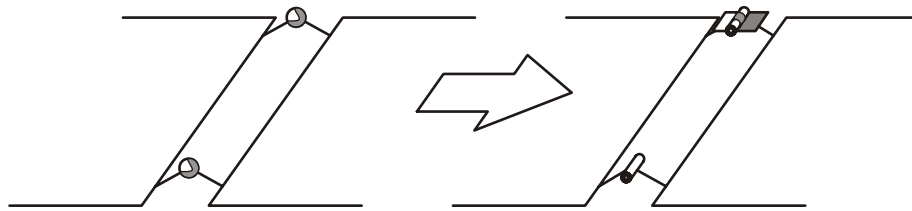


Figure 3.3.4-1: Modified joints in flexible model

Being close to reality is not the only reason that justifies this change in the model. Forces or sensors formulae often refer to angular rotation of markers located in the hinges. If we use spherical joints in a flexible body environment we can observe the behaviour shown in Figure 3.3.4-2. The markers of the two connected bodies are no more coplanar and if we try to calculate their mutual angular displacement ADAMS returns an error.

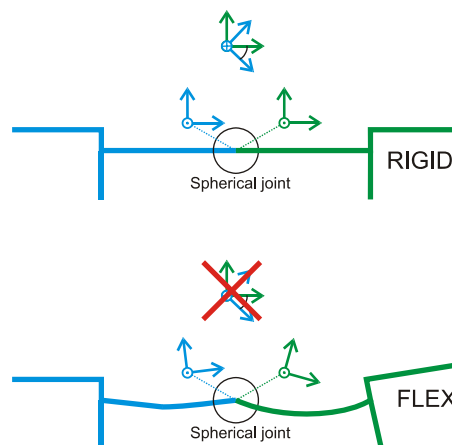


Figure 3.3.4-2: Loss of coplanarity in a flexible model with spherical hinges

The change of joint types implies also a change in friction properties of the hinges.

Figure 3.3.4-3 shows how the friction properties were modified to get comparable result between the two models for what concern the friction forces.

In a flexible model simulation a low value of the *stiction transition velocity* as the ones showed can create some converge problems in the corrector formula of the integrator. These problems usually happen in the very first instant of motion (when the model starts moving) and can be avoided by increasing the value of this velocity by one order of magnitude.

The resultant friction forces after these changes are close to the previous.

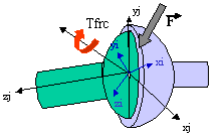
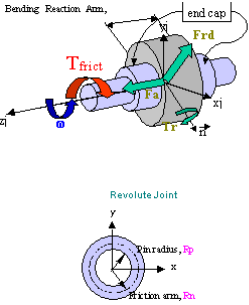
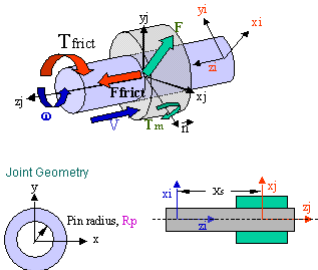
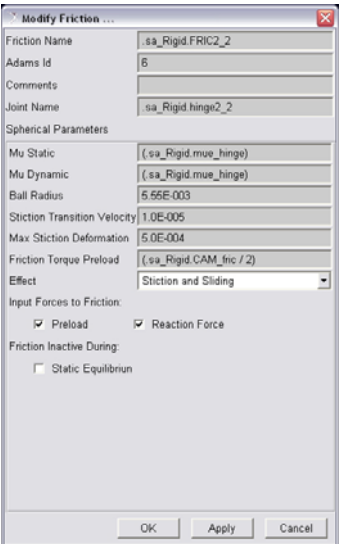
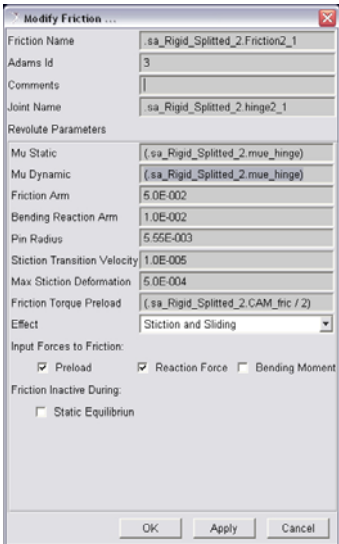
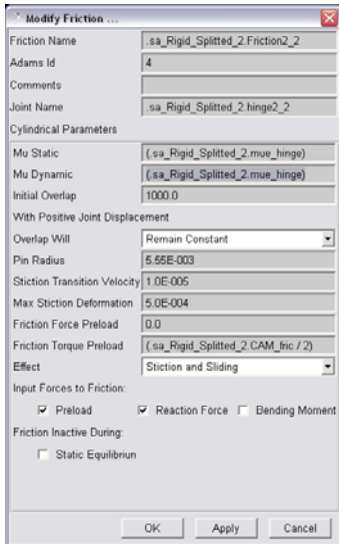
ADAMS spherical joint (Rigid model)	ADAMS revolute joint	ADAMS cylindrical joint
		
		

Figure 3.3.4-3: Equivalent friction properties for different kinds of joints

3.3.5 Introducing kinematical locking

In the rigid model we have seen that the locking of two panels is realized using latching spring. This solution is also appropriate for the semi-flexible model but is useless for the pure-flexible model where all the stiffness properties are inside the bodies.

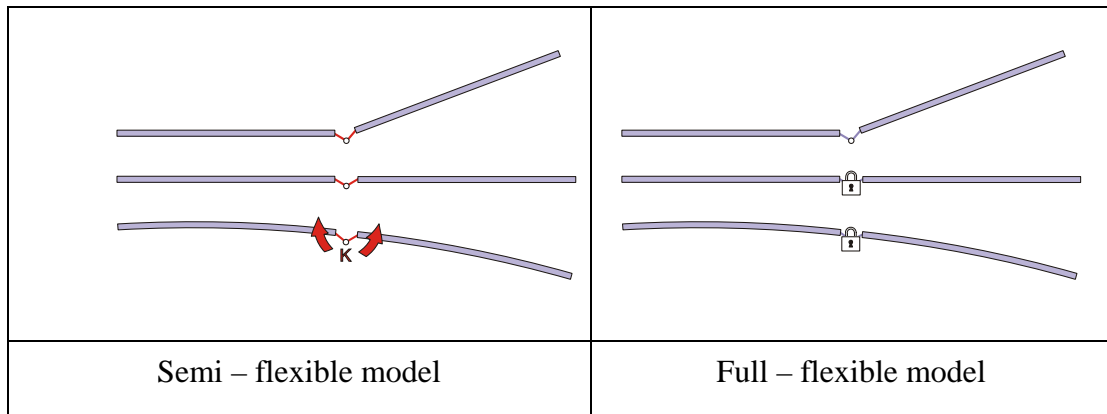


Figure 3.3.5-1: Latch-up mechanism in Semi-flexible and full-flexible model

A very rough approach could be to increase the stiffness of the latching springs to very high values but this may create numerical problems.

So the best way is to act on the relative rotations.

There are three different ways to fix the relative rotation of two bodies connected by the joints and they are shown in Figure 3.3.5-2.

The first one consists in two coincident joints, one revolute and one fix joint, coincident in the same hinge location. Before reaching the 180° the revolute joint is activated and the other is deactivated. After the 180° the activation is reversed and the fix joint starts working.

The deactivation of the revolute joint has however a negative aspect; the friction associated is deactivated as well. This doesn't influence the analysis because the role of friction has terminated after the locking, but some problems in the ADAMS postprocessor are generated. The user in fact is unable to plot the right trend of friction torque.

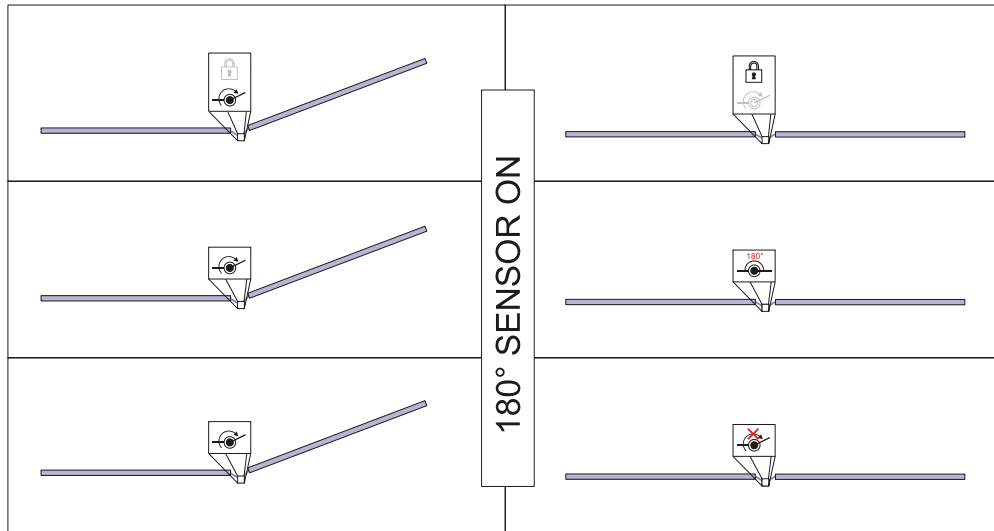


Figure 3.3.5-2: Different ways to fix the rotational DOF

One way to avoid this could be leave the revolute joint active but this would increase the number of redundant constraints of the model. For this reason is better to use one of the other alternative solutions proposed.

The other two solutions are quite similar. One fixes the angle of the revolute joint after the reaching of 180° , the other imposes a zero rotational speed after the locking.

Due to the fact that we decided to use just one sensor to feel the 180° deployment angle the solution that impose a zero rotational speed is recommended (we avoid a sudden rotation of the hinge not monitored by the sensor towards 180°).

For more details about the ADAMS solver scripts please refer to paragraph 3.4.2.5.

3.3.6 Modifying the ADAMS/solver script

An ADAMS rigid body simulation is usually controlled by a user written script. The commands are written in a particular language (e.g. ADAMS/solver language), that describes the behaviour of model elements within the course of the simulation. It is easy to divide the simulation in different phases, for example characterized by different time-step control, or activate/deactivate options of forces or other elements in the model.

The scripted control enables also the user to select a particular integrator for the equations of motion integrations. The default integrator, GSTIFF integrator, is the one used for the rigid model simulations. This kind of integrator will be maintained also in the flexible simulations.

The ADAMS/solver script used in the rigid simulation usually is not suitable for a flexible simulation.

Besides the fact that forces ID are changed (due to the splitting and movements) and new elements like locking devices are usually present when we pass to a flexible model we have also to reconsider the different time stages of the simulation.

According to Chapter 1 it is clear that the numerical problem behind the flexible model is more complex in comparison to rigid one. Besides the equations of motion, a system of non-linear coupled differential and algebraic equations due to large displacements and rotations during the deployment process, in a flexible model we have to deal with bodies deformations and their modal representation.

For these reasons a first point to correct is the entity of integrator time-steps. If we want to catch the effect of some high frequencies we have to decrease the integrator time-step.

We can use the example used for the fix-interface modes (refer to paragraph 3.2.2) to show the effect of different time steps on the latching torque.

Figure 3.3.6-1 shows the sensitivity of the latching torque due to variations of the HMAX integrator parameter. HMAX defines the maximum time-step that the integrator is allowed to take. There are no particular rules about how to choose the right value of HMAX. The best way is to make different attempts and take the bigger one that generates an accurate solution.

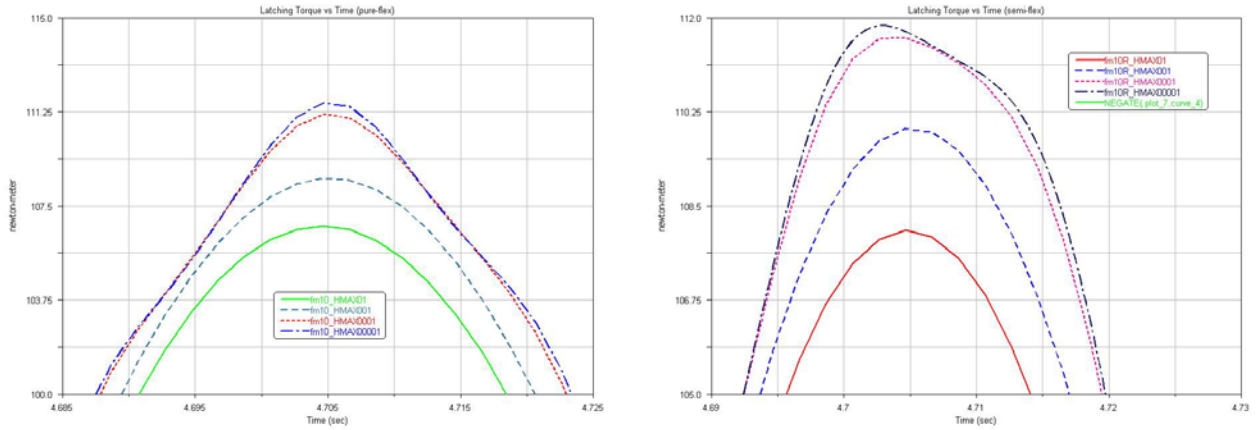


Figure 3.3.6-1: HMAX sensitiveness for full-flexible and semi-flexible model

Referring to the figure for example a good choice could be the solution *fm10_HMAX0001* generated by an $HMAX = 0.0001$.

It is always better not exceed in decreasing the time-step because the computational times increase rapidly and mostly we can encounter corrector failures at small step sizes. These occur because the Jacobian matrix is a function of the inverse of the step size and becomes ill-conditioned at small steps.

Another way to modify the integrator time-step could be increase the number of output-steps of the simulation. The output-step is the step that ADAMS use for plotting results and HMAX is always smaller or equal to it.

Anyway is not advisable to use output-step smaller than the one necessary to have a good graphical representation of results (the output files become uselessly big) so the best procedure is to fix the right step for the output and then tune the model with HMAX. Figure 3.3.6-2 shows the effects of different output-steps on the output.

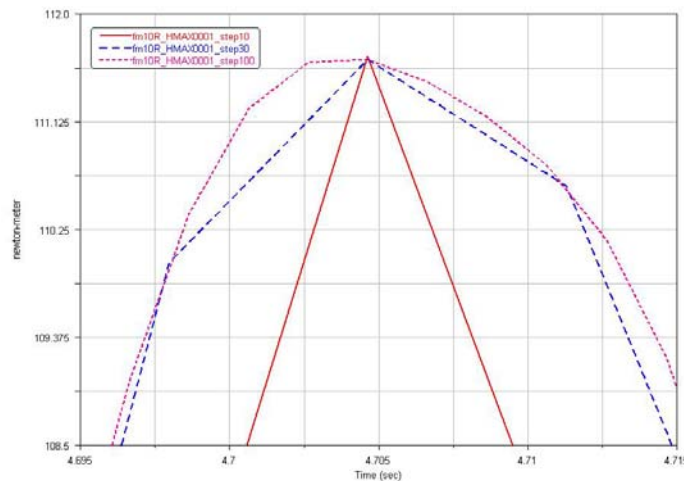


Figure 3.3.6-2: Effect of different output-step on the plot of results

3.4 Applied Exemples

In the following paragraph we will show two examples of flexible modelling

- BEPI COLOMBO Mercury Polar Orbiter (MPO) solar array
- AMOS-3 solar array
 - In orbit model
 - On ground model

The flexible model will be obtained from the related rigid model (refer to paragraph 2.3). The following paragraphs report a brief explanation of the changes between the two models. For more details about generation of flexible bodies or about how to import them in ADAMS environment please refer to Appendix A and D.

3.4.1 BEPI COLOMBO MPO solar array – semi-flexible model

As first application example of the ADAMS flexible model will be considered the BEPI COLOMBO MPO solar array.

As we have seen in Chapter 2 this solar array is composed by two panels and their deployment is driven by a system of deployment springs.

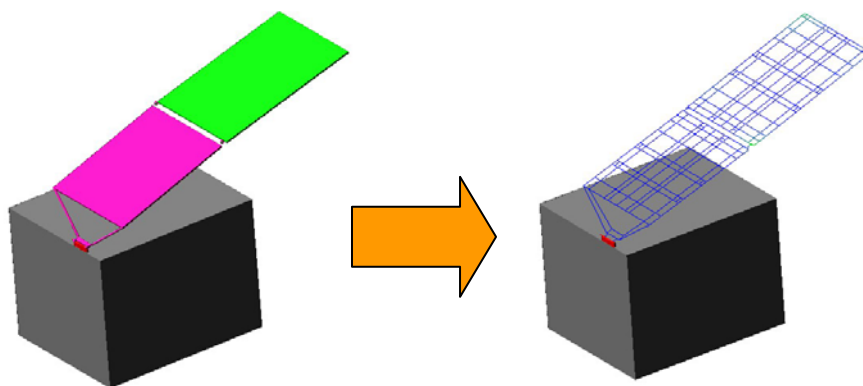


Figure 3.4.1-1: BEPI COLOMBO MPO rigid and semi-flexible model

The flexible model will consist of two flexible panels as shown in Figure 3.4.1-1.

Since in this case we know the stiffness of the latched-up hinges on HL2 we will use a semi-flexible model according to what said in paragraph 3.1.2. The beam elements that represent the hinges on HL1 in the FEM will be included in the flexible body of panel 1.

3.4.1.1 Splitting and repositioning of forces

Starting from the rigid model the first step will be split the forces and relocate them in their application point as reported in the sketch of Figure 3.4.1-2 for the HL2. The picture on the right shows the final result after the import of flexible panels.

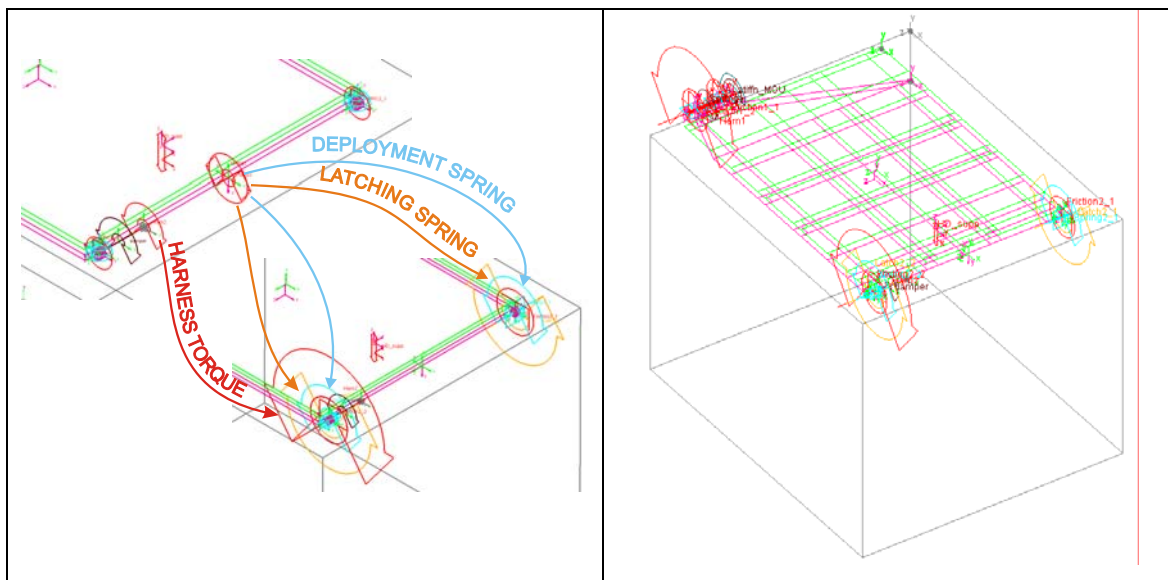


Figure 3.4.1-2: Forces splitting

As we can see in the picture the harness torque is not split. This is because usually the cables pass from one panel to the other by only one of the two hinges.

3.4.1.2 Modifying the kinds of hinges and friction

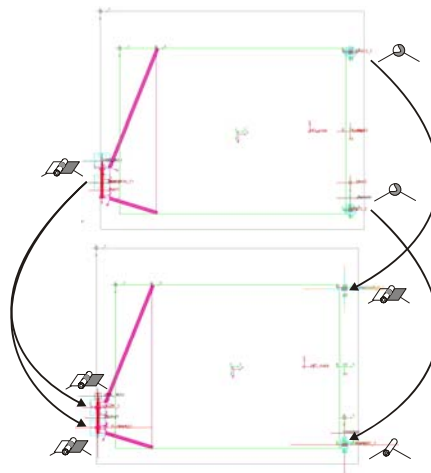


Figure 3.4.1-3: Joints modification

For what concern the joints the spherical joints of the rigid model at HL2 are changed to revolute and cylindrical joints while the revolute joint on HL1 is changed to 2 revolute joints. The friction properties of the joints will be changed as reported in following Table 3-4.

	RIGID MODEL	FLEXIBLE & SEMI-FLEXIBLE MODEL
HINGE LINE 1		
HINGE LINE 2		

Table 3-4: Differences between rigid and flexible model friction properties

3.4.1.3 Locking devices

The locking stiffness of the hinges on HL2 are introduced using the two latching torques at the hinges locations. As we saw in the Chapter 2 we know the test data for the stiffness of these hinges. This time anyway we don't need to correct this value to consider the stiffness of the structure (see § 2.2.8) because the panels are now flexible; we have just to introduce the spline function obtained from tests and reported in the following chart.

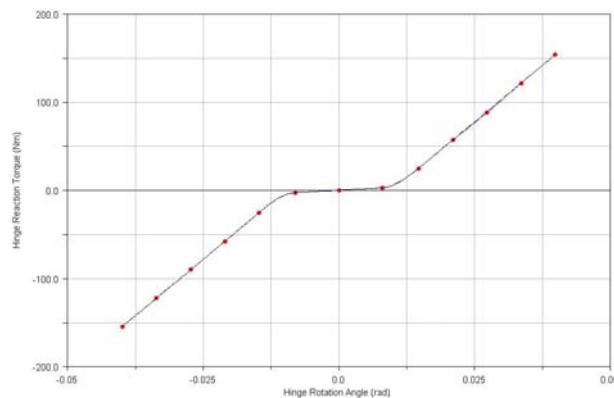


Figure 3.4.1-4: Measured Latch-up torque spline

The chart represents the stiffness of the hinge-line (two hinges) so for obtaining the right value of each one of the latching springs we have just to take half of the value reported (the two hinges work as parallel spring).

3.4.1.4 Flexible panels

The flexible panels used for the semi-flexible analysis are reported in Figure 3.4.1-5. The zoom box shows the APs and the rigid hinges. The right column reports the FEM models used for obtaining the flexible bodies on the left. As shown in Figure 3.4.1-6 the hinges arms are superimposed by RBE2 elements to make these parts rigid conserving their mass properties (inside the BEAM element).

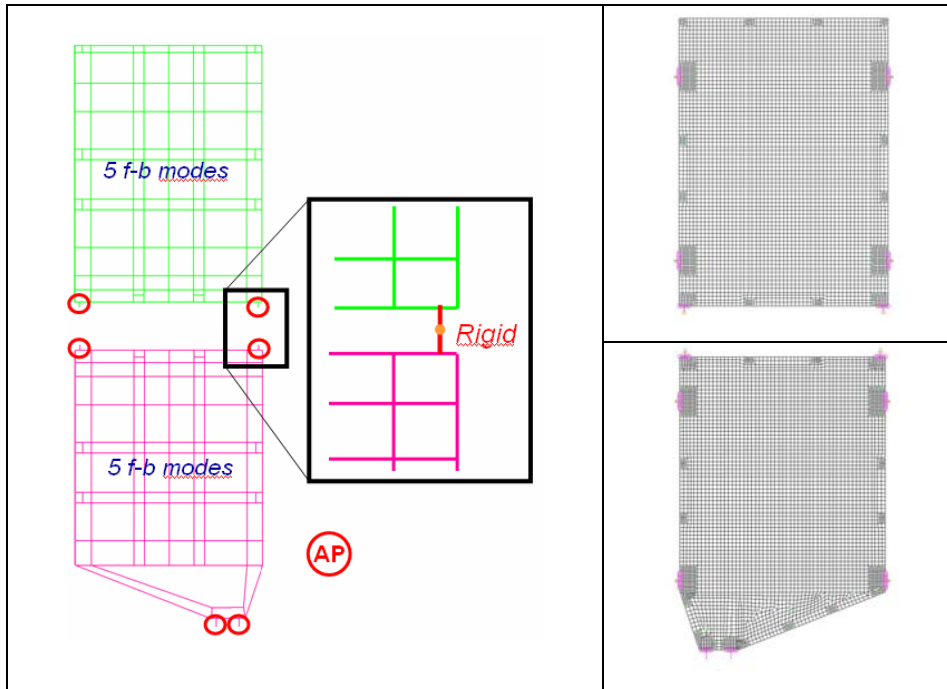


Figure 3.4.1-5: BEPI COLOMBO MPO Flexible model characteristics

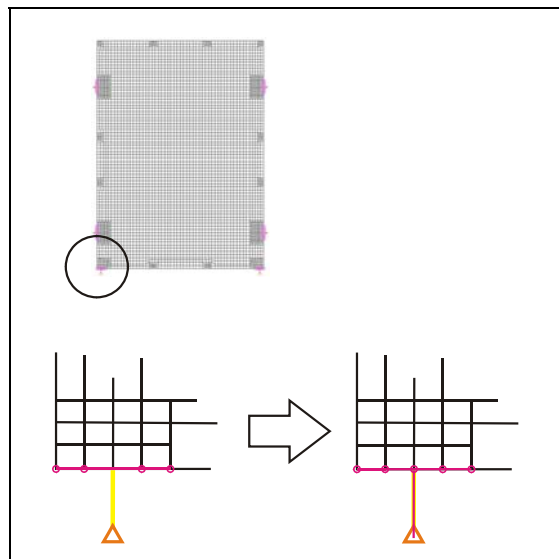


Figure 3.4.1-6: Rigid hinges obtained by RBE2 superimposition

We have 4 APs for panel1 and 2 APs for panel2. If we take 5 fix-interface modes we obtain:

$$\begin{aligned}
 N_{\text{modes P1}} &= 5 + 6 \cdot 4 = 29 \xrightarrow{-6 \text{ r-b modes}} N_{\text{FLEX modes P1}} = 23 \\
 N_{\text{modes P2}} &= 5 + 6 \cdot 2 = 17 \xrightarrow{-6 \text{ r-b modes}} N_{\text{FLEX modes P2}} = 11
 \end{aligned}$$

3.4.1.5 ADAMS solver script

The following picture shows how the script of the rigid model was adapted to the semi-flexible one.

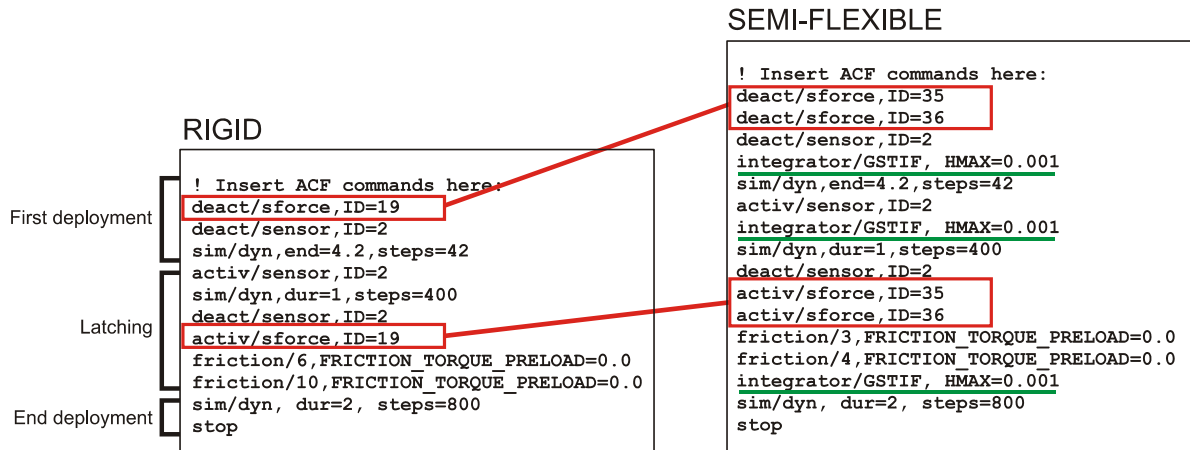


Figure 3.4.1-7: Main differences between Rigid and Semi-flexible solver scripts

The only significant changes consist in the latching torque splitting (red) and the addition of a limit on the HMAX for each phase of the deployment (green).

3.4.2 AMOS-3 solar array Full-flexible model – in orbit model

The second flexible body model application example is based on AMOS-3 solar array. As shown in Chapter 2 this solar array includes some more complicated aspects compared to BEPI COLOMBO MPO.

This solar array is in fact composed by three bodies, yoke, panel1 and panel2 coupled together by a Closed Cable Loop (CCL) synchronization system.

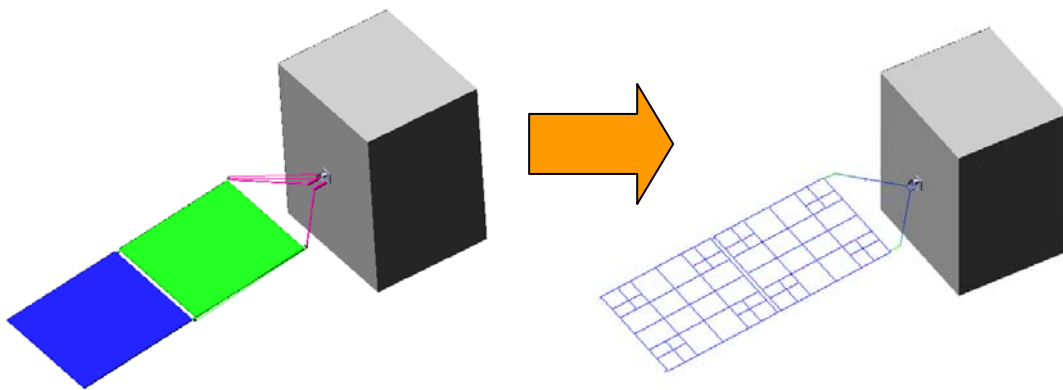


Figure 3.4.2-1: AMOS-3 rigid and full-flexible model

In this case we don't have any information about the hinge stiffness and for this reason we will adopt a full-flexible model for this solar array. That means that we will introduce a kinematical locking as shown in Figure 3.3.5-2 to obtain the latch-up of the bodies.

3.4.2.1 Splitting and repositioning forces

All we have seen about the splitting and replacement of forces in the previous example is also valid for this model (see § 3.3.1 and 3.4.1.1). The presence of the CCL mechanism however will introduce a complication when we import the flexible panels in the rigid model. While in fact in BEPI COLOMBO model all the loads of interest for the dynamic analysis acted directly on AP location in this model the load application points are offset relative the AP as shown in Figure 3.4.2-2.

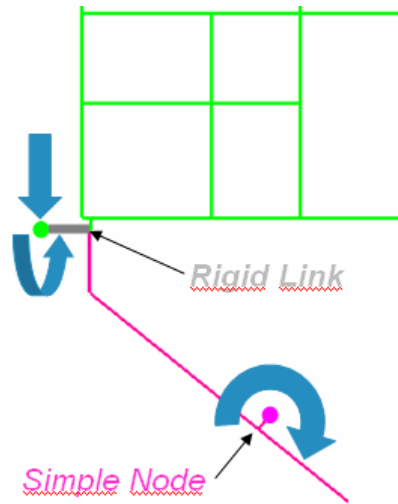


Figure 3.4.2-2: Offset of CCL loads

The problem of the offset is due to the fact that the pulleys are not represented in the FEM model and their mass is simply added to the mass of the hinges. This means when we import the flexible bodies we don't have a node to apply the loads on. This problem can be solved preserving the location of the offset load relative to near hinge node (AP). ADAMS will automatically generate the rigid link showed in Figure 3.4.2-2.

The same Figure shows also a load that acts on a simple node; it is the torque acting on the yoke arm which results from the CCL guidance. The user in this case has simply to manually select the node to apply the load on, otherwise ADAMS will apply the load to the nearest AP.

For a better comprehension of the importing flexible bodies process please refer to Appendix D. Figure 3.4.2-3 shows the final flexible model with split and relocated forces.

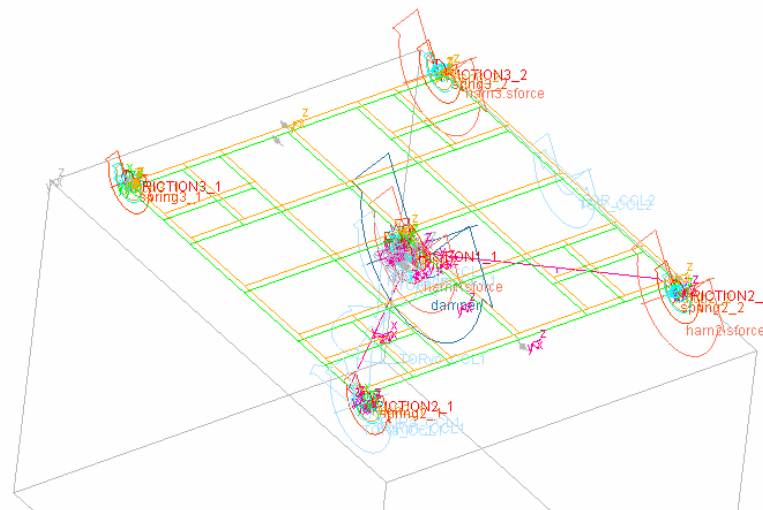


Figure 3.4.2-3: AMOS-3 full-flexible model

3.4.2.2 Modifying the kinds of hinges and friction

For what concern the hinges and friction modification there are no differences between this model and BEPI COLOMBO one. All spherical hinges will be changed by couple of revolute and cylindrical joints as shown in picture Figure 3.4.2-4.

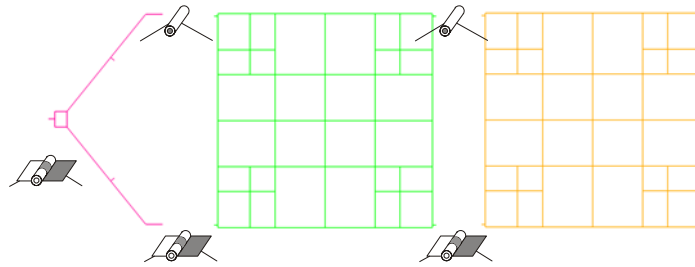


Figure 3.4.2-4: New set of hinges

3.4.2.3 Locking devices

As advised in paragraph 3.3.5 for locking the relative motion between bodies we will fix the rotational DOF of each HL imposing zero rotational speed at the latch-up as shown in Figure 3.4.2-5.

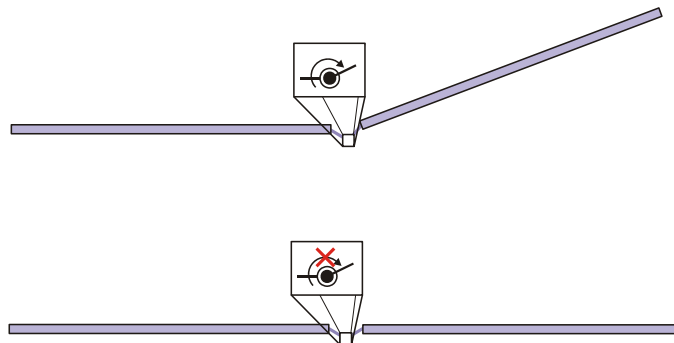


Figure 3.4.2-5: Rotation DOF suppression by fixing the rotational speed

The ADAMS/solver script to obtain this locking will be shown in paragraph 3.4.2.5

3.4.2.4 Flexible bodies

Figure 3.4.2-6 shows the flexible panels used for the full-flexible analysis. The flexible yoke has been defined using only 3 AP (see § 3.2.1)

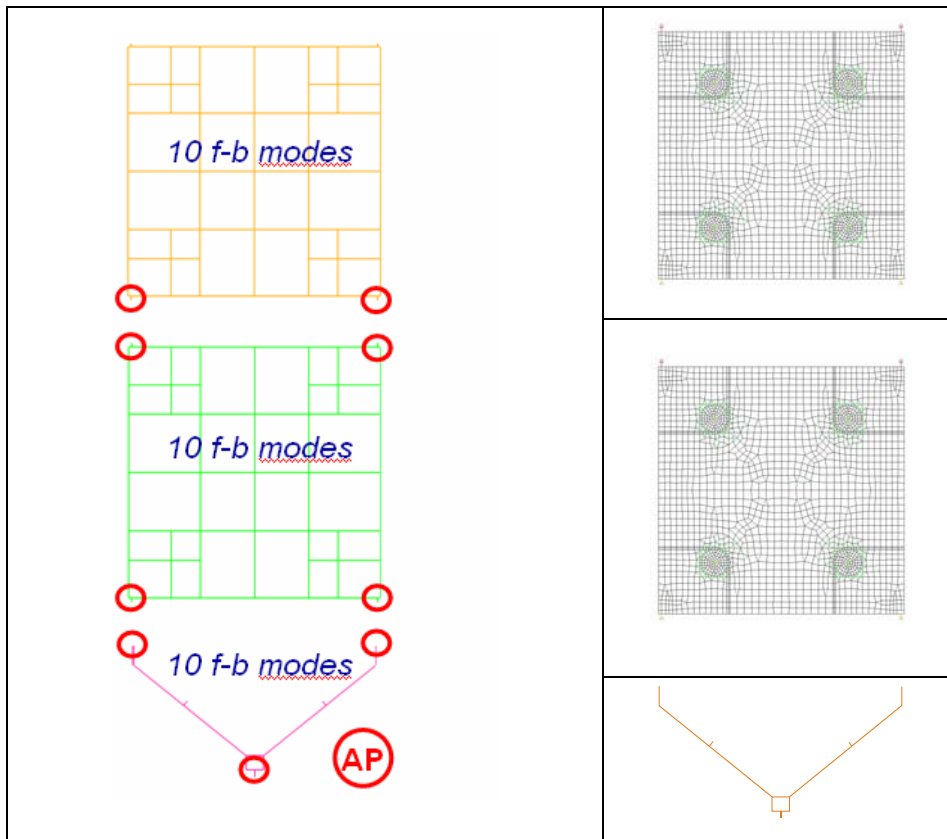


Figure 3.4.2-6: AMOS-3 full-flexible model characteristic

The number of modes that we obtain this time for each flexible bodies is reported below

$$\begin{aligned}
 N_{\text{modes P2}} &= 10 + 6 \cdot 2 = 22 \xrightarrow{-6 \text{ r-b modes}} N_{\text{FLEX modes P2}} = 16 \\
 N_{\text{modes P1}} &= 10 + 6 \cdot 4 = 34 \xrightarrow{-6 \text{ r-b modes}} N_{\text{FLEX modes P1}} = 28 \\
 N_{\text{modes YO}} &= 10 + 6 \cdot 3 = 28 \xrightarrow{-6 \text{ r-b modes}} N_{\text{FLEX modes YO}} = 22
 \end{aligned}$$

3.4.2.5 ADAMS solver script

The solver script has, compared to BEPI COLOMBO one, the particularity shown in Figure 3.4.2-7. This time we don't have to activate a torque but we define a new ADAMS element, a MOTION, that we used to fix the rotational DOF of revolute and cylindrical joints.

```
! Insert ACF commands here:
deact/sensor, ID=2

deact/motion, ID=5
deact/motion, ID=4

integrator/GSTIF, HMAX=0.001
sim/dyn, end=4.2, steps=42
activ/sensor, ID=2
integrator/GSTIF, HMAX=0.001
sim/dyn, dur=1, steps=400
deact/sensor, ID=2

activ/motion, ID=4
activ/motion, ID=5
motion/4, velocity, func=0.0
motion/5, velocity, func=0.0

friction/3, FRICTION_TORQUE_PRELOAD=0.0
friction/4, FRICTION_TORQUE_PRELOAD=0.0
integrator/GSTIF, HMAX=0.001
...
```

Figure 3.4.2-7: Full-flexible model script example

3.4.3 AMOS-3 solar array Full-flexible model – On ground model

The on-ground model of AMOS-3 solar array is shown in Figure 3.4.3-1.

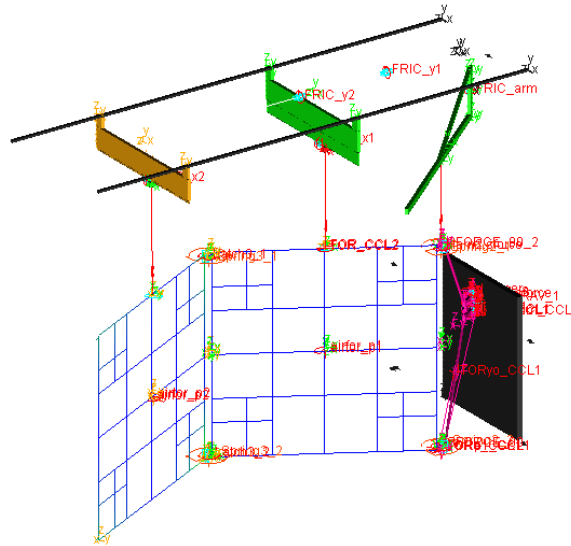


Figure 3.4.3-1: AMOS-3 on-ground hybrid model

This model can be obtained in an analogous way as for the in-orbit one but there are three different aspects that are useful to take in evidence.

- Aerodynamic load applied on simple nodes
- Support bracket represented as different bodies
- Coexistence of rigid and flexible parts in same model (hybrid-model)

3.4.3.1 Aerodynamic load applied on simple nodes

As we have already seen in early paragraph 3.2.1 we are interested only in aerodynamic global effects. To consider the air drag that they generate, we can apply them to the central node of each panel (the closer to the centre of mass) as shown in Figure 3.4.3-2

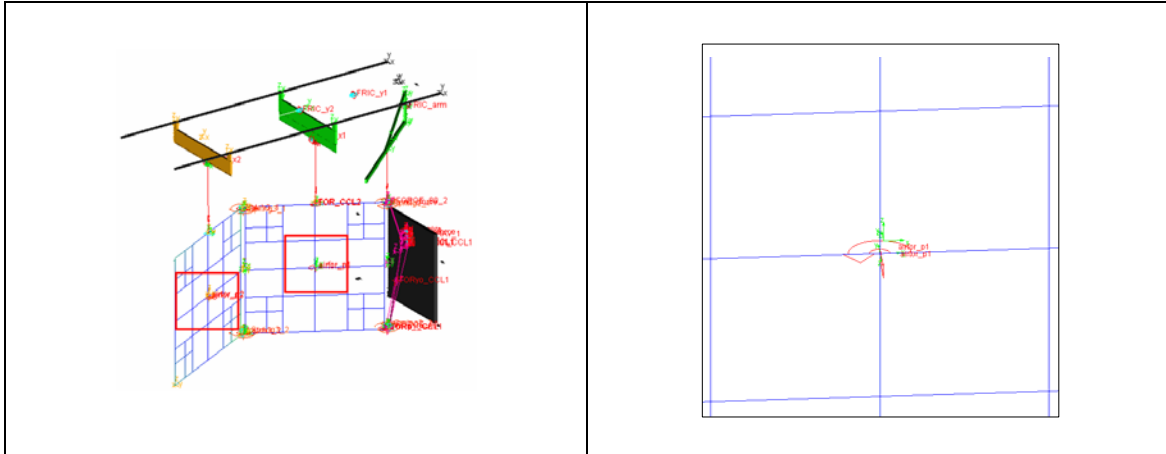


Figure 3.4.3-2: Aerodynamic loads on the panles

3.4.3.2 Support brackets represented as different bodies

The system of springs that compensates the gravitational forces on the structure is connected to the panels and to the yoke by brackets. While in the rigid model we could include their masses and their inertia properties inside the rigid body which they were connected to, this time we have to consider them as separate entities.

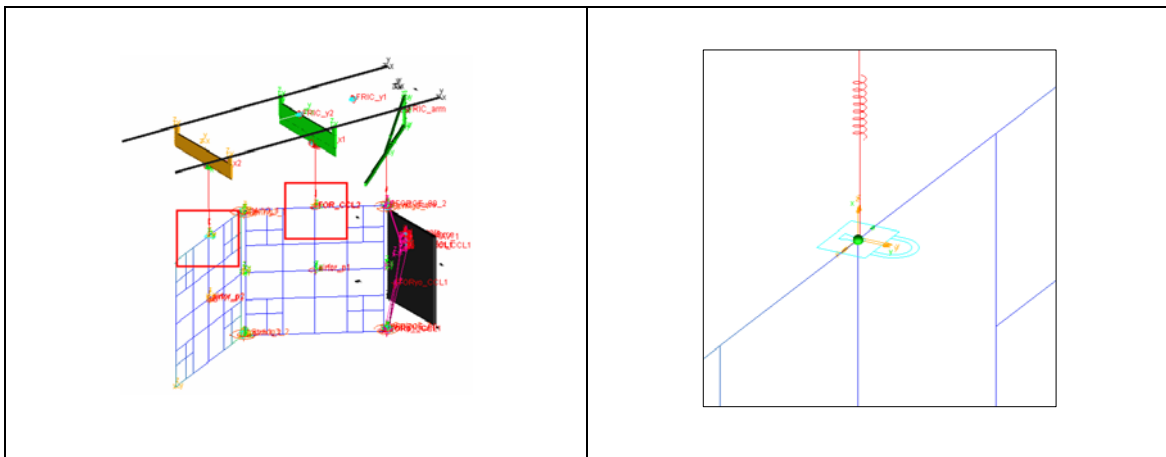


Figure 3.4.3-3: Supporting brackets interfaces

Figure 3.4.3-3 shows the particular of the bracket. As we can see by the picture the bracket is represented in ADAMS by a sphere of known mass rigidly connected to the panel by a fix joint (the cyan padlocks of the picture on the right).

3.4.3.3 Coexistence in same model of rigid and flexible parts (hybrid-model)

The on-ground flexible model of AMOS-3 , beside the results of the dynamic analysis, is important to notice the possibility of building ADAMS hybrid models with rigid and flexible parts.

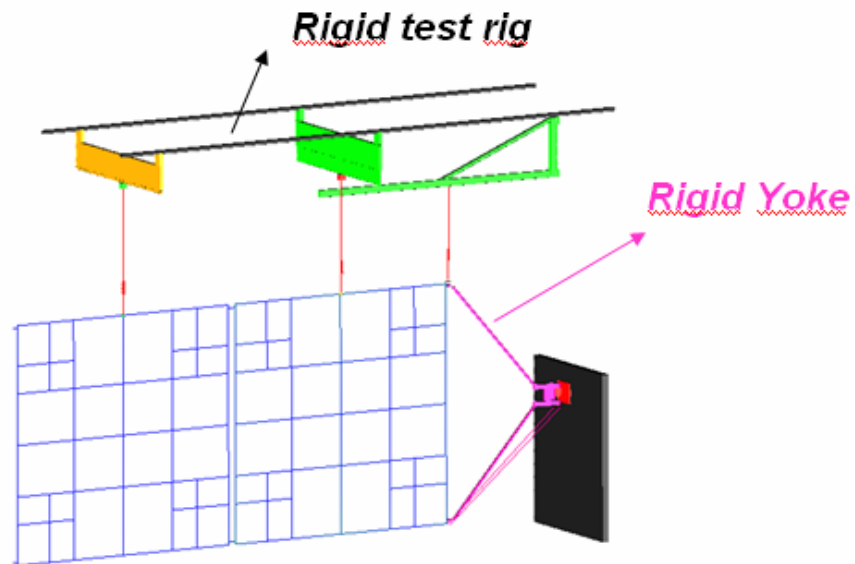


Figure 3.4.3-4: Rigid and flexible parts in the same model

Figure 3.4.3-4 shows the rigid parts of the model. The problem that emerges due the presence of the rigid yoke is how to include the stiffness properties of this element inside the model.

The solution is obtained in a way similar to the way we included the stiffness in the rigid model. We will use two latch-up springs between the rigid element and the flexible one tuned on the value obtained by the FEM linear modal analysis as shown in Figure 3.4.3-5.

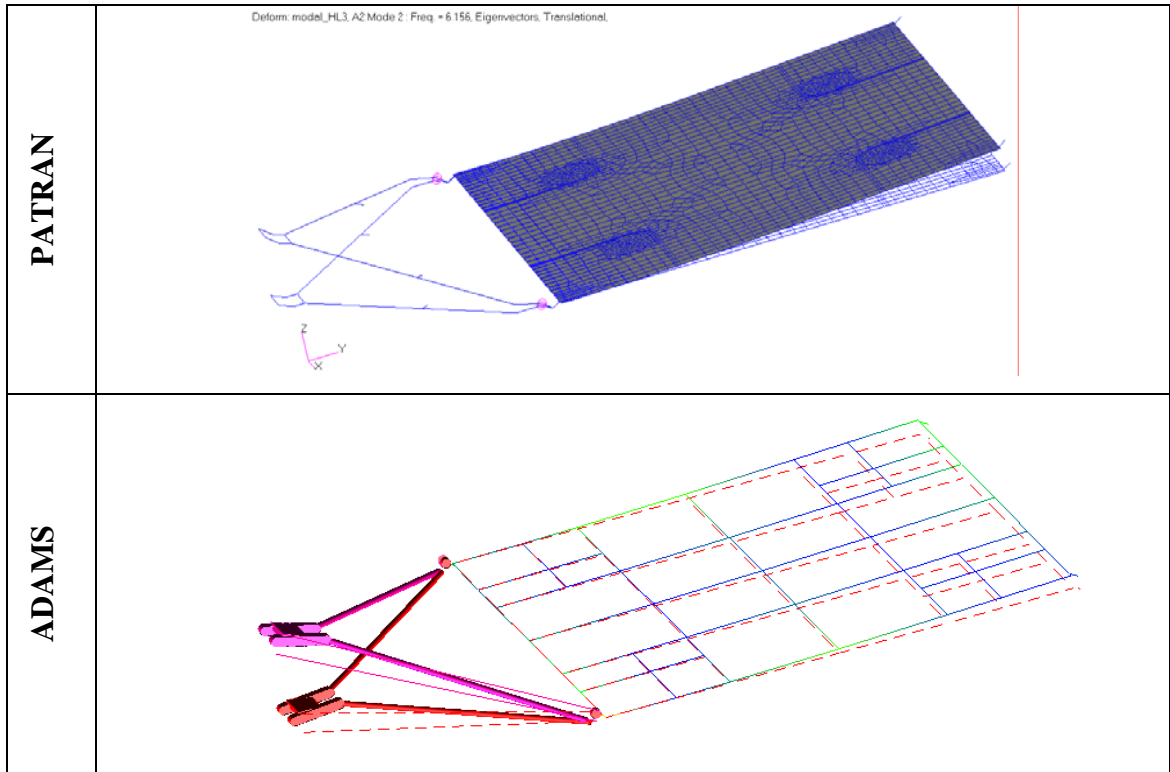


Figure 3.4.3-5: Latch-up spring tuning procedure

Chapter 4

Analysis of Results

4.1 BEPI COLOMBO MPO S/A – Semi-flex vs Rigid Model

The following paragraph shows a comparison between the Semi-Flexible and Rigid dynamic analyses of BEPI COLOMBO MPO solar array deployment.

4.1.1 Solar array Deployment

Sequence of Figure 4.1.1-1 shows the comparison between the deployments of the two models. Even from the short sequence we can see how the two models are quite synchronized. The deformation of bodies, as expected, doesn't create any problem in the flexible model.

The flexible model is the one on the right. As we can see by the sequence of pictures the use of PLOTTEL instead of the FEM mesh grid inhibits the rendering in ADAMS.

The colour-fringe plot present in the PLOTTEL wire-frame during the deployment indicates the magnitude of body deformation.

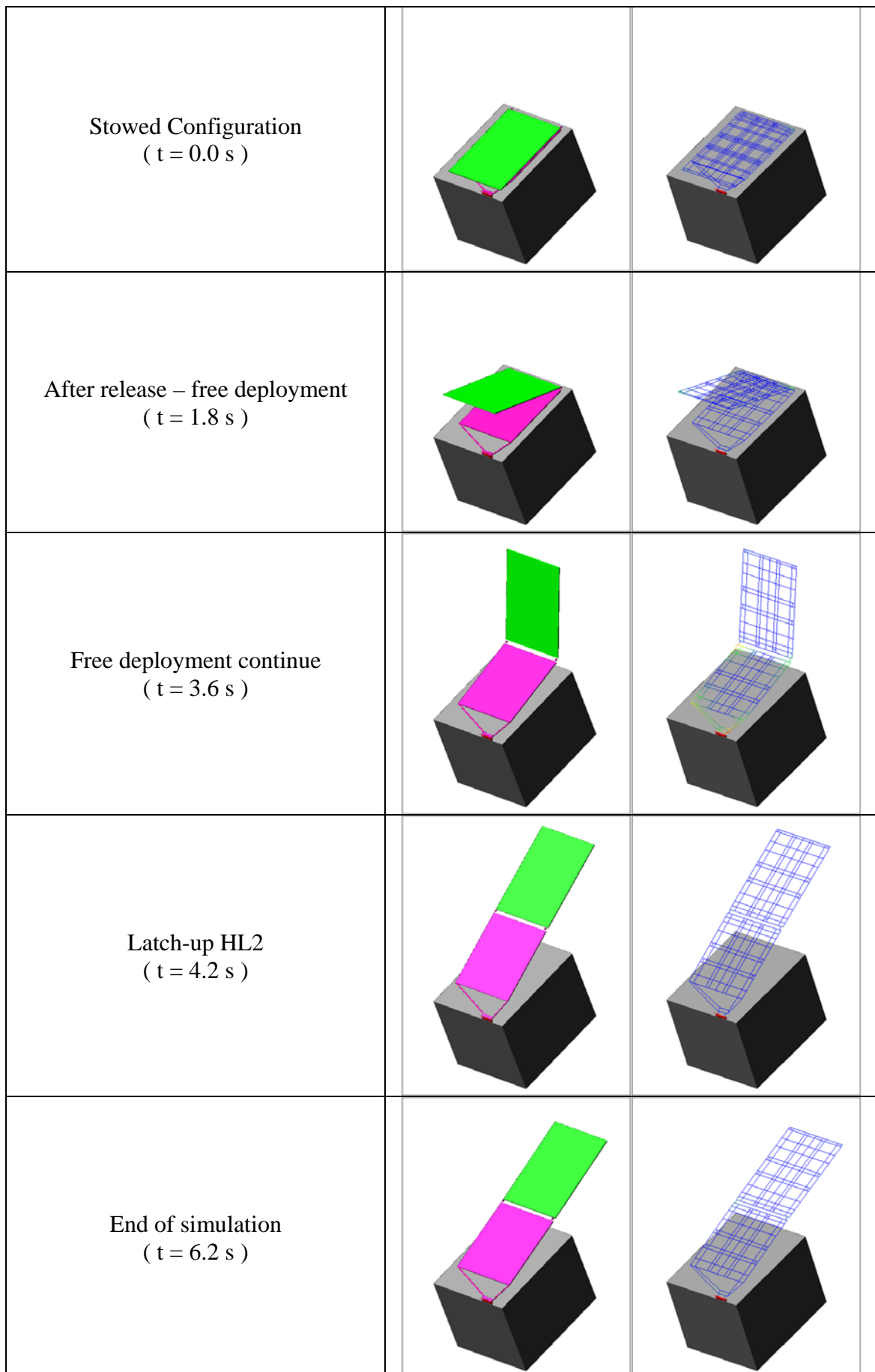


Figure 4.1.1-1: Rigid vs Semi-flexible deployment

4.1.2 Latch-up torque

The estimation of latch-up torque represents the main target of our investigation. Using this torque in fact we are able to understand the entity of the loads associated with the latching shock and find out the stress condition in the hinges surrounding areas.

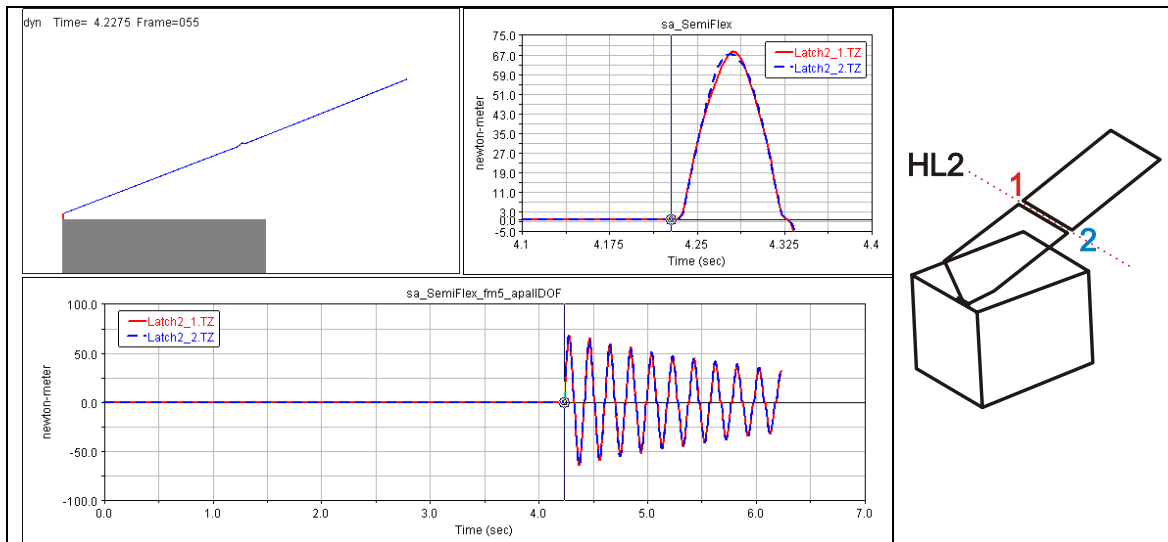


Figure 4.1.2-1: Latch-up torque on HL2

Figure 4.1.2-1 show the latch-up torque vs time chart for the semi-flexible model. Top left picture shows the starting time-step of the latch-up.

Even if the problem is slightly asymmetric (the two panels are different and the harness torque involves only one hinge) the two functions are in phase and the two maxima are quite the same as shown in **Errore. L'origine riferimento non è stata trovata.** In this figure we can also recognize the flexibility from the non-linear experimental stiffness of the hinges (refer to Figure 3.4.1-4).

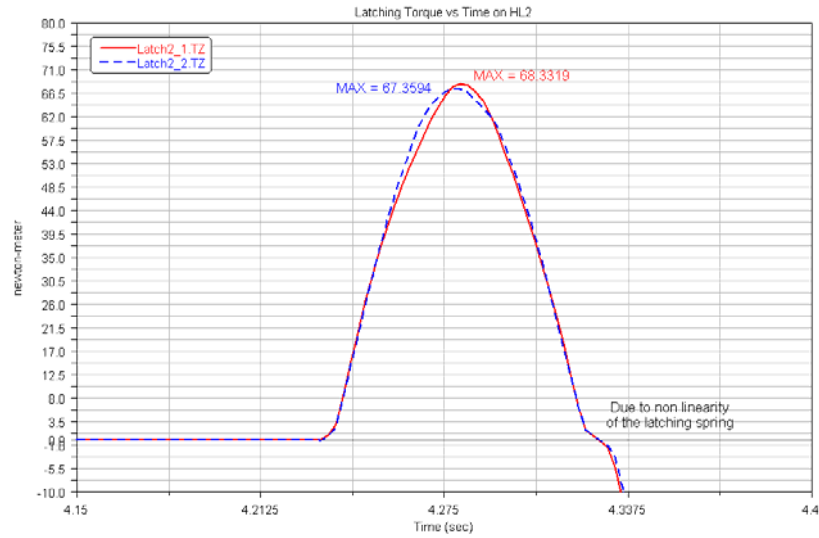


Figure 4.1.2-2: Close up on the maximum latch-up torque

For comparing these results with the corresponding ones from the rigid model we have to add the torque from the two hinges together since in the rigid model the latch-up torque is represented by only one torque for the hinge-line.

Figure 4.1.2-3 shows this comparison.

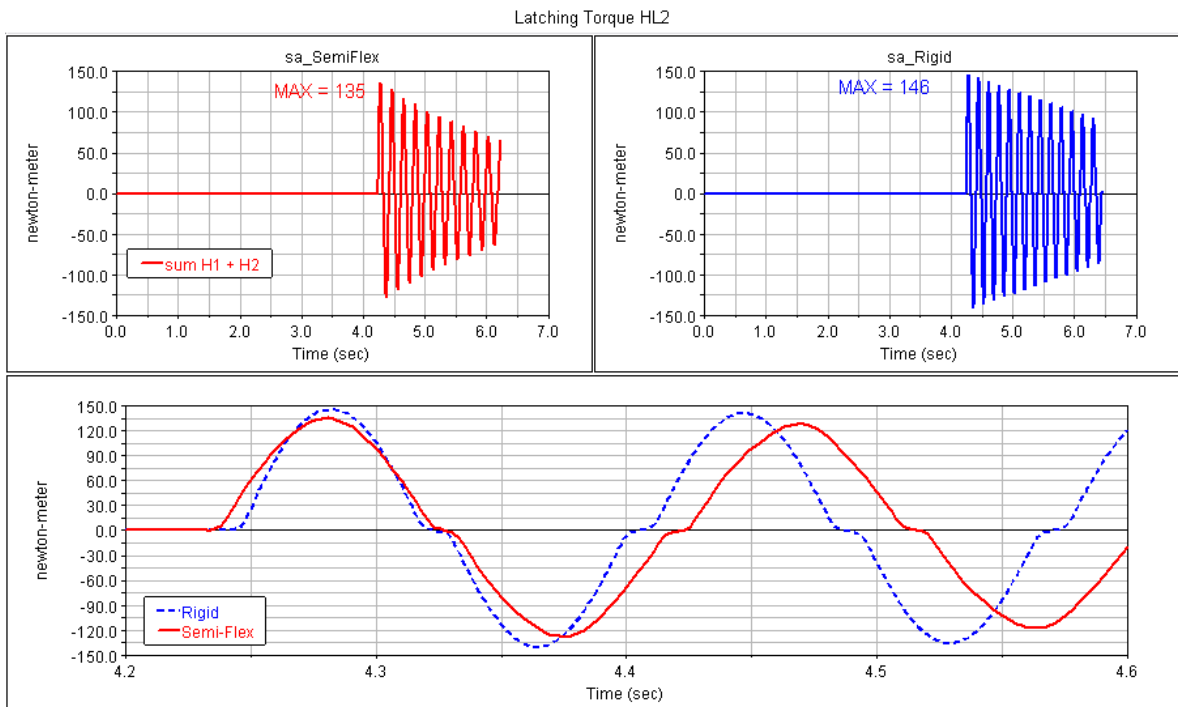


Figure 4.1.2-3: Comparison between Rigid and Semi-flex model latch-up torque

The charts show that we have a good match between the results of the two models. The rigid torque is characterized by a slightly higher peak value but that is not surprising considering the approximation used to estimate the structural stiffness contribution of

the latch-up spring based only on the frequency of the first flexible mode of the structure.

The small difference in the starting time of the latch-up (about 1 tenth of second) is due to the imperfect equivalence of frictions of different joints (spherical vs revolute and cylindrical) and to the differences in the integration steps between the two models. The use of smaller integration time-step for the semi-flexible model leads to a more accurate solution.

One more thing to notice is the different frequency of the oscillation. The lower frequency of the semi-flexible is related with the lower stiffness of the model in comparison with the rigid one.

4.1.3 Loads on SADM I/F

Other important loads to check in BEPI COLOMBO solar array are the loads on the SADM interface. This device represents the connection between the solar wing and the rest of the space craft. It is clear that in a solar array with such a deployment, it is important to check that these loads are in the allowable tolerance.

4.1.3.1 SADM I/F forces

The SADM is connected to the spacecraft by a fix joint; the SADM interface loads will be calculated reading the reactions in this joint.

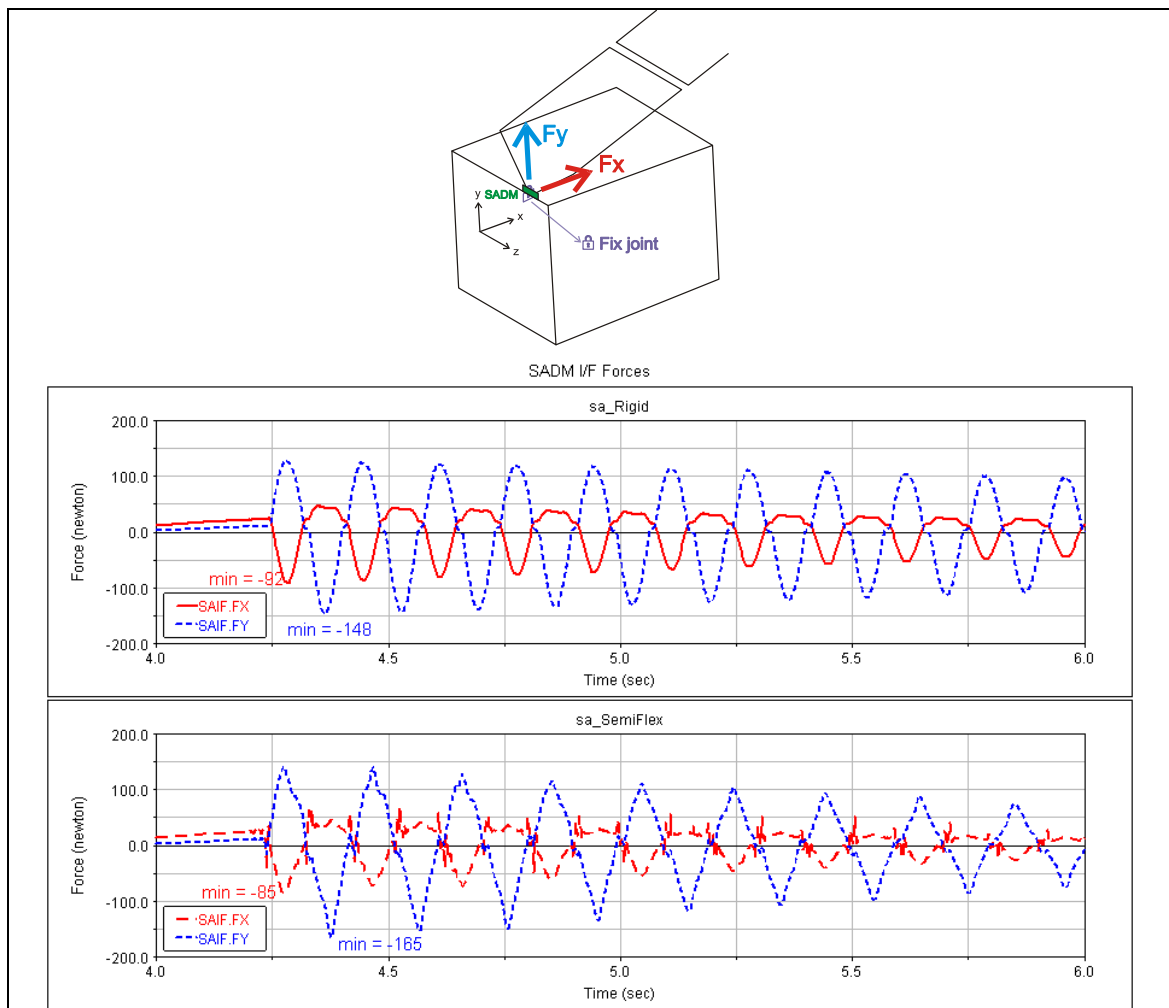


Figure 4.1.3-1: SADM forces comparison

Figure 4.1.3-1 shows the comparison between rigid model result (upper chart) and semi-flexible one (lower chart). As we can see also in this case the higher frequency effects are quite restrained. The trend of the two forces is the same and the error on the minimum value of F_y is about 10%.

4.1.3.2 SADM I/F torques

From Figure 4.1.3-2 we can see that for the torques on the SADM interface the two models show a quite different behaviour.

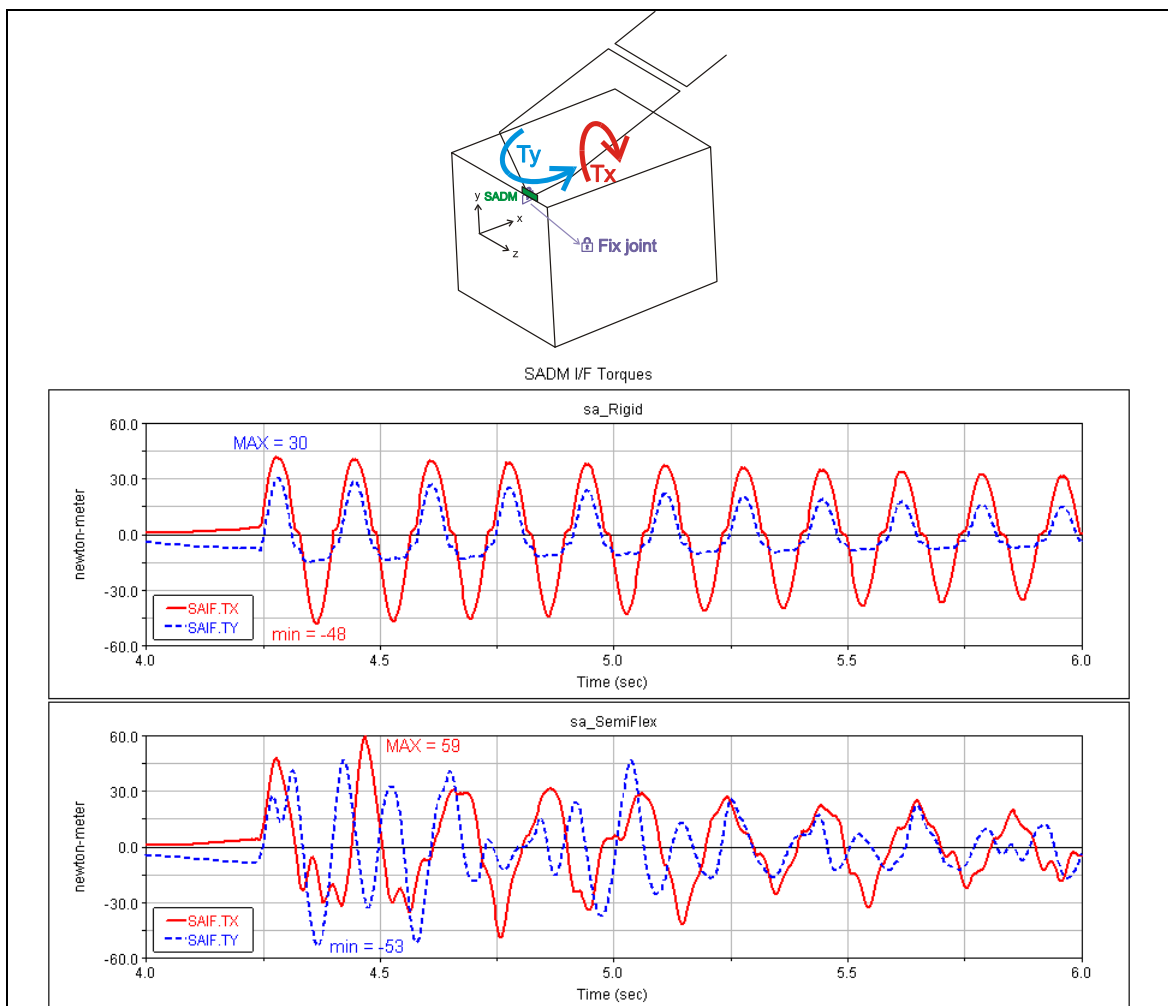


Figure 4.1.3-2: SADM torques comparison

The main difference is in the magnitude of T_y . The rigid model underestimates the magnitude of the torque around y by a factor of 1.77.

Beside this the trends of the curves, at least in a period of about 1 second after the latch-up, are quite different and for the flexible result weakly periodic too.

This behaviour and these differences can be explained considering the asymmetry of the structure of the solar array. The geometry and mass differences between the two panels excite asymmetric flexible modes that can't be captured with the 2 DOF approach of the rigid model.

4.2 AMOS-3 S/A in orbit – Full-flex vs Rigid Model

4.2.1 Solar array Deployment

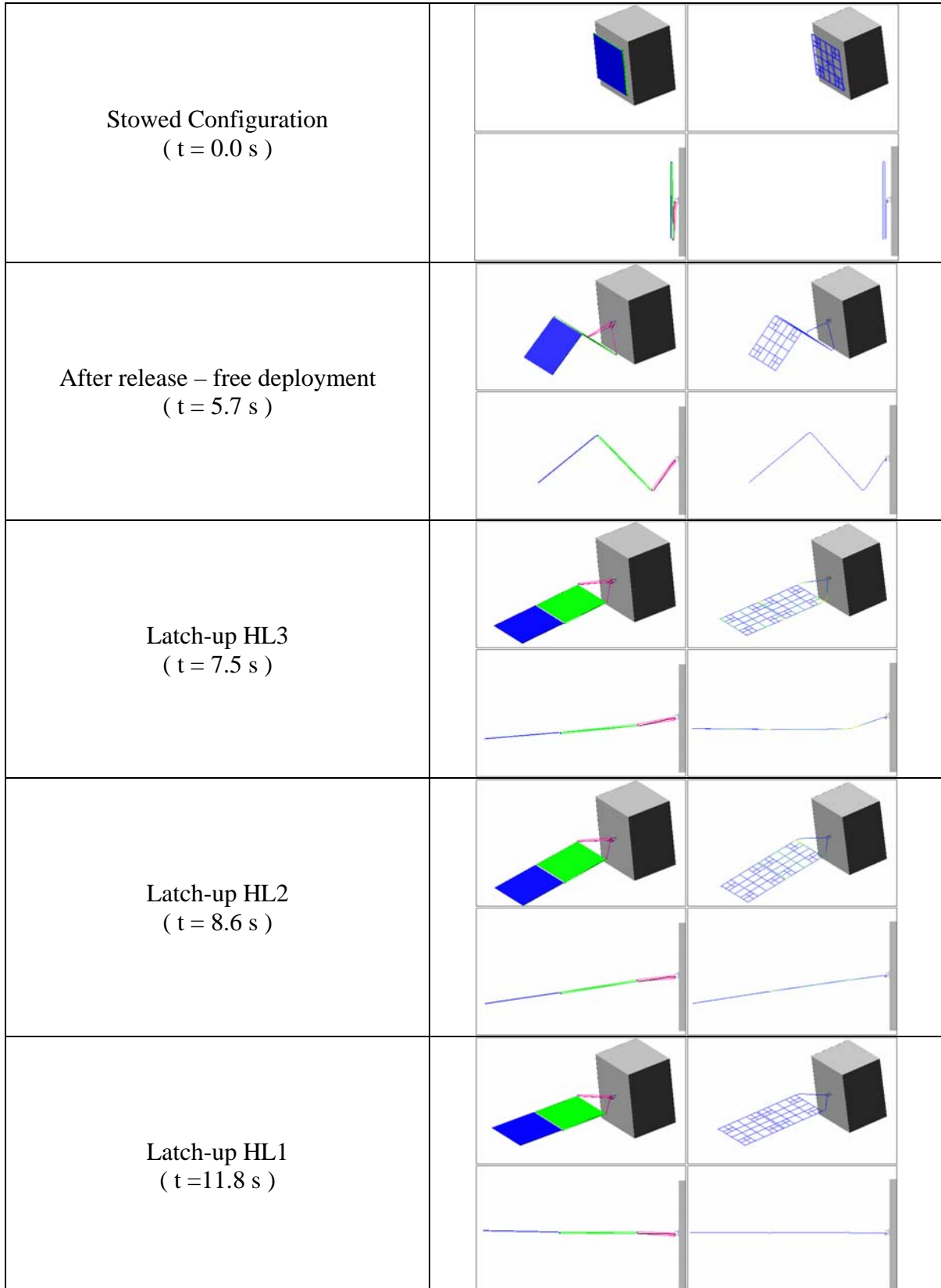


Figure 4.2.1-1: Rigid vs Full-flexible deployment

The sequence of Figure 4.2.1-1 shows the comparison between the rigid and the flexible model deployment. Also here, as we already saw for BEPI COLOMBO semi-flexible model, the deployment of the flexible mechanism performs in good correspondence with the equivalent rigid model.

4.2.2 Latch-up torque

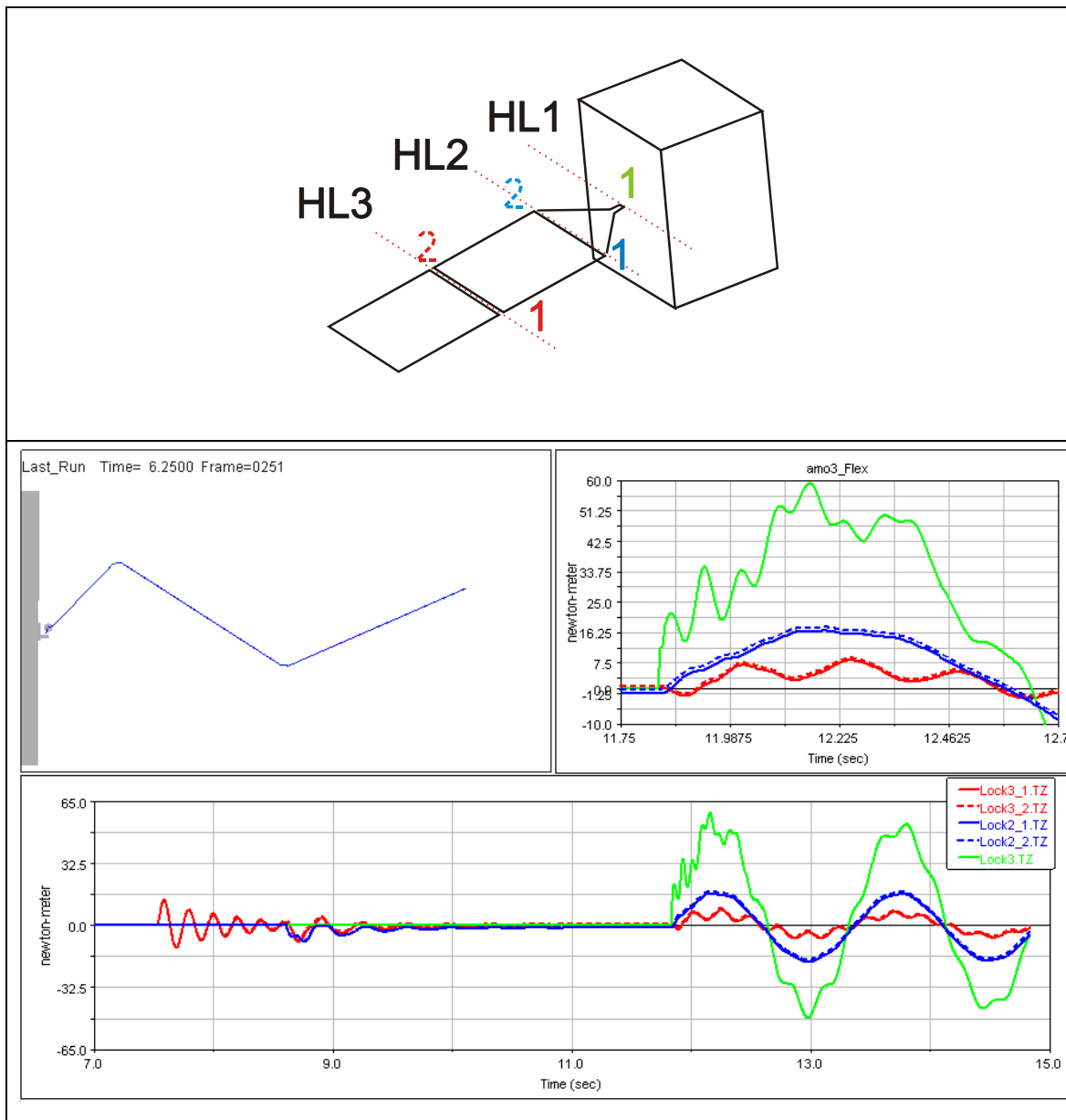


Figure 4.2.2-1: Full-flexible model latch-up torque on the 3 HLs

Figure 4.2.2-1 shows the latching torques vs time behaviour. As shown in the upper-right zoom there is a good agreement between the curves related to two different hinges of the same hinge-line (dot-line vs solid line of the same colour).

In the following paragraphs these latch-up torques will be compared with the ones obtained by the rigid model. The two torques of each hinge-line from the flexible model are add together to be compared with the rigid latching torque.

4.2.2.1 HL3 latch-up

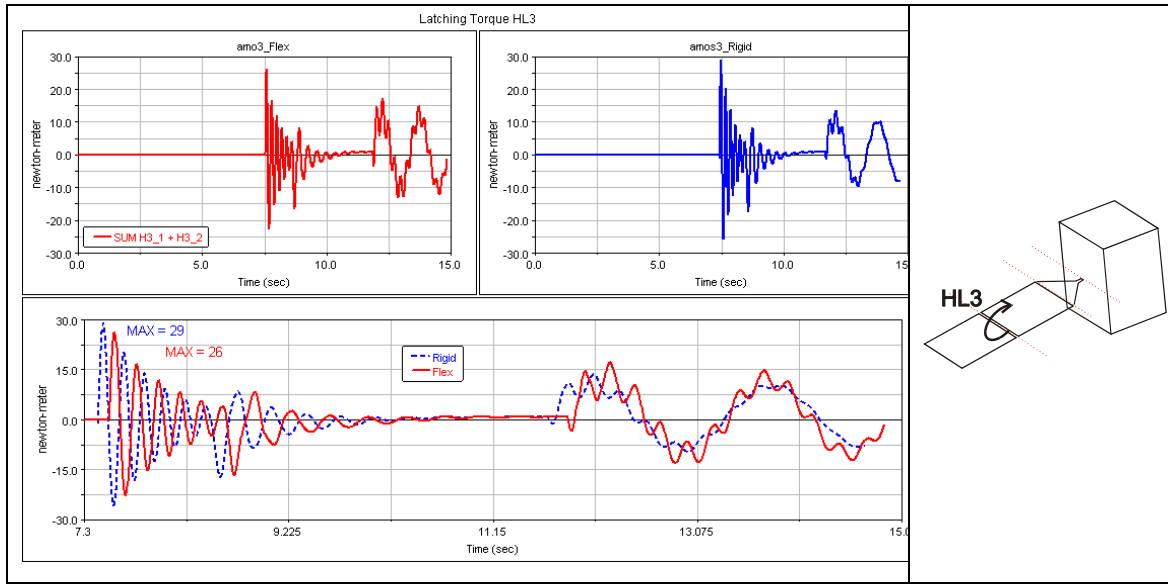


Figure 4.2.2-2: Comparison between Rigid and Full-flexible latch-up torque on HL3

Figure 4.2.2-2 shows the comparison between rigid and flexible latch-up torque on HL3. The two evolutions are quite similar; the maxima and the timings are comparable.

4.2.2.2 HL2 latch-up

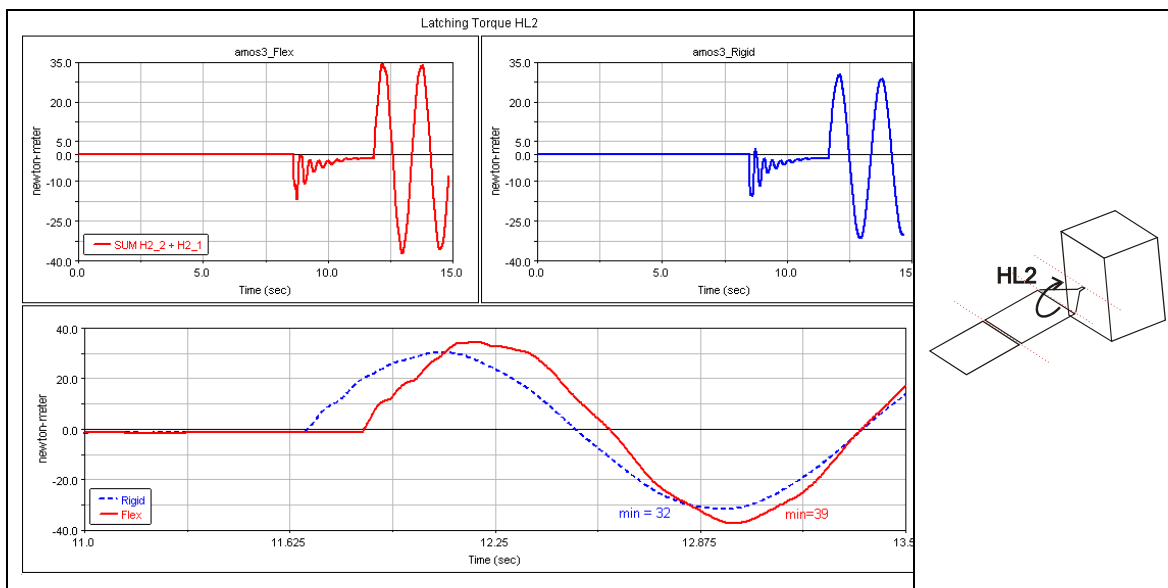


Figure 4.2.2-3: Comparison between Rigid and Full-flexible latch-up torque on HL2

The latch-up torque on HL2 is reported in Figure 4.2.2-3.

4.2.2.3 HL1 latch-up

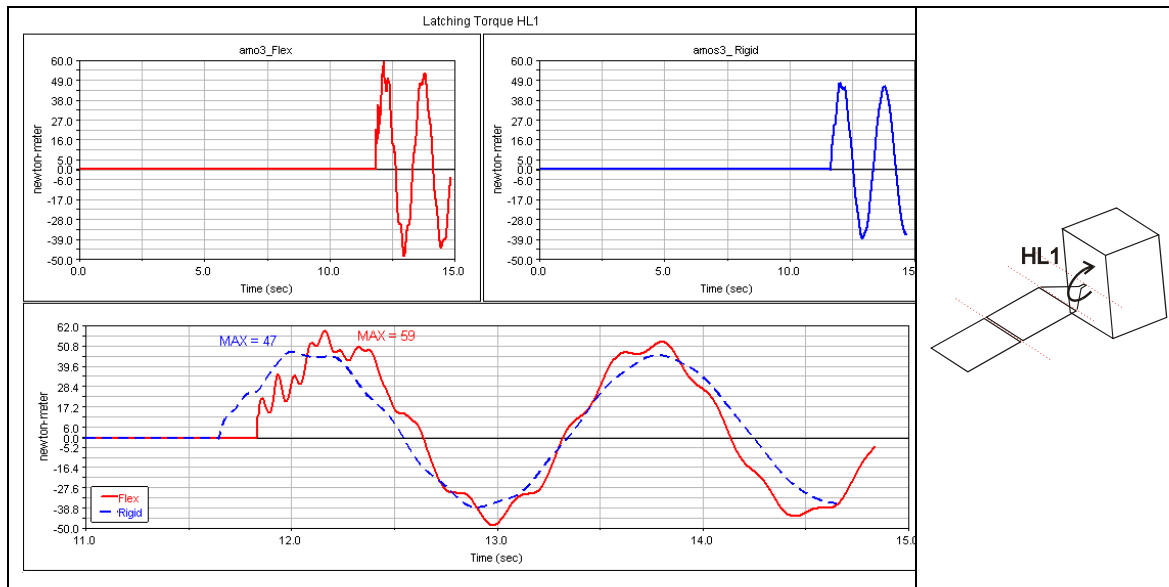


Figure 4.2.2-4: Comparison between Rigid and Full-flexible latch-up torque on HL1

The latch-up torque on HL1 is reported in Figure 4.2.2-4. In the flexible solution some higher frequencies are excited and damped out rapidly. The overall peak from the flexible solution is about 20% higher than for the rigid model.

4.2.3 CCL forces

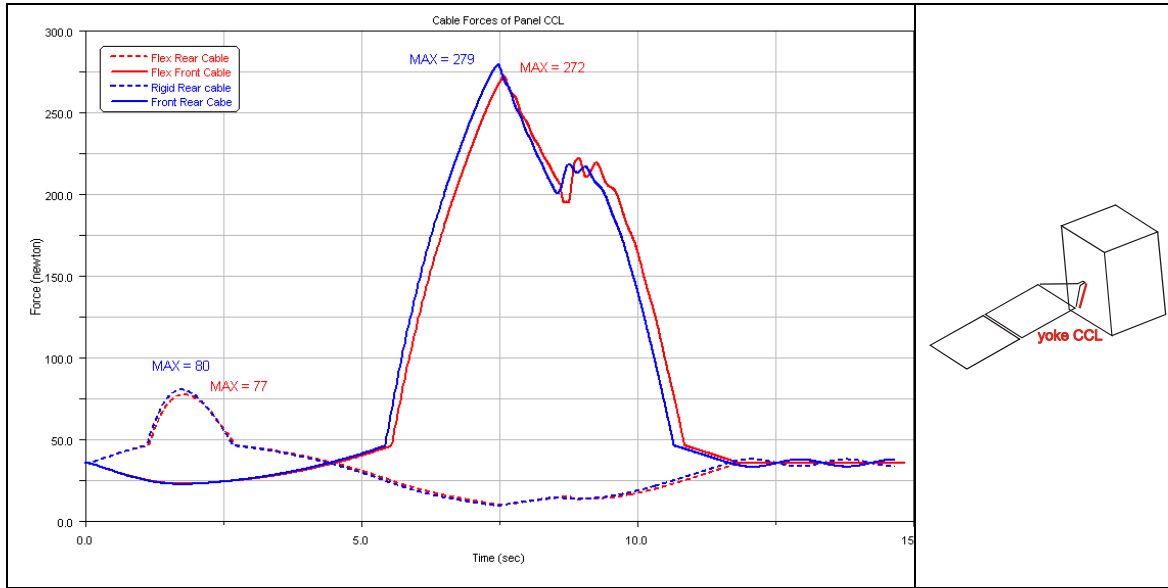


Figure 4.2.3-1: Comparison between Rigid and Full-flexible yoke CCL forces

Figure 4.2.3-1 and Figure 4.2.3-2 show the comparison of the CCL forces. Also in this case we have a good match of results that can be explained with the high in-plane stiffness of the panels. In other words the cables lengths are not really affected by the flexibility of the model because the in-plane deformations of panel and yoke are small.

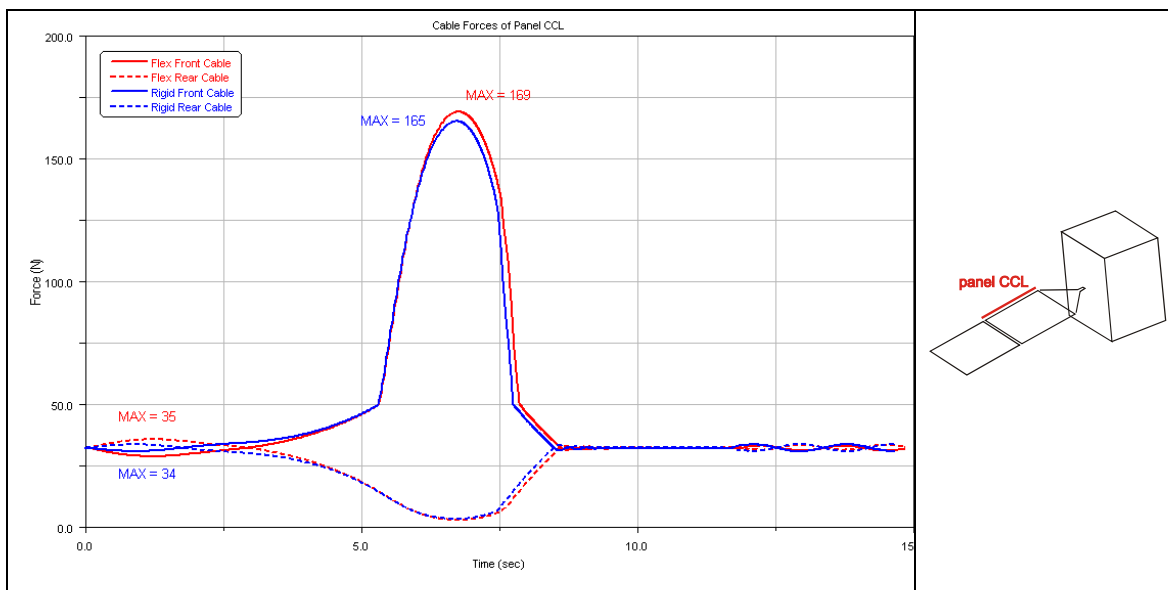


Figure 4.2.3-2: Comparison between Rigid and Full-flexible panel CCL forces

4.2.4 Eddy current dumper

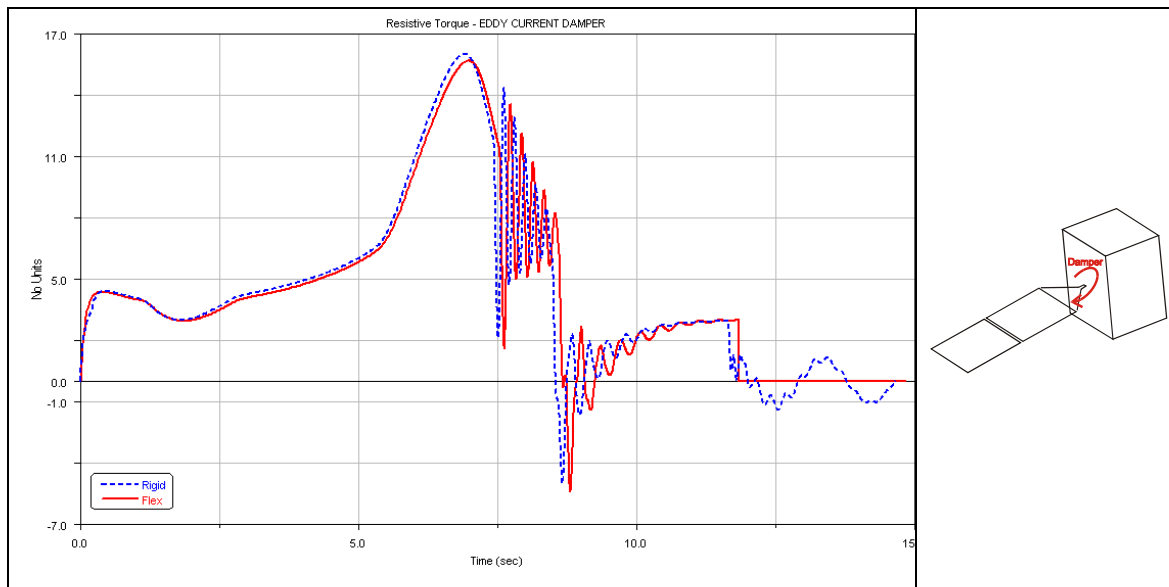


Figure 4.2.4-1: Comparison between Rigid and Full-flexible eddy current damper torque

The behaviour of the resistive torque generated by the eddy current damper is reported in Figure 4.2.4-1. The only relevant difference between the two models is after the latching of HL1. After the latching of HL1 at about 12 [s]. We see that the rigid solution keeps on oscillating around zero while the flexible solution goes straight to zero.

This difference is generated by the different latching devices used in the two models. The locking spring of the rigid model enables the damper to work even after latch-up. In the flexible model instead the relative rotation is fixed by the MOTION element (see §3.3.5).

4.2.5 Torque on SADM I/F

The loads on the SADM are not critical for AMOS-3 solar array. Anyway we want to warn the user about the problem of preload.

Figure 4.2.5-1 shows the Torque along y direction on the SADM I/F. As we can see in the red square the first 4 seconds of the flexible simulation are characterized by a high frequency oscillation. The reason for this behaviour is the lack of preload in the yoke. ADAMS at the very first instant of simulation suddenly applies the set of CCL loads on the yoke establishing that oscillation response shown in the picture.

The best solution to avoid this effect is to run a first static analysis fixing the hinge DOF. This static simulation has only to load the yoke and after it we can start the dynamic simulation with the preloaded yoke.

Figure 4.2.5-2 shows the same torque of Figure 4.2.5-1 obtained by a dynamic analysis preceded by a static equilibrium in which we have fixed the HL DOF using the same MOTION elements that will be used in the following dynamic analysis. The pick at around second 12 is a numerical artefact generated by the latch-up of HL1; to fix it one can decrease the time steps preceding the latch-up.

It is clear that the pre-load effects are not present in the rigid body (blue-dot line) model.

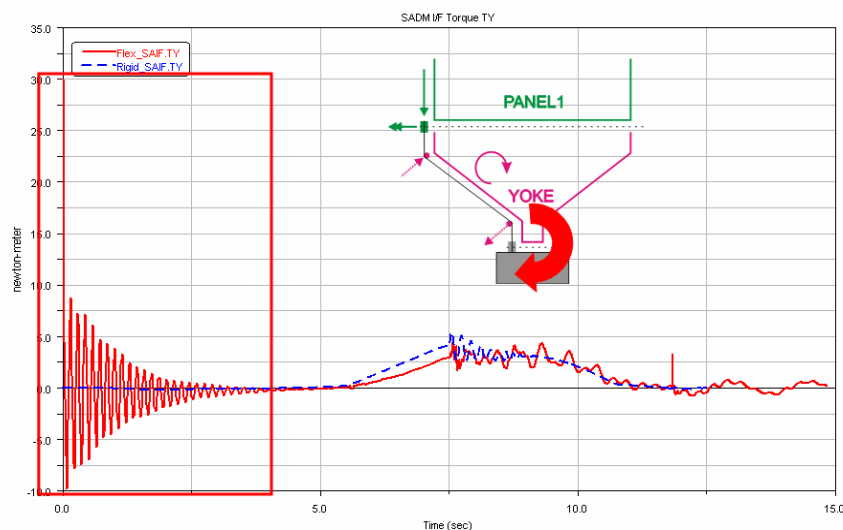


Figure 4.2.5-1: Effect on the lack of preload on Yoke Ty torque

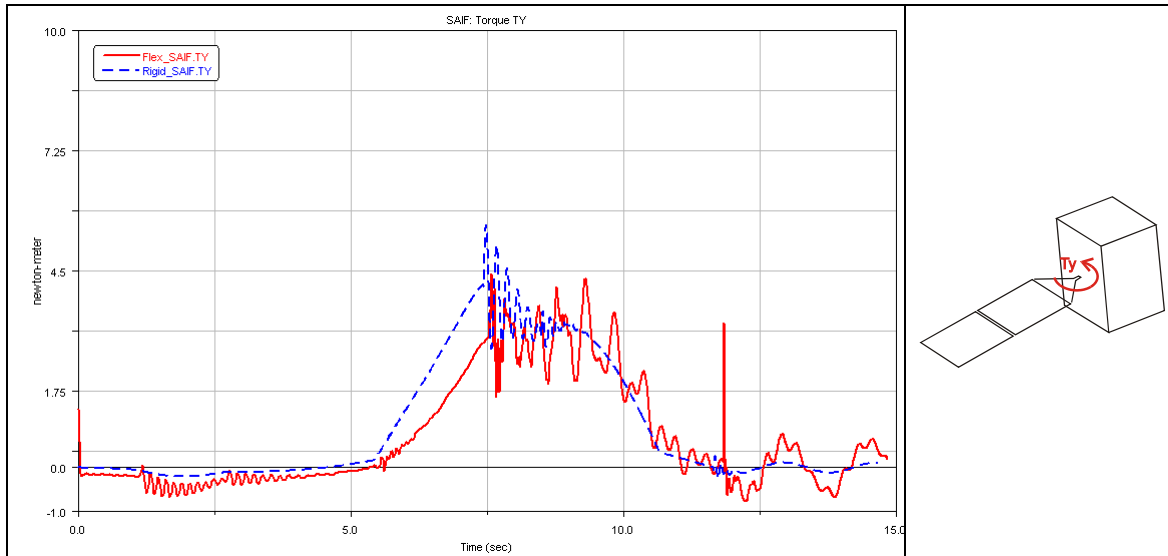


Figure 4.2.5-2: Yoke Ty torque considering the preload

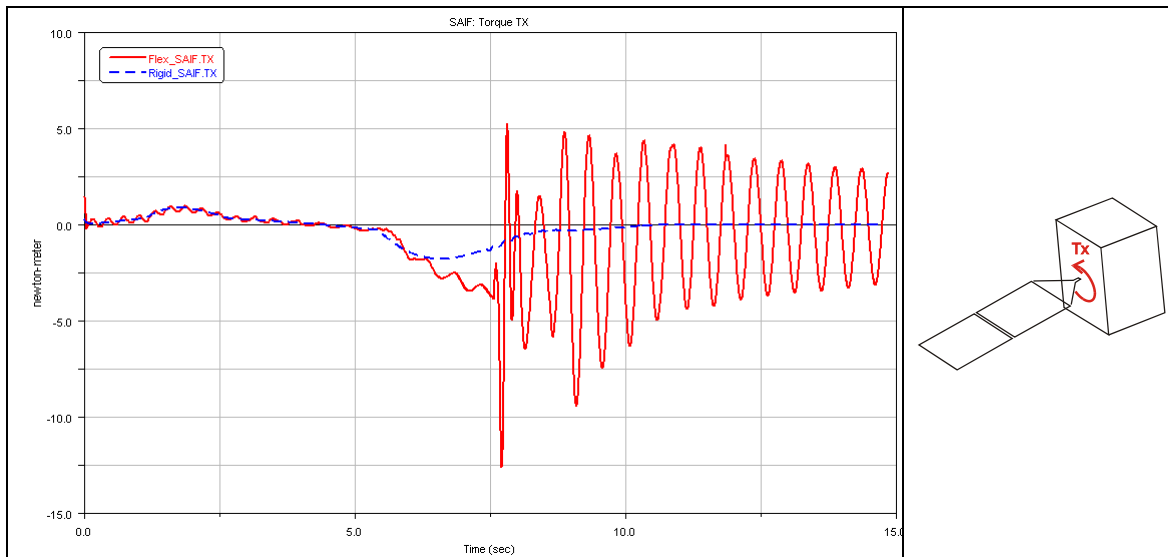


Figure 4.2.5-3: Yoke Tx torque

Figure 4.2.5-3 shows the torque on the SADM along x direction. In this case again, as already seen for BEPI COLOMBO SA, we find that the rigid model is inadequate to capture the dynamic in the plane transversal to the deployment one. Although the loads on the SADM are moderate the difference between the two models is evident.

These dynamics, as for BEPI COLOMBO, are excited by asymmetries in the model. Also for AMOS-3 in fact, although if we have a symmetric geometry of the bodies we have asymmetries in mass distribution (pulleys) and in some elements of the model (harness torque and CCL system). The yoke with is low stiffness against T_x load, emphasizes this dynamic and contributes to the big difference between the two models.

4.3 AMOS-3 S/A on ground – Hybrid vs Rigid

4.3.1 Latch-up torque

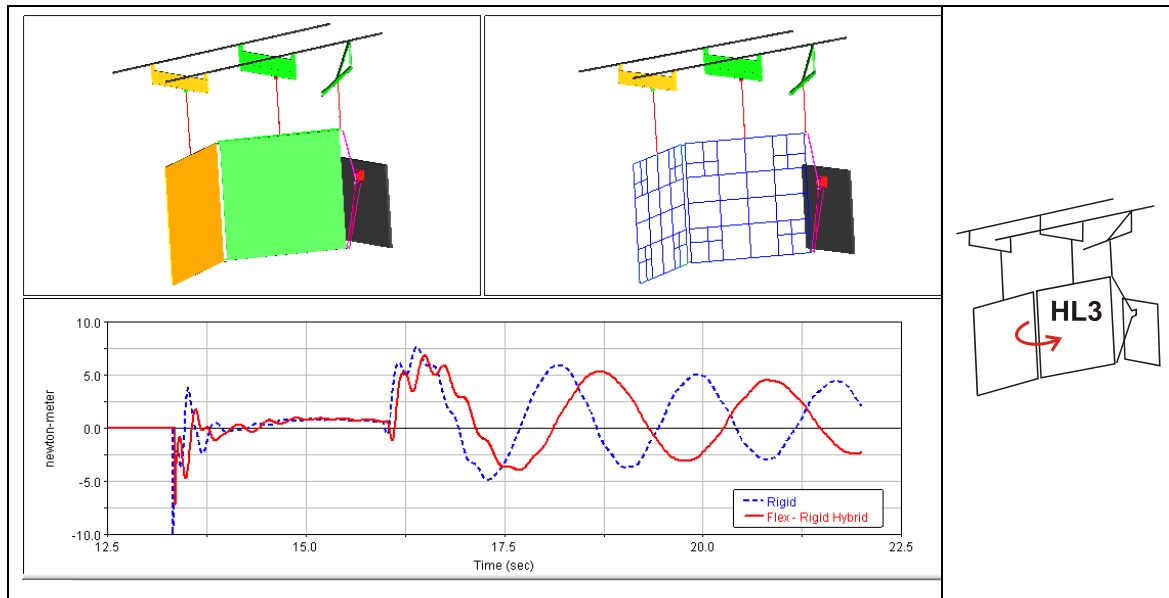


Figure 4.3.1-1: Amos-3 on-ground model Latch-up torque on HL3

Figure 4.3.1-1 show the comparison between flexible and rigid latch-up torque on HL3. Apart from the difference in the frequency we found also in this simulation a good match of results. One can conclude from this result that flexible modelling only for some selected bodies of a rigid model (see § 4.4) is a useful option.

Chapter 5

Summary and Outlook

5.1 Rigid vs Flexible – Pro & Con of the two models

The comparison of analyses in Chapter 4 had shown a substantial good correlation between the results of the two rigid and flexible (full & semi) models. Speaking about the latch-up torque we have seen that the rigid is able to catch the essence of the problem with the minimum number of DOF.

This fact demonstrates that the approximation of the latch-up stiffness in the rigid model is essentially correct:

The latching torque is influenced mainly by the lowest bending mode of the two structures involved in the latching, and the contributions of the other higher frequency modes can be neglected.

Thanks to this result we are able to affirm that for the stress analysis of the structure in NASTRAN a transient analysis is not mandatory. The low sensitivity of the latching torque on the higher frequency dynamics of the structure will in fact allow us to

represent the structural flexibility in a rotational spring with a stiffness value identified from a simple modal analysis.

Anyway the flexible analysis has put in evidence some limitations of the rigid model. As we have seen the rigid model can't include higher frequency effects and, most of all, can't capture the dynamic effects outside the deployment plane as shown in Figure 5-1. The rigid model represent a good approximation for the dynamics in the green plane of the figure (latch-up torque) but we loose the flexible dynamic effects related to the other two plane.

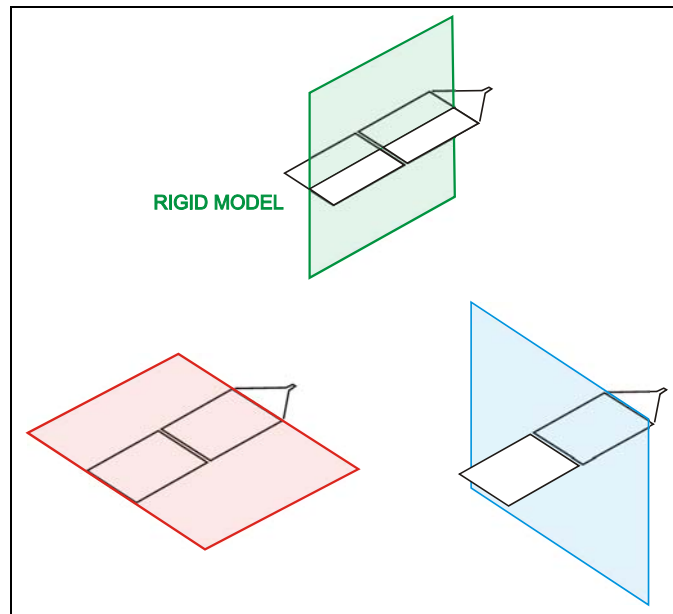


Figure 5-1: Deployment and transversal planes

So if we are interested in latch-up torque analysis this work has shown that the rigid model approach is very good and that the flexible model solution represents only a secondary improvement.

Otherwise, if we are interested in results that are influenced by transversal dynamics, the flexible approach is advisable, mainly in those cases where we have important asymmetries in the deployment plane.

The BEPI COLOMBO MPO example has shown that if we trust the rigid model we have a torque on the SADM that is nearly half of the one obtained by the flexible approach, and so the resulting margin of safety for that interface is strongly overestimated.

Table 5-1 summarizes the conclusions that can be taken after the comparison of the analysis of the two models.

	Flexible(Semi&Full) model	Rigid model
PRO	<ul style="list-style-type: none"> • No latching spring tuning required • Higher frequency effects considered • Out of deployment plane effects considered 	<ul style="list-style-type: none"> • Simple ADAMS model • Good approximation of latch-up torque
CON	<ul style="list-style-type: none"> • Flexible bodies generation and rigid model modification required • High frequency modal content in the ADAMS model (more sensitive w. r. t. time-stepping) 	<ul style="list-style-type: none"> • Latching spring tuning required • Higher frequency effects neglected • Problem with asymmetric structure

Table 5-1: Flexible vs Rigid model

Since the requirements on the easiness of generation have been matched and the effort required for the flexible analysis is not much bigger compared to the latching spring tuning process in the rigid model, the use of the flexible model is advisable.

In addition as been positively tested the possibility to use the flexible model also for quasi-static simulation. This increase the versatility of the model that can so also be used for torque margin analysis (see § 2.1).

In this prospective the rigid model preserve its importance for the preliminary design of the solar array and as first step in the generation of the flexible model.

5.2 Developments of Hybrid model

The result obtained by the hybrid model (see § 4.3) brings us to the conclusion that the flexible approach, when necessary, can be restricted only to the parts of interest.

This will give us the option to study more complicated solar arrays restricting the flexible analysis only on the bodies that, for example, are subjected to higher dynamic load.

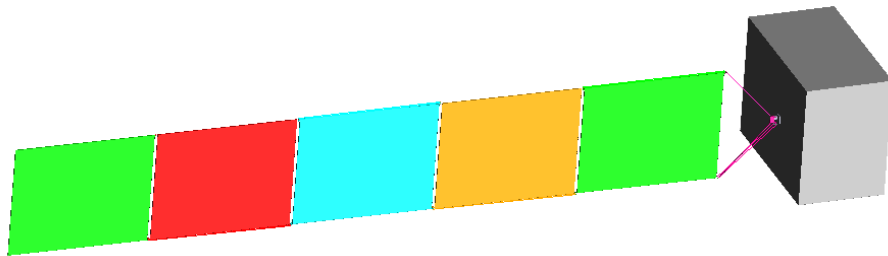


Figure 5-2: ARABSAT deployed configuration

A typical example suitable for this approach can be found in ARABSAT solar array. This 6 bodies solar array (5 panels and yoke) is characterized by a first free spring driven deployment of the first panel (see sequence of Figure 5-3) while all the others are kept stowed.

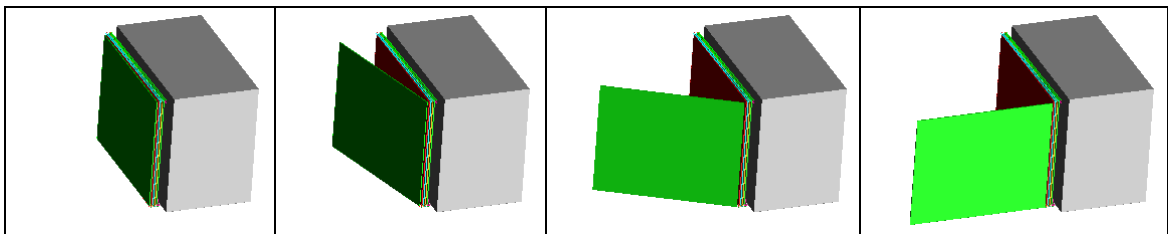


Figure 5-3: ARABSAT first phase deployment

This first free 90° deployment is necessary to provide an initial power supply that will later on also be used to drive the complete the deployment (Figure 5-4 sequence).

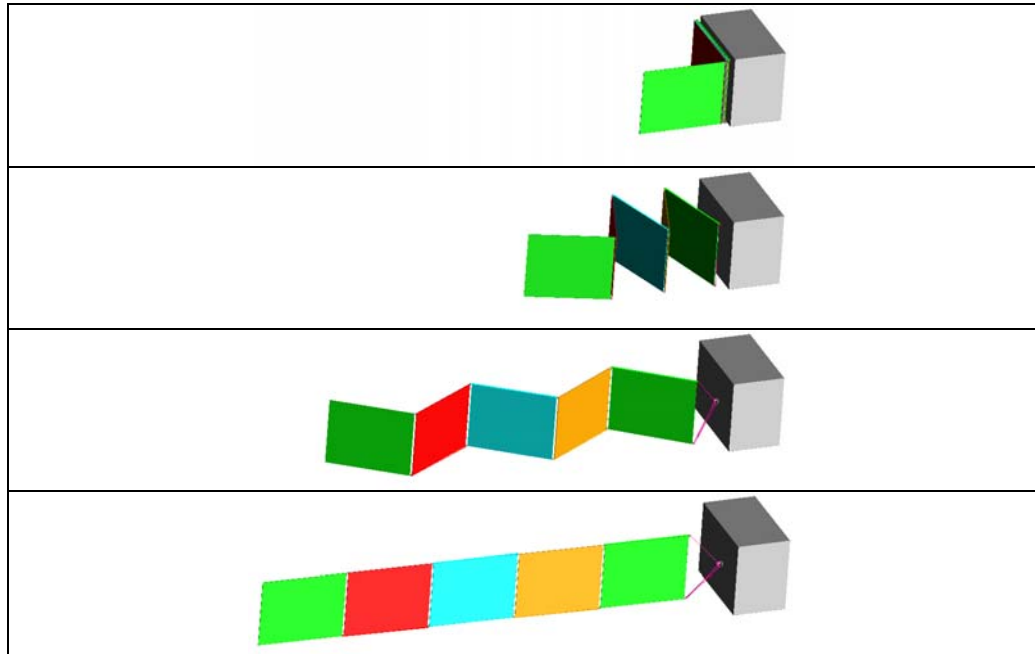


Figure 5-4: ARABSAT second phase deployment

It is evident that in this case there is no need to create a full-flexible model that, due to high number of bodies in the model, would be very complicated. The flexible analysis can be restricted to the last two outboards panels that are subjected to the higher dynamic loads of the spring driven deployment while we can keep the rest of the model rigid since the engine driven phase is very slow and can be considered quasi-stationary.

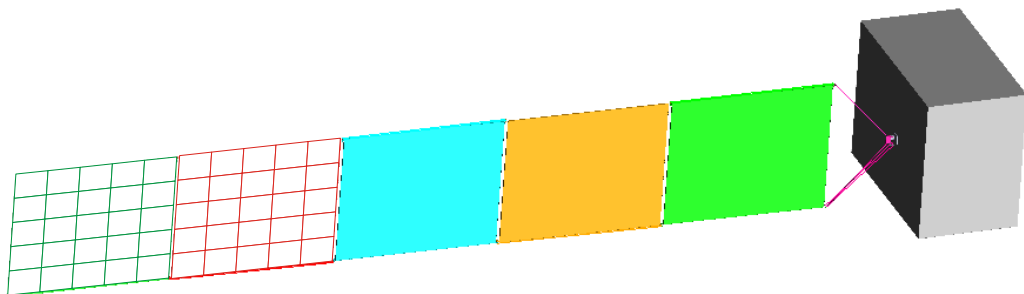


Figure 5-5: ARABSAT hybrid model

Chapter 6

Alternative Fields of Application

6.1 Alternative application of the flexible approach

This chapter show two other possible fields of application of ADAMS/flex

- Stress & Strain in ADAMS environment
- Vibration Analysis

These two alternative applications need two plug-ins of ADAMS, ADAMS/Durability for stress & strain evaluation and ADAMS/Vibration for vibration analyses.

6.1.1 Stress & Strain in ADAMS environment

During the generation of flexible bodies in the NASTRAN – ADAMS interface we can decide to include in the MNF file information concerning grid point stresses and strains. We can use then this information to get an evaluation of stress & strain directly in ADAMS environment.

The grid point stress and strain information are determined by the related element properties. So this time the FEM elements have a more important role than the mere generation of a graphical grid for the flexible bodies visualization in ADAMS; the use of the PLOTEL elements can anyway be useful as shown in Figure 6.1-1.

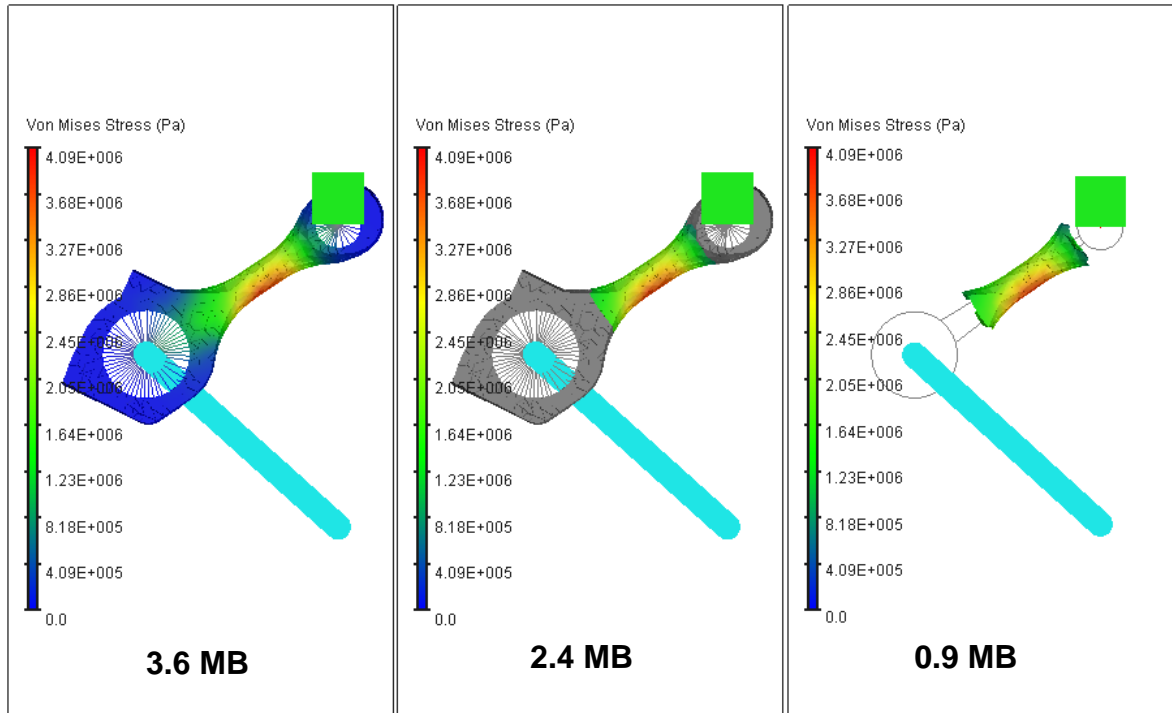


Figure 6.1-1: Stress visualization in a loaded rod with three different approaches

The three rods of Figure 6.1-1 show three different approaches to the problem.

The first flexible body on the left contains stress information for each grid point of the FEM mesh. The middle one solution instead stores stress information only about the middle part of the rod but anyway the total mesh grid is used for visualization purpose in ADAMS. The last one is the solution obtained by the use of PLOTEL and, with the same stress results as for other solution, is able to minimize the file size of the MNF file.

6.1.2 Flexible model impact analysis

What we have seen for the example of the rod can be useful if we want to have an overview of stresses on the solar array during the deployment. As for the rod in fact, also for the solar panels, we know the critical areas subjected to the higher dynamic loads.

Figure 6.1-2 shows the FEM model to use for generating a flexible body of BEPI COLOMBO MPO panel 1.

We use the fine FEM mesh only in the hinges surrounding areas and in a central circle because we want to analyze the effect of an eventual impact on the structure of panel 1.

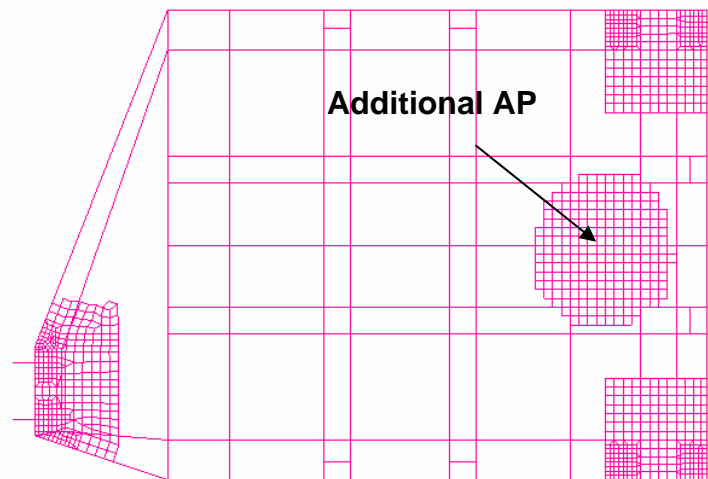


Figure 6.1-2: BEPI COLOMBO MPO panel 1 FEM model for the impact analysis

This time, in contraposition for what we have seen for example for aerodynamics loads, we define an AP on the impact node because we want to have a full local resolution in this point.

Figure 6.1-3 shows the model used for the impact analysis; analysis. Panel 1 is kept close the space craft side wall by an increased friction in HL 1 such that panel 1 will suffer a collision at the contact point (location of hold-down device) when the outboard panel runs into the latch-up mechanism.

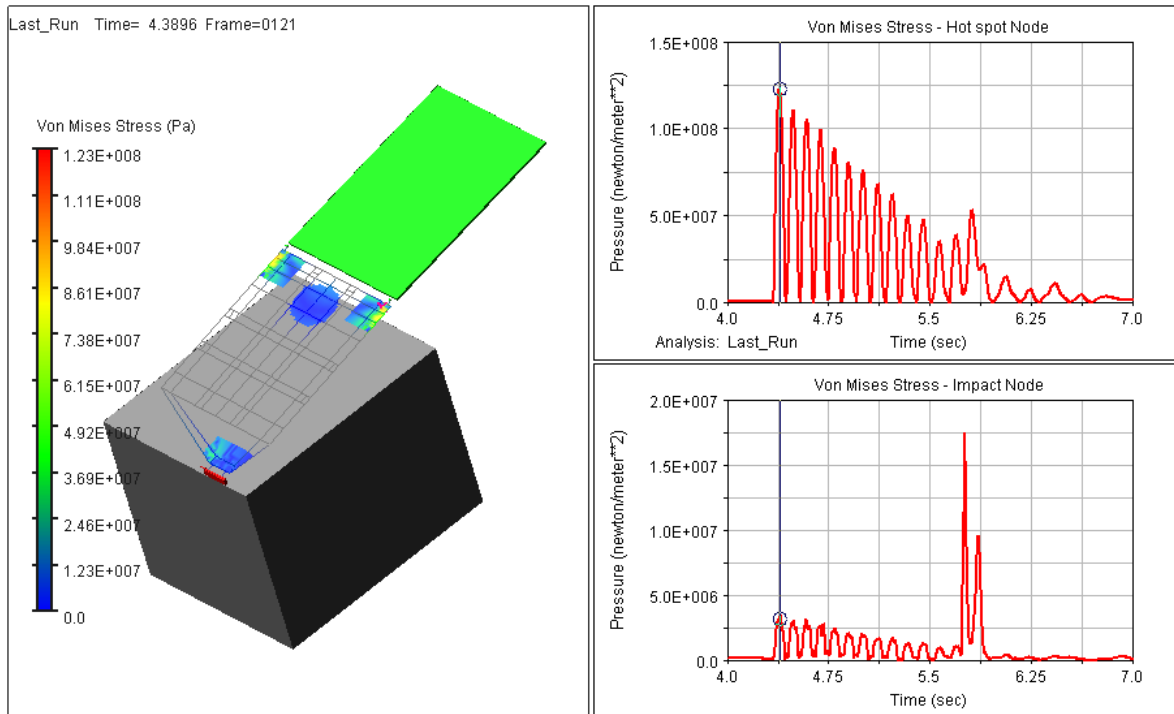


Figure 6.1-3: Impact and hot spot stress analysis

The two right charts show the evolution of Von Mises stresses in the hot spot node (red point below the right hinge in the picture) and in the impact node, respectively.

In this analysis we see that the impact is not critical with respect to the latch-up since the maximum of the stress related to the latter is one order of magnitude bigger than the one related to the former.

The user has to be aware that this stress analysis is anyway quite coarse and not sufficient for a real stress analysis. In other words ADAMS\Durability does not substitute the stress analysis in NASTRAN but anyway it can be useful in the design of the solar array deployment to see how different choices influence directly the stresses.

6.1.3 Vibration Analysis in ADAMS

Another possible application of ADAMS\Flex is the vibration analysis with the ADAMS plug-in ADAMS\Vibration.

As for the stress & strain analysis of previous paragraph this plug-in has not the claim to substitute frequency response analysis in NASTRAN but it represents a user friendly option to analyse complex problems that in NASTRAN environment require great effort.

Figure 6.1-4, taken from “getting started using ADAMS\Vibration tutorial” by MSC, shows a model of a spacecraft stored in its vector launcher.

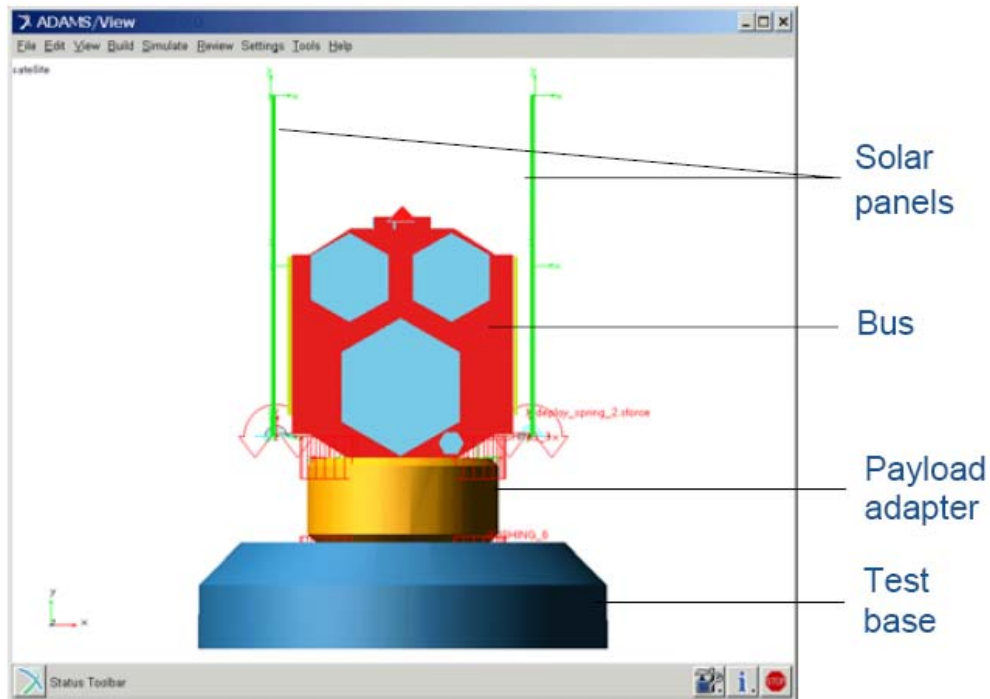


Figure 6.1-4: Spacecraft model ready for vibration analysis

Using the same procedure that we have seen to generate flexible panels for the dynamic analysis we are able to generate the panels needed for this analysis. It is clear that for this vibration analysis we have to generate flexible bodies with a higher number of fix-boundary normal modes compared to the ones used in the dynamic analysis.

In ADAMS environment we are able for example to study a whole structure of a spacecraft using different flexible bodies for each subgroup of the structure.

Figure 6.1-5 shows the example of GAIA space-craft. For each subgroup on the left we can generate an MNF file and then reassemble the spacecraft in ADAMS environment. This let us for example to define for each flexible body a particular damping function.

The same picture shows also another important aspect. The payload can be represented also by a super-element. Often the payload FEM model is available only in terms of a super-element model or directly the MNF file of the payload (since each of them is just a condensed model from which is impossible to go back to the generating FEM model). Using ADAMS the spacecraft designer can generate the related MNF from the super-element of the payload and include it in the ADAMS model and has the complete model ready for modal analysis.

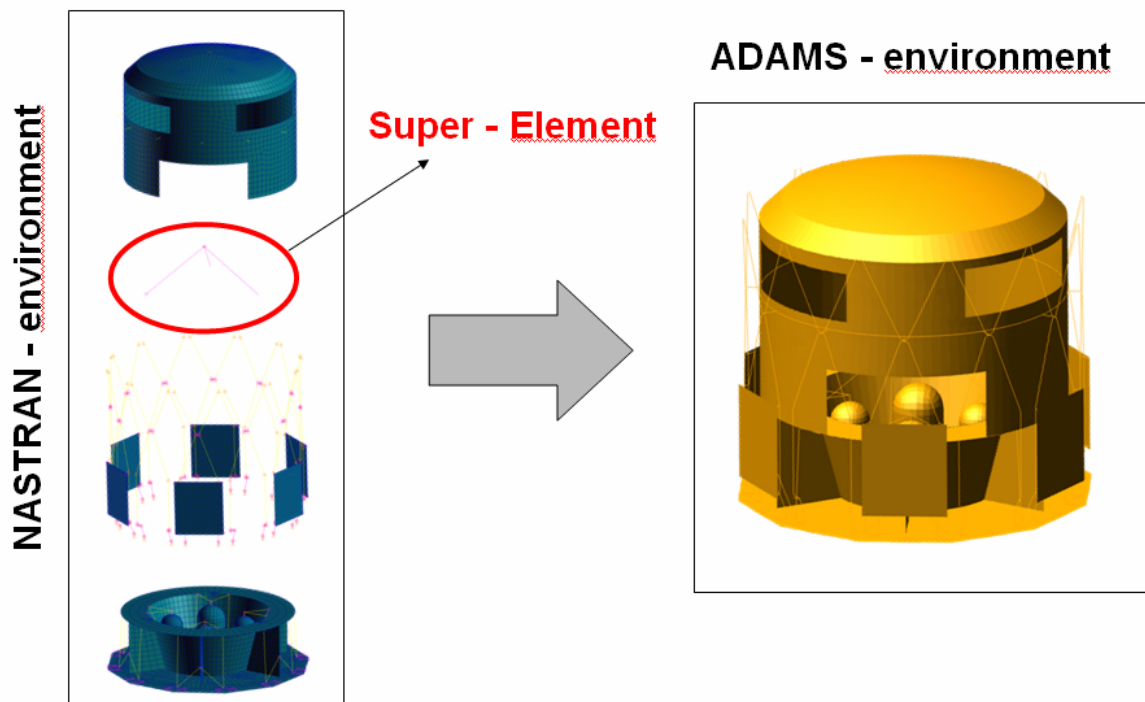


Figure 6.1-5: Generation of an ADAMS model using different flexible sub-groups

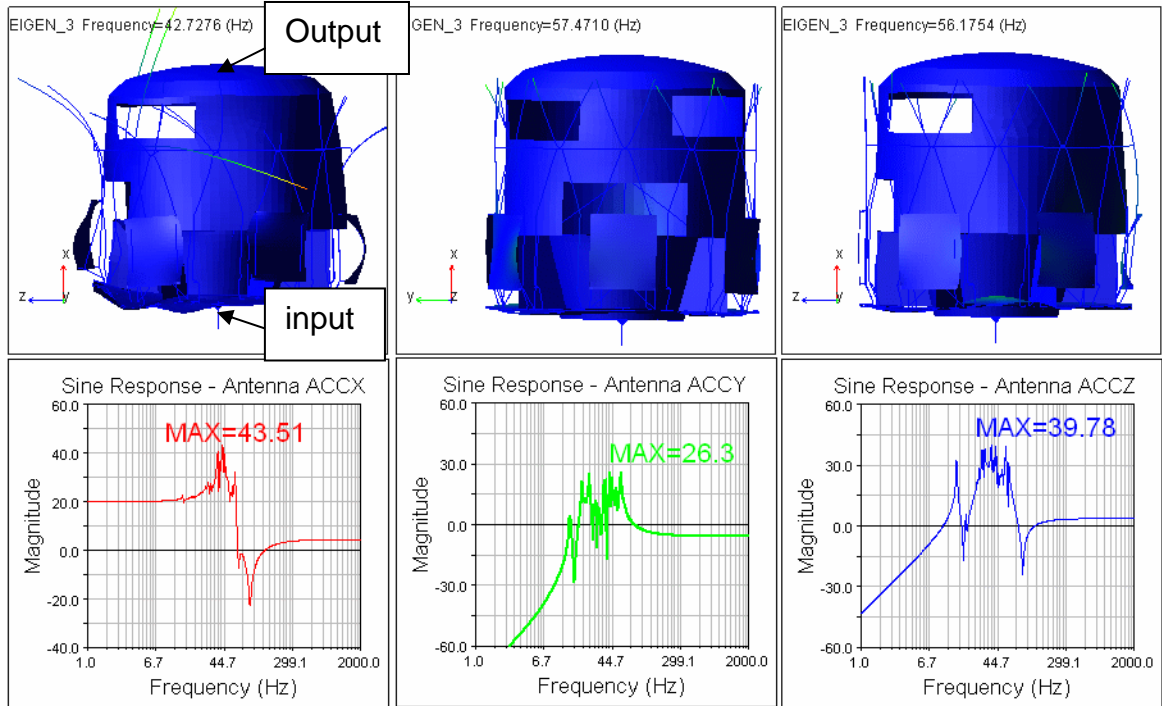


Figure 6.1-6: Response analysis of GAIA s/a ADAMS flexible model

Figure 6.1-6 shows the result of a sine response analysis along x direction. The excitation input has been applied to the base of the satellite and the response has been evaluated at the base of the antenna on the top of the cover.

Appendixes

The following appendixes represent some practical guides and tutorials in ADAMS and PATRAN/NASTRAN environment. The appendixes will show some practical aspects introduced in the first conceptual part.

The software version used in these tutorials are:

MSC.ADAMS 2005 r2

MSC.PATRAN 2005 r2

MSC.NASTRAN 2005

Appendix A

Latch-up spring Tuning

The following tutorial explains how to use ADAMS to tune the latch-up spring of the rigid model. This tuning process can be performed also in PATRAN (using BUSH element to simulate the spring DOF at the HL) but the ADAMS way is easier and more intuitive.

The target for this condensation is that the first mode of two systems, one rigid with only 1 DOF (rotational along the hinge line) and the other flexible, has the same frequency for the first deformation mode.

With this choice we implicitly assume that the flexibility effects are mainly due to the first flex bending mode of the two bodies involved in the latch-up.

The following tutorial is based on BEPI COLOMBO MPO solar array.

A.1 Getting data from NASTRAN

The first step of the tuning process is a modal linear analysis in NASTRAN. This analysis will give us the frequency to use for tuning the springs in ADAMS. The normal modes analysis has to be run with a model consisting of two bodies connected by the HL. These two bodies are panel1 and panel2 for the BEPI COLOMBO example.

We have here to distinguish two cases according to which kind of stiffness we are interested in.

- **Total Stiffness** (structure + hinges stiffness) – to use in the rigid model when we don't know the stiffness of hinges separately

In this case the FE model to use has flexible hinges as shown in Figure A.1-1

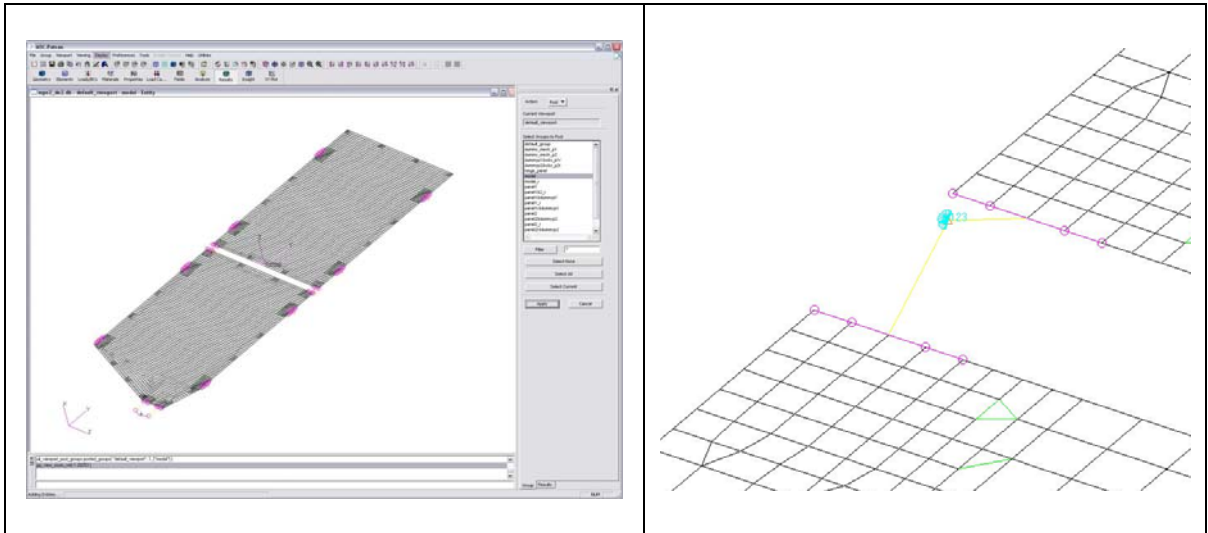


Figure A.1-1: Full-flexible model in PATRAN

- **Structure Stiffness** – to use in the rigid model when we know the stiffness of the hinges.

In this case the model to use has rigid hinges as shown in Figure A.1-2

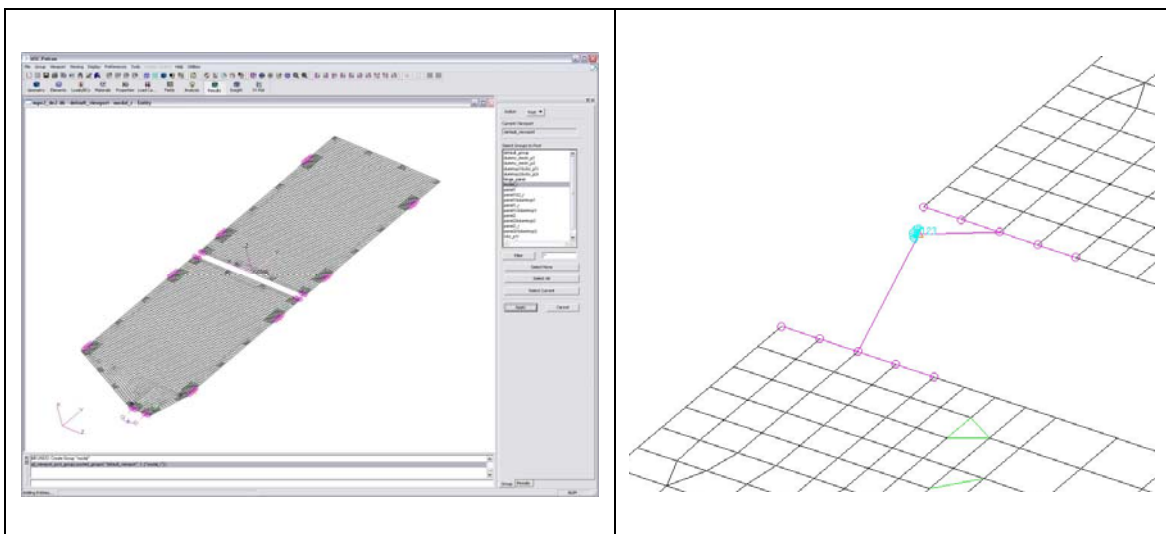


Figure A.1-2: Semi-flexible model in PATRAN

A.1.1 Constraining the PATRAN model

A key aspect to consider is how to constrain the model on the HL for the linear modes analysis in NASTRAN. One could think that the best way is to leave the model free, in fact during the deployment the HL is free from any constraint.

However, such an approach often leads to the wrong result. The only thing we can be sure is in fact the deformation of the rigid model in ADAMS. This model has only one flexible DOF and so its first and only flexible mode will be the one reported in Figure A.1-3.

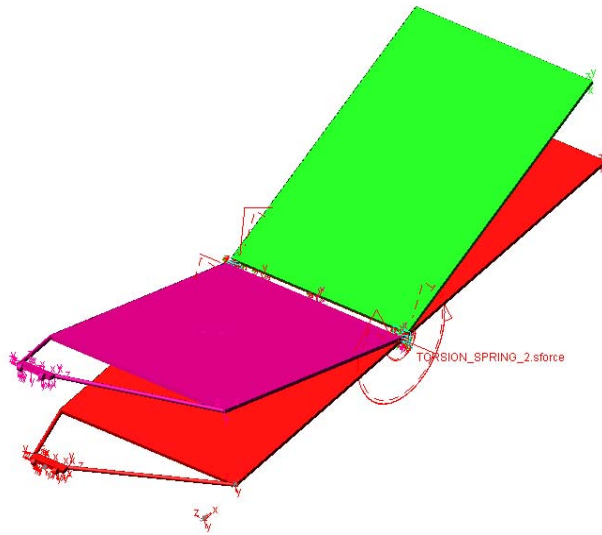


Figure A.1-3: Flexible mode in ADAMS rigid model

Now, if we run a free-free modal analysis in NASTRAN it is not certain that we will obtain a similar mode deformation.

In the case of BEPI COLOMBO solar array for example the first two flexible modes that we find with a free-free linear modes analysis are reported in Figure A.1-4

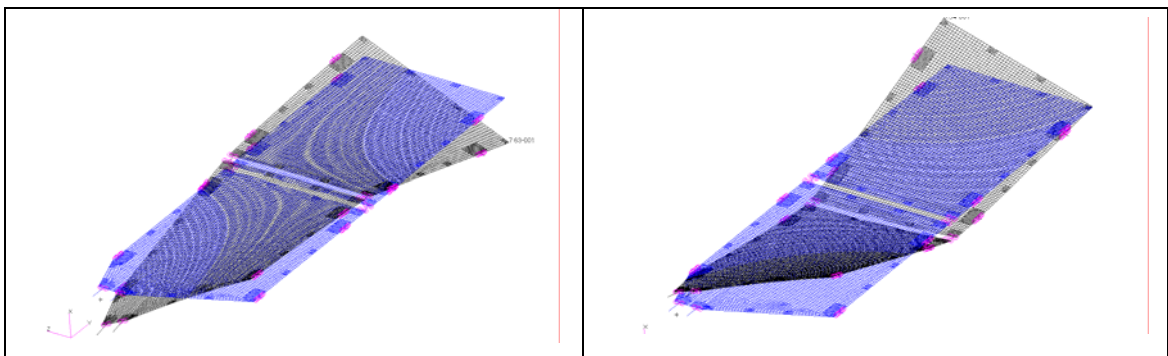


Figure A.1-4: First two flexible modes in NASTRAN obtained from a free-free analysis

These two modes shapes are impossible to obtain with our rigid model in ADAMS. For this reason we have to introduce a set of constraints on the HL.

If we fix the translational DOF of the two hinges as shown in Figure A.1-5 the first flexible mode that we obtain is characterized by the deformation reported in Figure A.1-6

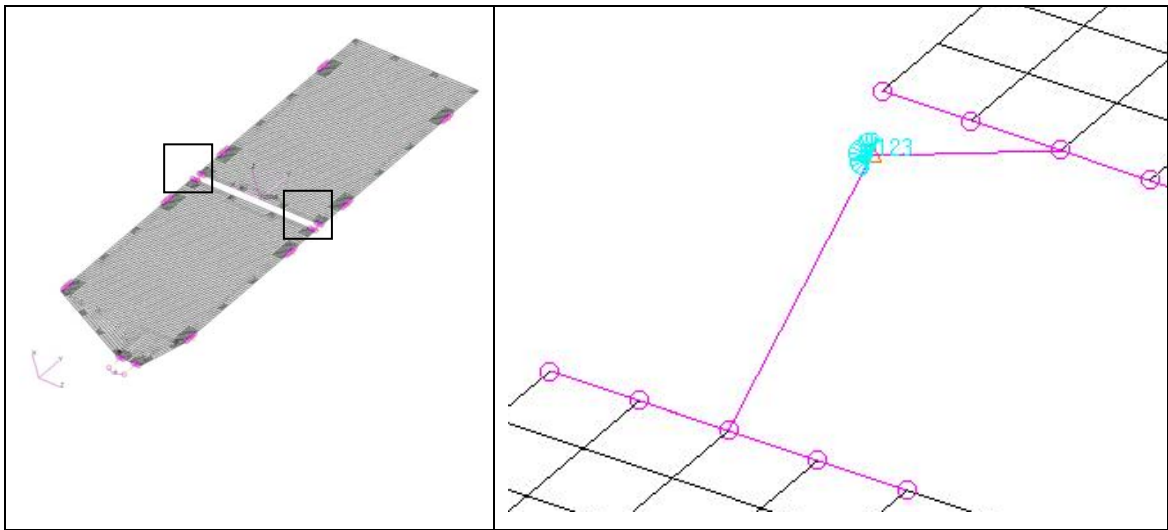


Figure A.1-5: Constraints on HL2

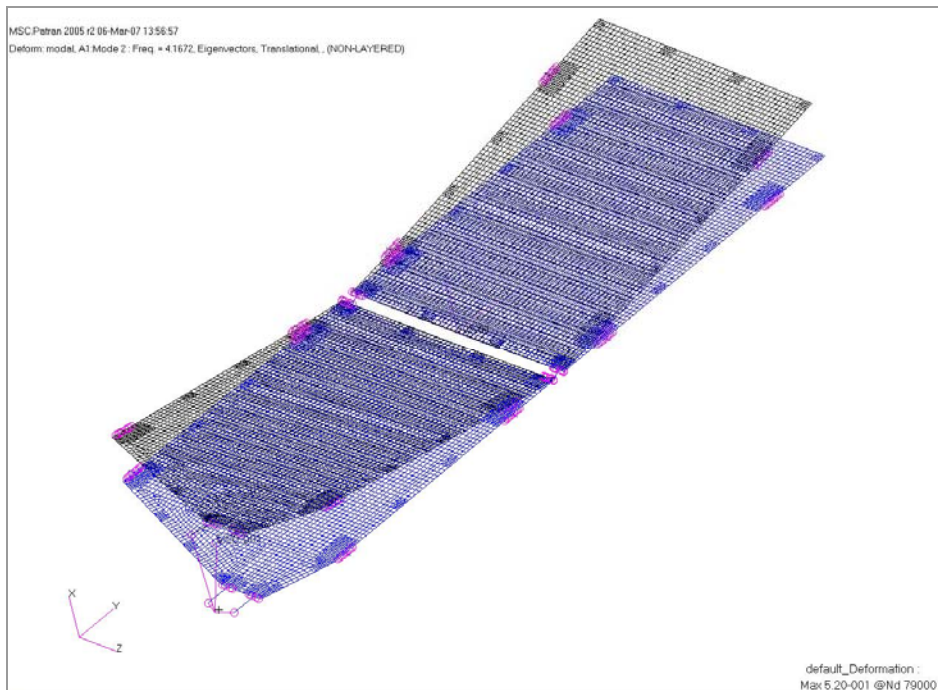


Figure A.1-6: First NASTRAN constrained model flexible mode

The mode shape that we obtain constraining the HL is similar to the one that we can obtain in ADAMS.

A.1.2 Flexible mode frequency

Once we have run the normal modes analysis we obtain the frequency related to the first flexible mode of each model

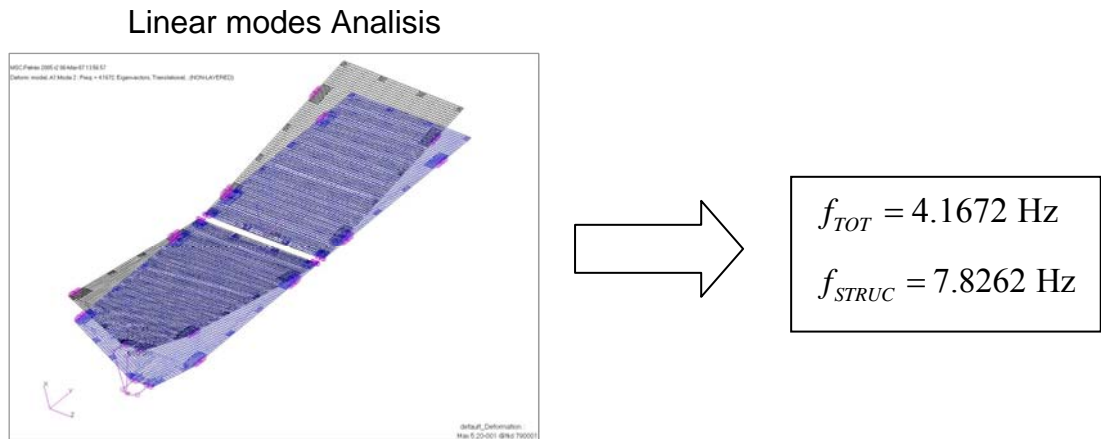


Figure A.1-7: NASTRAN first flexible mode frequencies

Where the frequency related to the merely structure is higher because it has been generated from a stiffer model.

A.2 ADAMS model

The first step in ADAMS environment is to create a partial rigid model containing only the bodies involved in the latching. Since usually we have a complete rigid model of the solar array the faster way is copy the model into a new database, delete all the unnecessary parts, and orient the two parts according to the deployed configuration.

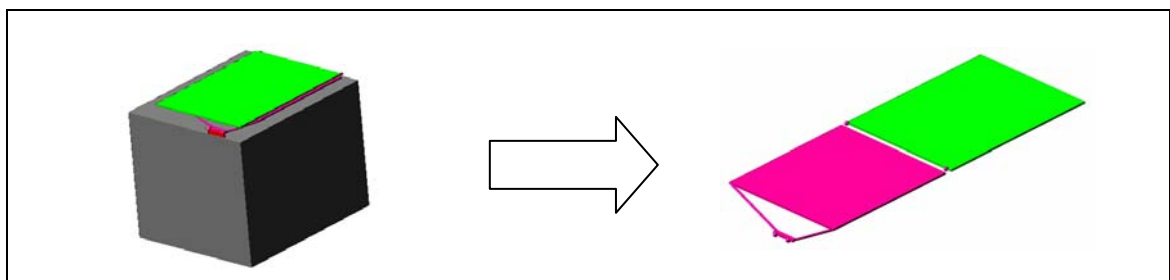


Figure A.2-1: ADAMS model obtained from the spacecraft model

The result to obtain is shown in Figure A.2-1.

A.2.1 Constraining the ADAMS model

After completion of the rigid model we have to constrain it in the same way we constrained the NASTRAN FEM. For our example the constraints are shown in Figure A.2-2

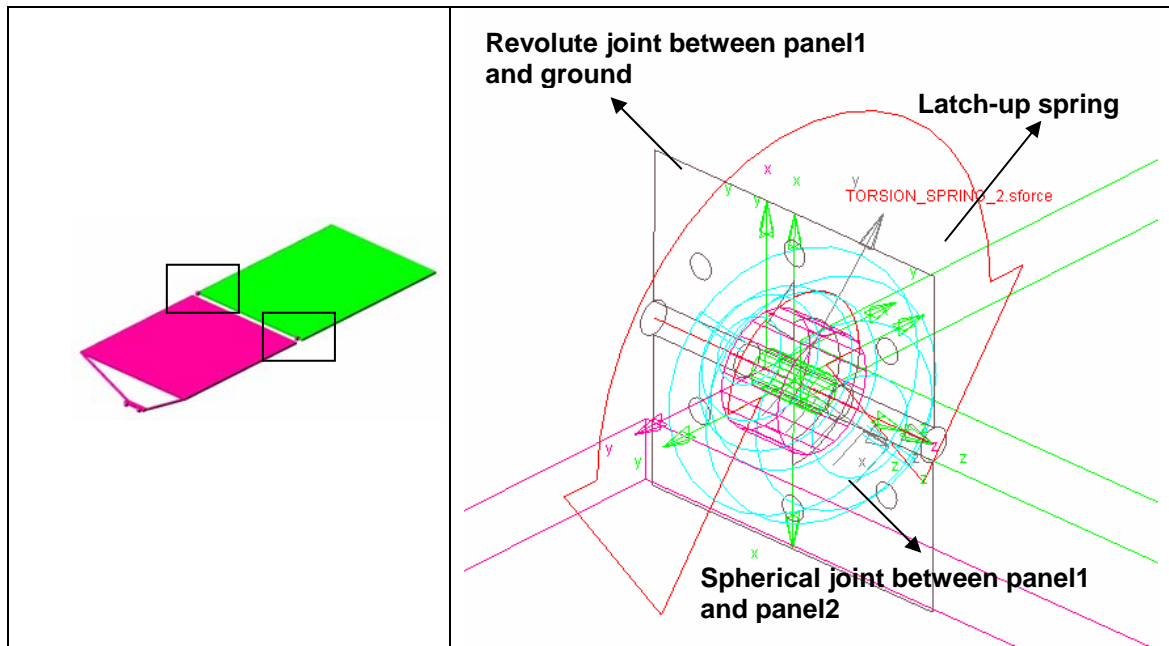


Figure A.2-2: Constraints in the ADAMS model

The spherical and revolute joints that fix the system to the ground is equivalent to the translational constraints used in the NASTRAN model.

The latch-up spring of Figure A.2-2 is the spring that we have to tune for matching the frequency. In this case we have used two springs but since the model is rigid we can obtain the same result with just one spring (with double stiffness).

A.2.2 Spring Manual Tuning

The sketch represented in Figure A.2-3 shows the procedure to adopt for tuning the latch-up springs. We start with a guess value for the stiffness and we obtain a frequency with a linear analysis in ADAMS; if this frequency is bigger than the NASTRAN one we have to decrease the stiffness and vice versa till we have found the right frequency. We can find the frequency manually after a few iterations, in next paragraph however a tutorial is reported to get it automatically in ADAMS.

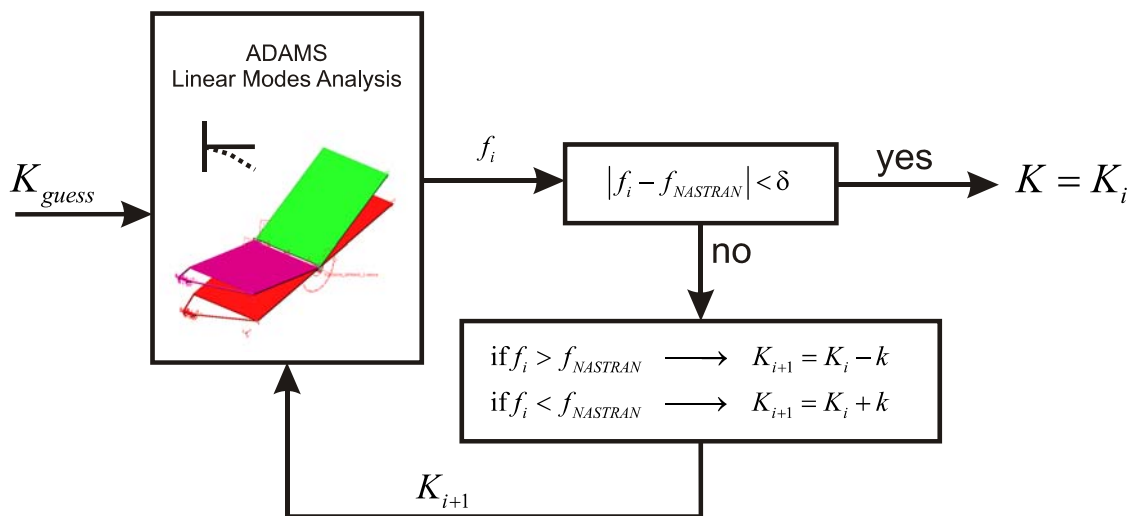


Figure A.2-3: Latch-up spring tuning pattern

A.2.3 Spring Automatic Tuning

This paragraph reports a tutorial that explains how to automatically tune the latch-up spring. Figure A.2-4 shows the starting model that will be used in this tutorial.

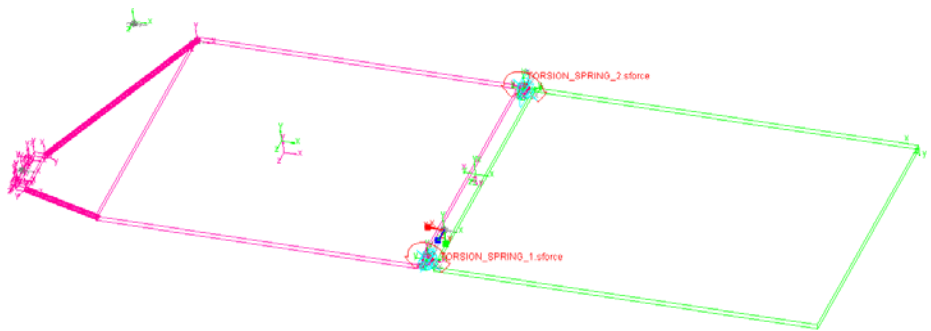


Figure A.2-4: ADAMS rigid model

The constraints on hinges are shown in Figure A.2-2. The stiffness of the two springs has to be defined as a design variable.

Select **Build** → **Design Variable** → **New**

We have to fill the box that appears as reported in Figure A.2-5.

The unit for the stiffness is Nm/deg.

The range used is quite wide because we want to be sure that the value we are looking for is included.

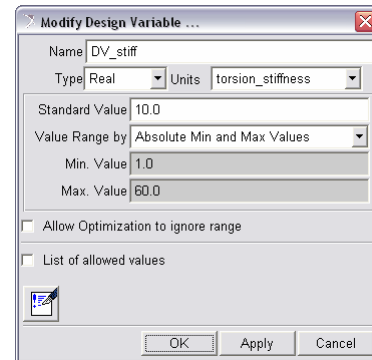


Figure A.2-5

The next step is to assign this just created variable as stiffness of the two springs as reported in Figure A.2-6

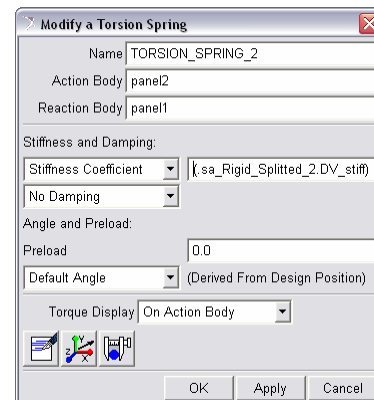


Figure A.2-6

Now we have to perform a linear mode analysis using ADAMS\Vibration. If it is off turn on the Vibration plug-in.

Select **Tools** → **Plugin Manager** → Load the ADAMS/Vibration by checking it

Now a new Vibration menu should appear

Select **Vibration** → **Test** → **Vibration Analysis**

Fill the box that appears as shown in Figure A.2-7.

We create a normal modes analysis called “normal_modes” without damping.

After clicking ok in few seconds the analysis is finished. Ignore the warning messages.

Go to ADAMS\Post-Processor and right clicking on a new page select **Load Vibration Animation**.

We find the flexible modes we are interested in is the third of the 3 normal modes found and is frequency is **2.9962 Hz**

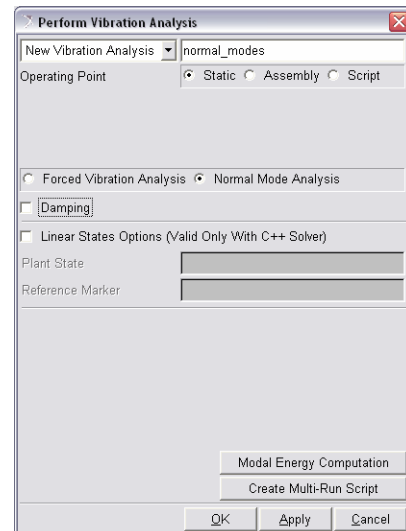


Figure A.2-7

Return to the modelling view.

Now we have to create a vibration design objective that measures the natural frequency error between the frequency of the third mode of the system and the value that we want to obtain, that can be assumed equal to 4.1672 Hz (see Figure A.1-7).

First of all we create a new design variable called “delta”. In this variable will be stored the difference between the actual frequency and the value to obtain. So the design problem will be minimize this variable varying the value of DV_stiff.

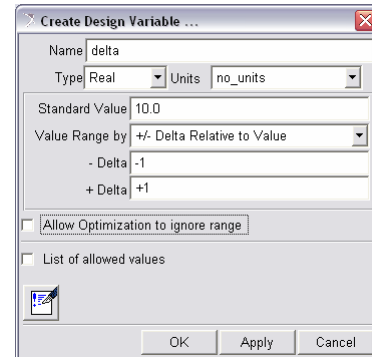


Figure A.2-8

Select **Simulate** → **Design Objective** → **New**
The Create Design Objective window appears.

Set **Definition by** to **/View Variable and Vibration Macro**

Fill the new box that pops up as shown in Figure A.2-9. After clicking ok the Create Design Objective window should appear as reported in Figure A.2-10. Don’t worry if the objective or macro number doesn’t coincide.

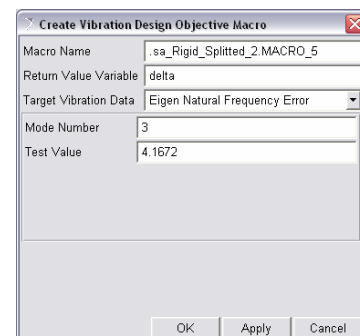


Figure A.2-9

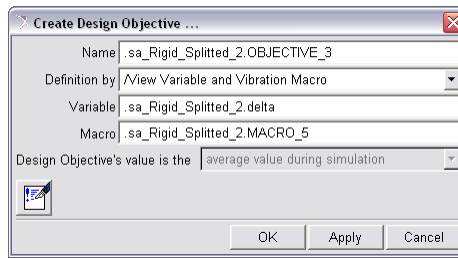


Figure A.2-10

The next step is the creation of a multi-run vibration analysis script

Select **Vibration** → **Test** → **Vibration Analysis**

Select the Vibration analysis previously created “normal_modes” and click on **Create Multi-Run Script** button.

Leave the default values in the box that appears and create the SIM_SCRIPT# by clicking on ok.

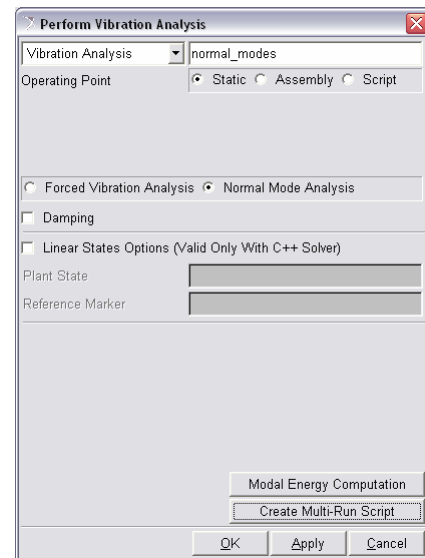


Figure A.2-11

Now we are ready to run the optimization study

Select **Simulate** → **Design Evaluation**

The window of Figure A.2-12 will appear. Select “DV_stiff” in the Design Variables box. The Goal is minimize the OBJECTIVE_3 previously created. Now we can set up the Optimizer by clicking on the corresponding button. For this analysis we can leave the default tolerances and run the optimization analysis by clicking on start.

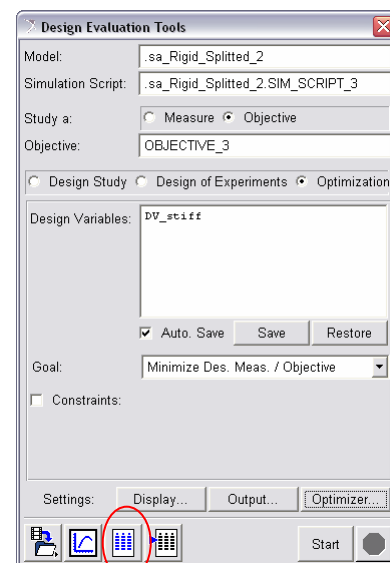


Figure A.2-12

ADAMS will run the analysis plotting the error on the objective for each iteration. After the process is converged we click on the table generator button (red circle in Figure A.2-12), click ok, and we generate the following output

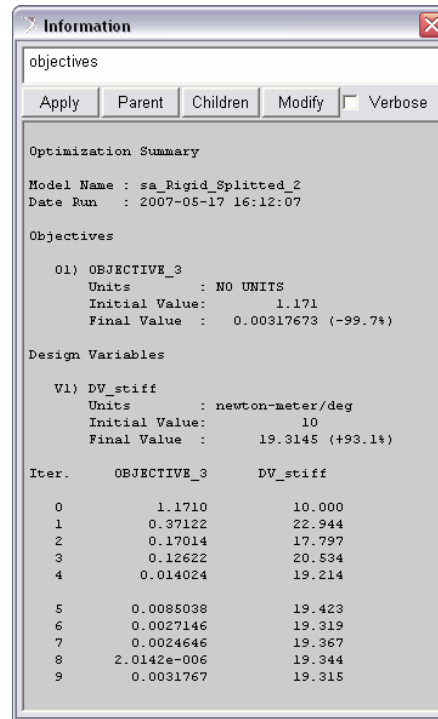


Figure A.2-13

From Figure A.2-13 we see that the minimal value of the OBJECTIVE_3 is reached for a value of 19.344 for the stiffness.

If we substitute this value in DV_stiff (since usually ADAMS set this value to the one obtained with the last optimization step, in this case 19.315) and we run a linear modes analysis (this time also using the interactive control dialogue box) we obtain for the third mode $f_3 = 4.167202$ Hz.

Appendix B

Flexible Body Generation

The following tutorial explains how to generate a flexible body in NASTRAN using the PATRAN interface. We will generate an MNF file with PLOTEL elements mesh for visualization purpose in ADAMS, for panel 2 of AMOS-3 solar array.

We will generate a part for a semi-flexible model. That means we will superimpose the BEAM of the hinges arms with rigid elements. The user can easily skip this part if interested to generate a full-flexible model.

B.1 Adapt the FEM model

The first step of the tutorial explains how adjust the FEM model and make it ready for the generation of MNF files.

Run PATRAN and open a F.E. data base (amos3_de.db in the example) as shown in Figure B.1-1.

A first thing to check is if are present or not PIN DOF on the hinge-lines BEAM elements. If present, delete the PIN DOF, modifying the properties of relative BEAMS. Their presence in fact can interfere with the modal reduction process since they are DOF of the Attachment points that we are going to generate.

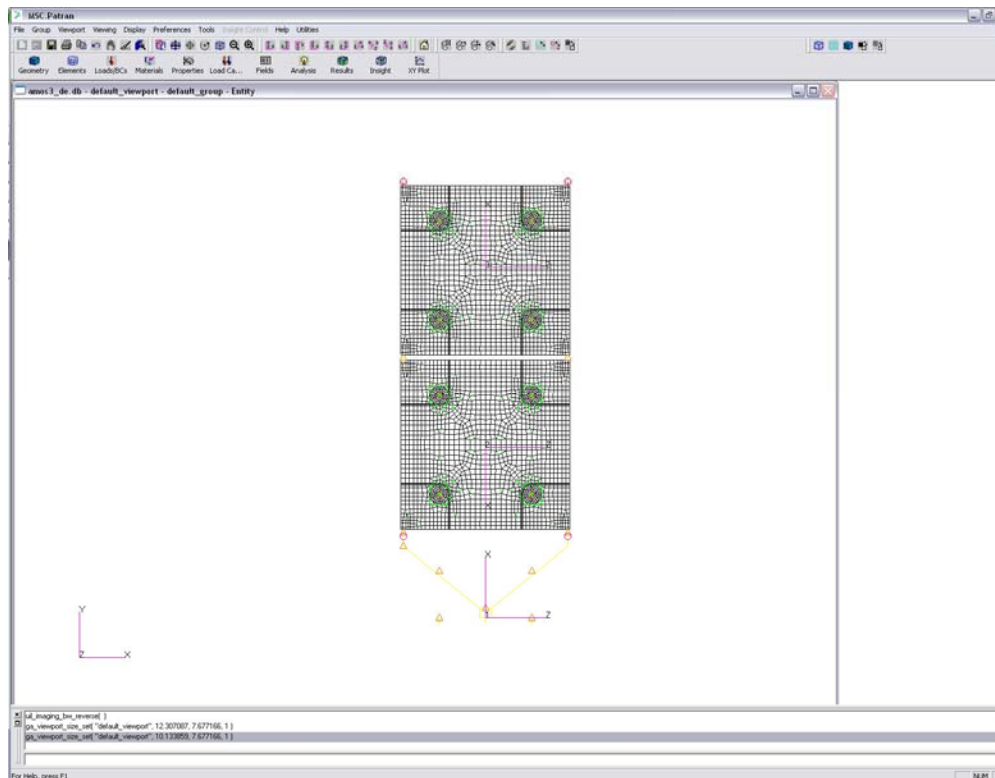


Figure B.1-1: AMOS-3 FEM model

B.1.1 Rigid hinges and mass splitting

Select the group corresponding to the panel 2

Group...

Post...

panel2

Apply

Create a new group called panel2_r. The letter r stands for *rigid*, that is because we will substitute the beams that represent the local hinge stiffness property with rigid elements (in the ADAMS model the flexibility of the hinges will be covered by the latching spring)

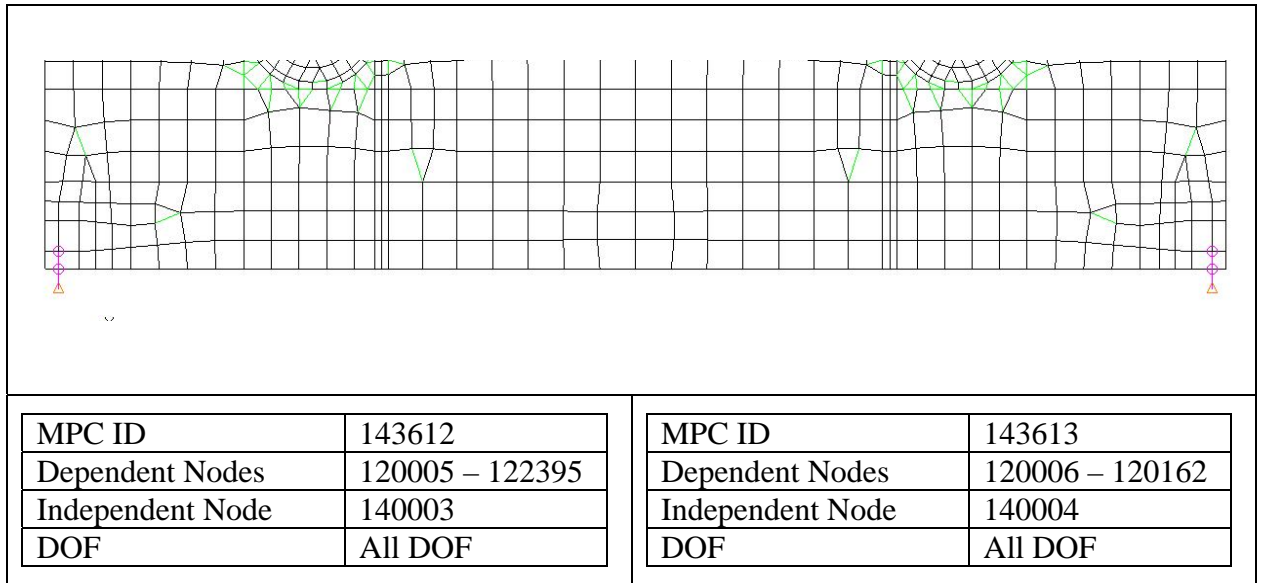


Figure B.1-3: RBE2 elements superposition on the panels

For panell1 and yoke we can proceed in the same way. Figure B.1-4 shows the new yoke_r group with rigid hinges

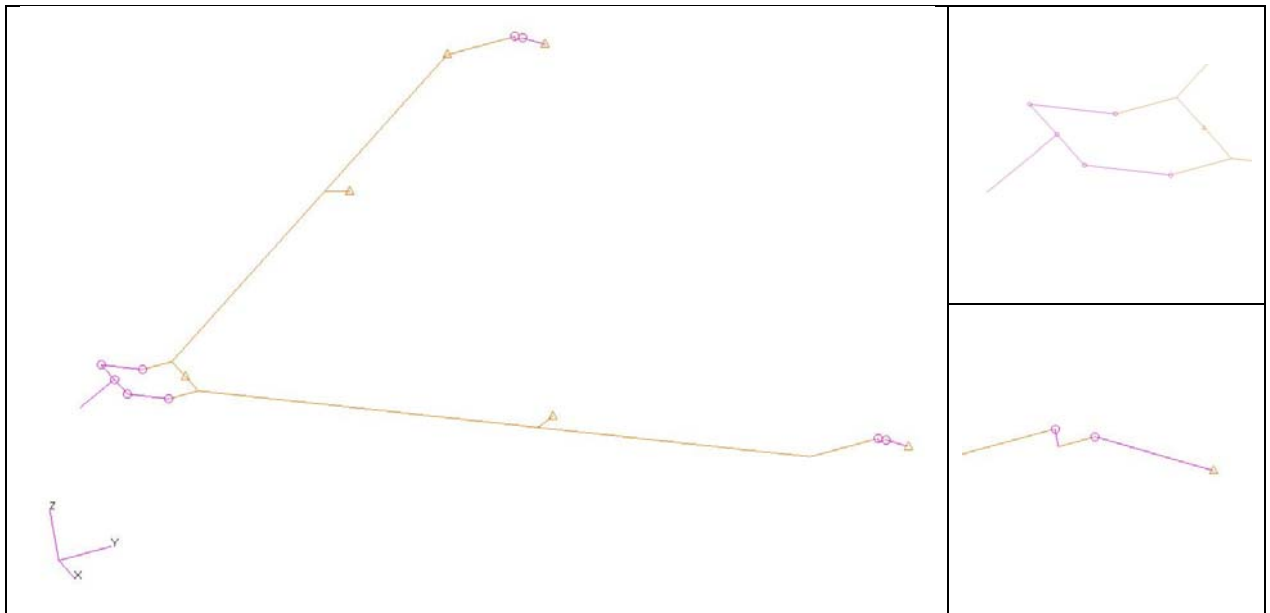


Figure B.1-4: RBE2 rigid elements superposition in the yoke

B.1.2 Attachment Points definition

The further step will be the definition of the attachment points (APs). The APs and their DOF define the generation of the *constrained modes* in the Craig-Bampton's modal reduction method (see Chapter 1).

The APs are all the interface nodes, in which two different bodies, in our example the hinge node of two panels or of the first panel and the yoke, exchange forces and torques. We will activate all 6 DOFs. This choice is not mandatory but if we not consider all their DOF, and so all the constraint modes connected to an AP, it should be like add additional constraints to the model (see Chapter 1).

◆ Element

Action:

Object:

DOF List name: "AP_p2"

Node List	140003 140004
DOFs	All DOFs

One has to be aware of some special aspects regarding the definition of APs in HL1 (hinge line 1).

Since the two real hinges of HL1 are collocated in the ADAMS model in only one revolute joint, one has to define only one relative AP with all 6 DOFs as outlined in figure below

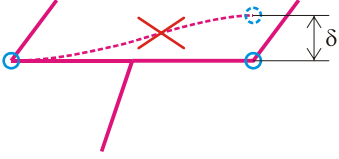
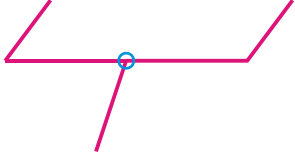


	
<p> It's not possible to define more than one AP on a rigid element because this conflicts with the definition of <i>constrained modes</i>.</p>	<p> We have to define just one AP. By the way we will have to modify the ADAMS model if more than one hinge are present.</p>

Figure B.1-5: APs definition on rigid parts

B.1.3 PLOTEL grid definition

Another important step for the implementation of a flexible body imported into ADAMS is the definition of a PLOTEL mesh.

A PLOTEL element is a dummy element that is used for visualization purpose only. A gross mesh of PLOTELS can be imported instead of the fine mesh of the FEM model decreasing the MNF (Modal Neutral File) file size and the GPU load during the ADAMS rendering phase.

Using a gross grid does not mean having worse results! In fact, the computational size of the flexible body in ADAMS is determined by the number of selected fix-interface normal modes and constrained modes.

Before starting the dummy grid we have to create a new group that will be the union set of panel2_r and its dummy mesh representation.

Group...

Create...

New group name “panel2_r&dummysp2”
Entity selection “...all entities of panel2 group”

Post “panel2_r&dummysp2”

Now we have to create a new property for the dummy elements of panel2

◆ Properties

Action:
Object:
Typet:
Property Set Name “dummy_p2”

<i>Property Name</i>	Dummy Property Data
<i>Value</i>	DUMMY
<i>Value type</i>	DUMMY

For an easy selection of the PLOTTEL we will start their numbering starting from 500

◆ Element

Action:
Object:
Element ID list “500”
Shape:
Topology:
Pattern:
 “dummy_p2”

There is not a particular strategy for creating the PLOTTEL elements mesh. It's clear that if we create a fine mesh we will have a better graphical result and a better comprehension of the deformation shape but we will pay this in terms of file size and computational time.

When defines the PLOTTELs lines one has to avoid the intersection between two or more PLOTTEL elements because this could generate misunderstanding. This situation is well explained in the example of Figure B.1-6 about a saddle deformation.

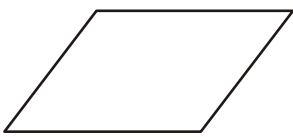
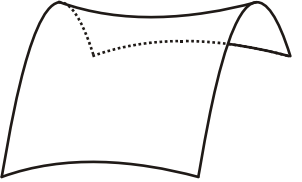

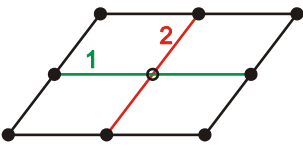
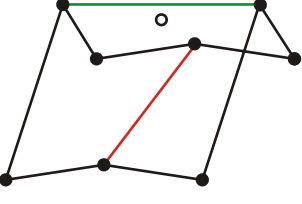

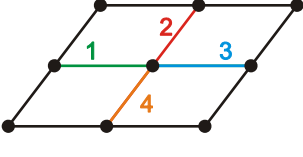
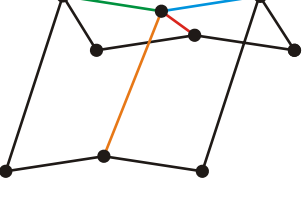
<p>A square plane undergoes a saddle deformation.</p>		
<p> The intersection between two PLOTTEL elements generate a bad deformation shape. The saddle geometry is lost.</p>		
<p> If we avoid the intersection we obtain a better approximation of the deformation shape.</p>		

Figure B.1-6: Visualization of a saddle deformation using plotel

A reasonable result of an 80 PLOTTEL elements grid is showed in figure below

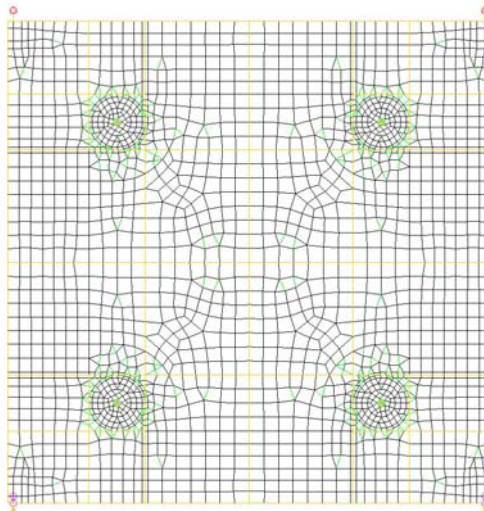


Figure B.1-7: Fine mesh + PLOTTEL mesh on panel 2

Now we can create a new group for the dummy grid

Group...

Create...

New group name “dummysp2”

Entity selection “Elm 500:579”

Post “dummysp2”

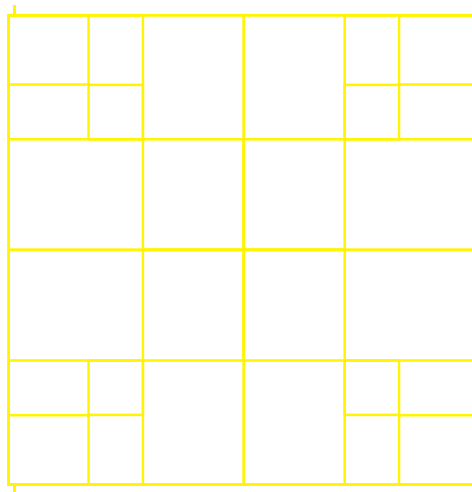


Figure B.1-8: PLOTTEL mesh grid

Notice that for a correct working of the NASTRAN – ADAMS interface the nodes that define the PLOTTEL elements in the dummysp2 group have to be a subset of the nodes from the fine mesh.

B.2 Definition of Load Cases

For creating the MNF to import in ADAMS we have to run a free-free modal analysis. The related *free-free* load case without any forces or displacement is defined below.

◆ Load Cases

Action:

Load Case Name "free"
 ...empty

B.3 Analysis

Now everything is prepared to go through the analysis phase. If we repeat the steps before for each body of the solar array at this point we have the groups of Table B-1 ready for the analysis. We have now to run three different analyses, one for each of the three bodies that form the solar array.

Group for the analyses	Related PLOTTEL mesh groups
panel1_r&dummysp1	dummysp1
panel2_r&dummysp2	dummysp2
yoke_r&dummysp0	dummysp0

Table B-1: Group for the analysis and related PLOTTEL mesh group

Going on using panel 2

Action:

Object:

Method:

Job Name "am3_p2_mnf"

 panel2_r&dummysp2

Translation Parameters...

...leave the default values

Solution Type...

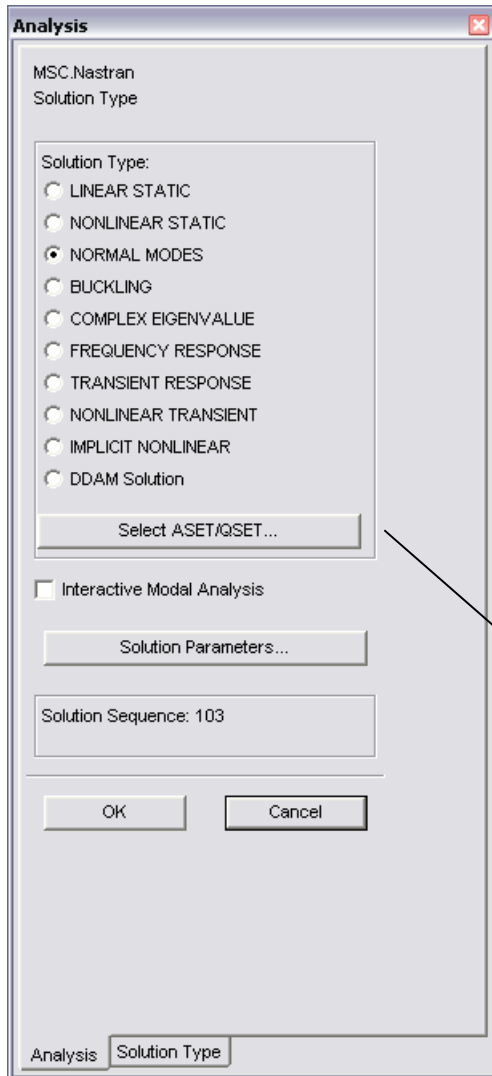


Figure B.3-1

The Solution Type window appears. As show in the picture aside.

Solution Type NORMAL MODES

Then we have to select the ASET/QSET. The new window that pops up enables us to chose one of the DOF list we have previously defined as APs DOF list.

Select ASET/QSET

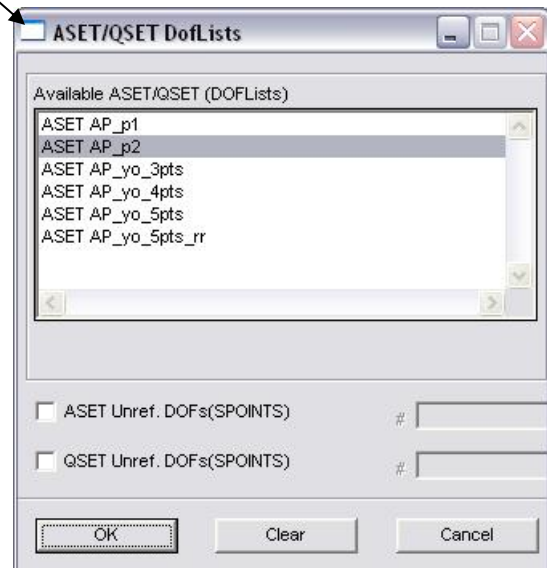


Figure B.3-2

Solution Parameters...

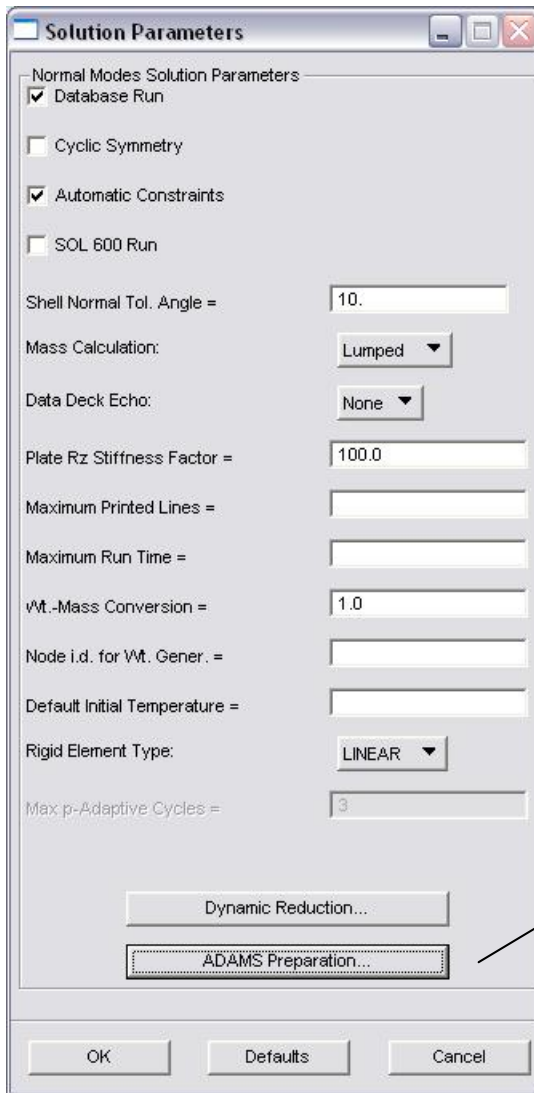


Figure B.3-3

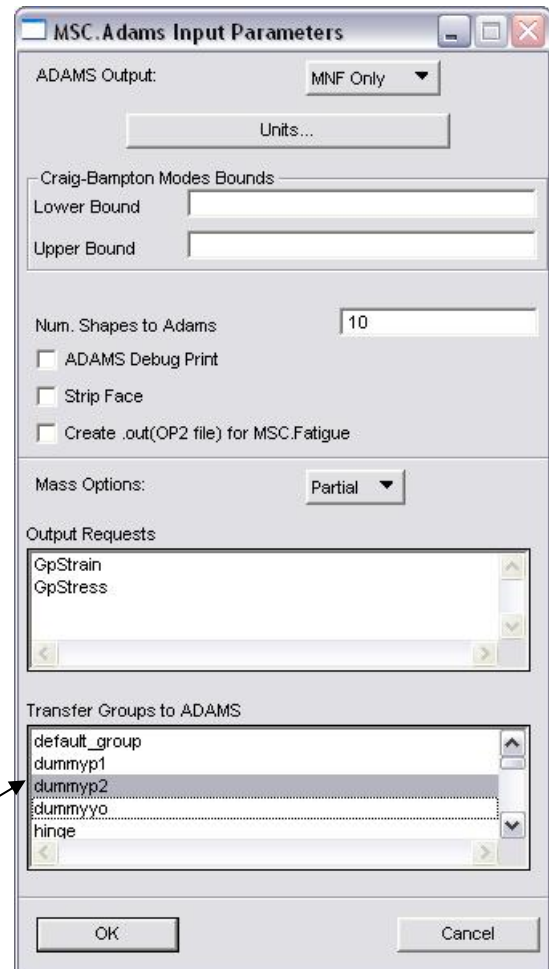


Figure B.3-4

We can leave the default values show in the figure above and finally enter the ADAMS Preparation menu.

ADAMS Output:

MNF Only

In the ADAMS output there is also the option “Full Run + MNF” run which creates the XDB file containing the modal results.

The modes that we obtain in this XDB file are those of the reduced model (Craig-Bampton orthogonalized) and not those of the full F.E. model.

Units...

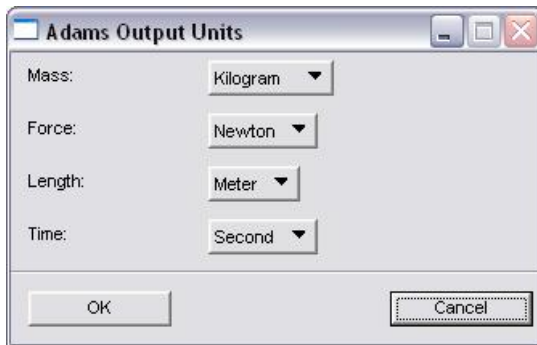


Figure B.3-5

Notice that ADAMS, differently from PATRAN, is not an unitless software. Please be sure to choose the right units for the model because this units will be stored in the MNF file and imported in ADAMS

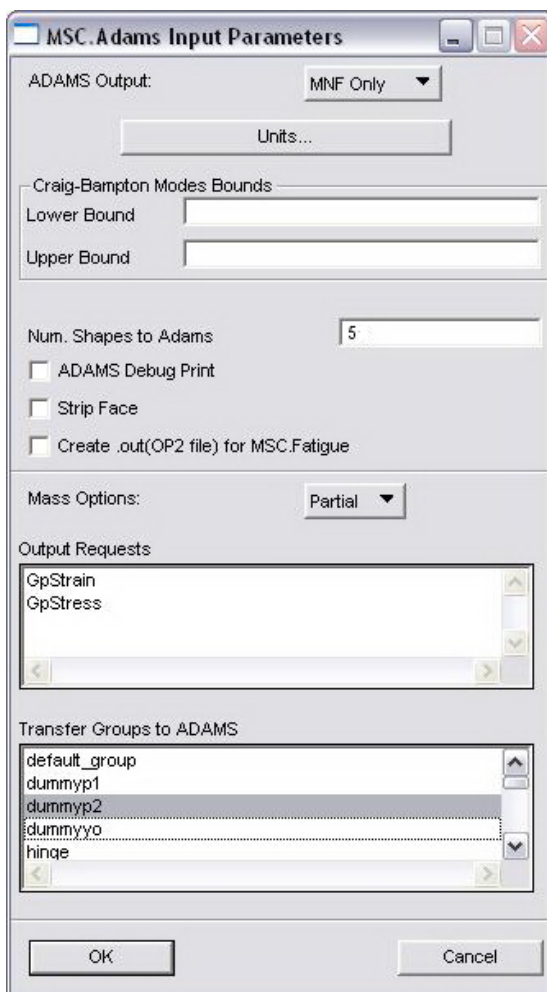


Figure B.3-6

We can leave blank the Craig-Bampton Modes Bounds. NASTRAN uses then the default values.

In the Num. Shapes to Adams we have to enter the number of dynamic modes (fix-interface normal modes) that will be calculated. 5 modes are enough in our example to have a good approximation of the flexible behavior of the panel during the deployment.

We don't select anything in the Output Requests window and for the Transfer Groups to ADAMS we select dummyp2. This will be the group that ADAMS will use to visualize the panel

After clicking OK we get two warning message from PATRAN that inform us that NASTRAN will use default values for Craig-Bampton bounds value.

Now we can come back to the analysis window and select the Subcases button.

Subcases...

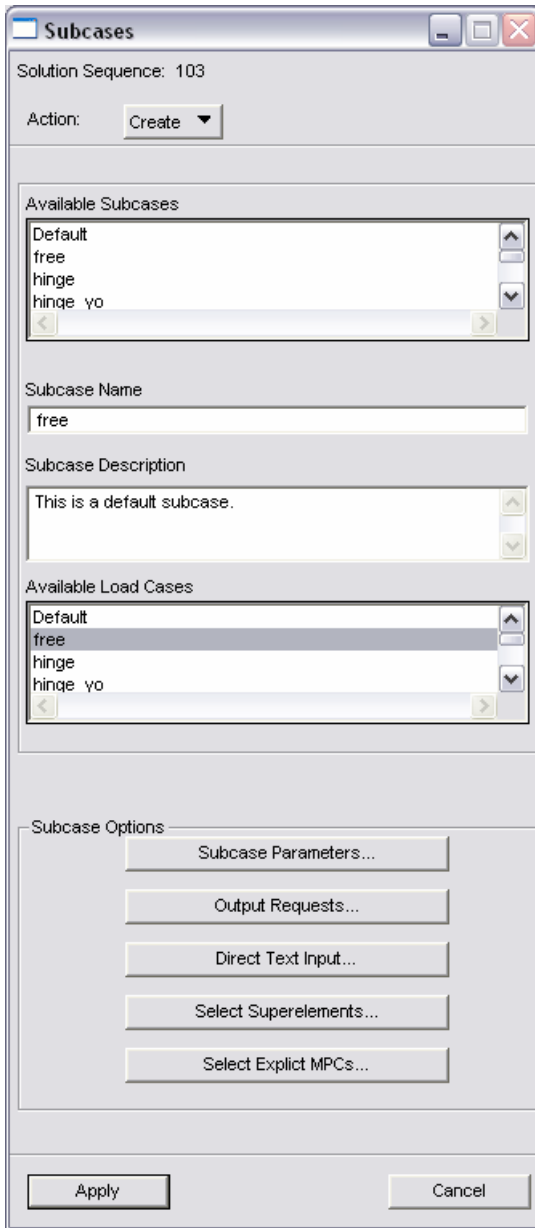


Figure B.3-7

We have to select the “free” load case that we have already created and then we can leave the other options at their default values.

Subcases Select...



Figure B.3-8

After the selection of the “free” subcase the analysis run can be submitted

From the analysis window

Apply

PATRAN will create the .BDF input file for NASTRAN.

B.4 Editing the BDF file

The next step describes a manual adjustment to the BDF file. This change is necessary because in the GUI of PATRAN is impossible to set the case control delimiter *OUTPUT* with the input *PLOT*.

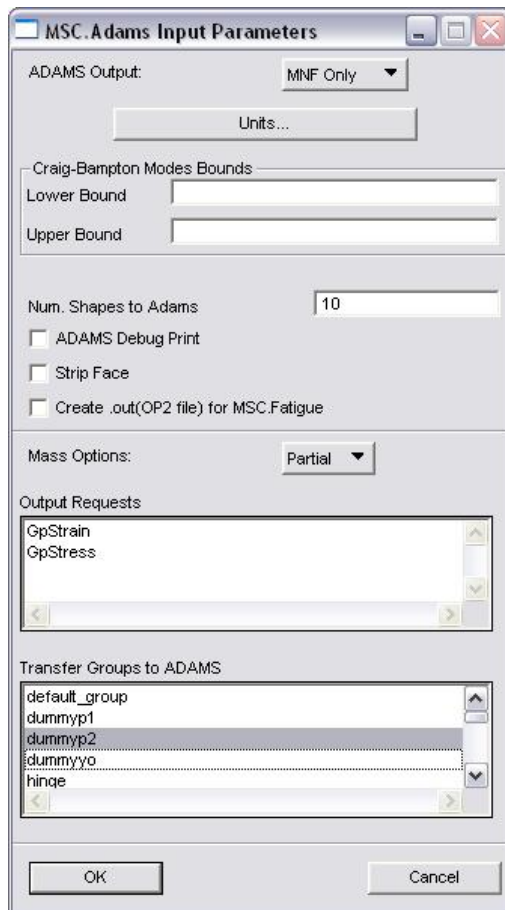


Figure B.4-1

PATRAN in fact set the *OUTPUT* command to *POST*, but this is the command for plotting grid points stresses or strains even if they are not requested in the Output Requests window as shown aside.

Instead we need *OUTPUT(PLOT)* which introduces the plotter commands responsible for the creation of the dummy mesh used by ADAMS for visualization purpose.

The strings reported in Figure B.4-2 show the simple change to apply at the BDF file

<pre> \$ NASTRAN input file created by the MSC MSC.Nastran input file \$ translator (MSC.Patran 13.1.116) on January 16, 2007 at 14:51:46. \$ Direct Text Input for Nastran System Cell Section \$ Direct Text Input for File Management Section \$ Normal Modes Analysis, Database SOL 103 \$ Direct Text Input for Executive Control CEND TITLE = AMOS-3 SOLAR ARRAY ECHO = NONE SET 1=2 ADAMSMNF FLEXBODY=YES,FLEXONLY=YES,PSETID=1 \$ Direct Text Input for Global Case Control Data SUBCASE 1 \$ Subcase name : free SUBTITLE=free METHOD = 1 VECTOR(PLOT, SORT1, REAL)=ALL SPCFORCES(PLOT, SORT1, REAL)=ALL \$ Direct Text Input for this Subcase OUTPUT (POST) \$ Elements for group : dummysp2 SET 2 = 500 THRU 578,579 BEGIN BULK PARAM POST 0 PARAM SNORM 10. PARAM PRTMAXIM YES ... </pre>	<pre> \$NASTRAN input file created by the MSC MSC.Nastran input file \$ translator (MSC.Patran 13.1.116) on January 16, 2007 at 14:51:46. \$ Direct Text Input for Nastran System Cell Section \$ Direct Text Input for File Management Section \$ Normal Modes Analysis, Database SOL 103 \$ Direct Text Input for Executive Control CEND TITLE = AMOS-3 SOLAR ARRAY ECHO = NONE SET 1=2 ADAMSMNF FLEXBODY=YES,FLEXONLY=YES,PSETID=1 \$ Direct Text Input for Global Case Control Data SUBCASE 1 \$ Subcase name : free SUBTITLE=free METHOD = 1 VECTOR(PLOT, SORT1, REAL)=ALL SPCFORCES(PLOT, SORT1, REAL)=ALL \$ Direct Text Input for this Subcase OUTPUT (PLOT) \$ Elements for group : dummysp2 SET 2 = 500 THRU 578,579 BEGIN BULK PARAM POST 0 PARAM SNORM 10. PARAM PRTMAXIM YES ... </pre>
--	---

Figure B.4-2: Modification to apply to the BDF file

The command *POST* is used for the generation of the stresses and strains grids, so if one forgets to substitute it with *PLOT*, the results obtained will be

- 1) The fine elements mesh for visualization in ADAMS. This comport a bigger file size and a slowing down in all rendering operations in ADAMS
- 2) The superimposition of the PLOTEL mesh

In figure below the two different results imported in ADAMS environment.

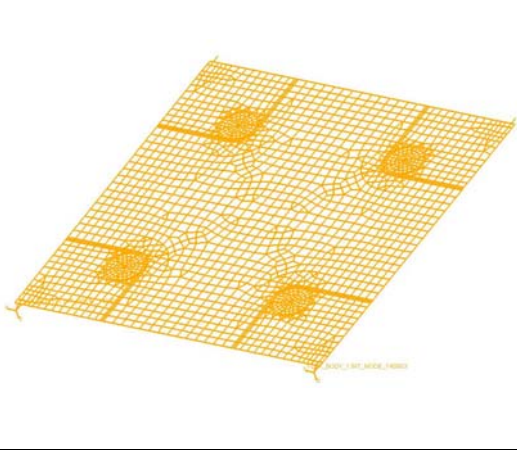
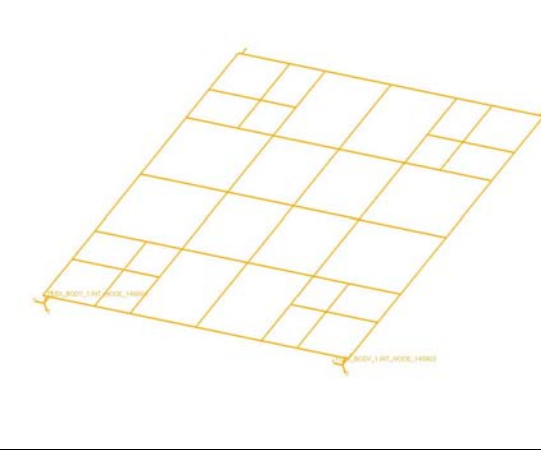
<i>OUTPUT(POST)</i>		<i>OUTPUT(PLOT)</i>	
			
Element Faces	2476	Element Faces	80
MNF File size	2537 KB	MNF File size	72 KB

Figure B.4-3: Sizes differences using or not the PLOTEL

Appendix C

Flexible Body with Stress & Strain

The following tutorial explains how to generate a flexible body containing stress & strain information in NASTRAN using the PATRAN interface.

Such an approach makes it possible to estimate the S&S due to the dynamic or to the latching torque using the same ADAMS model used for the deployment analysis (see Chapter 5). We will show now two different ways of doing that using the first panel of BEPI COLOMBO MPO solar array as an example.

C.1 Full mesh S&S

This first approach will generate a MNF file containing S&S information on the whole set of grid points of the mesh.

In this case we need just a group in PATRAN containing the first panel as shown in Figure C.1-1

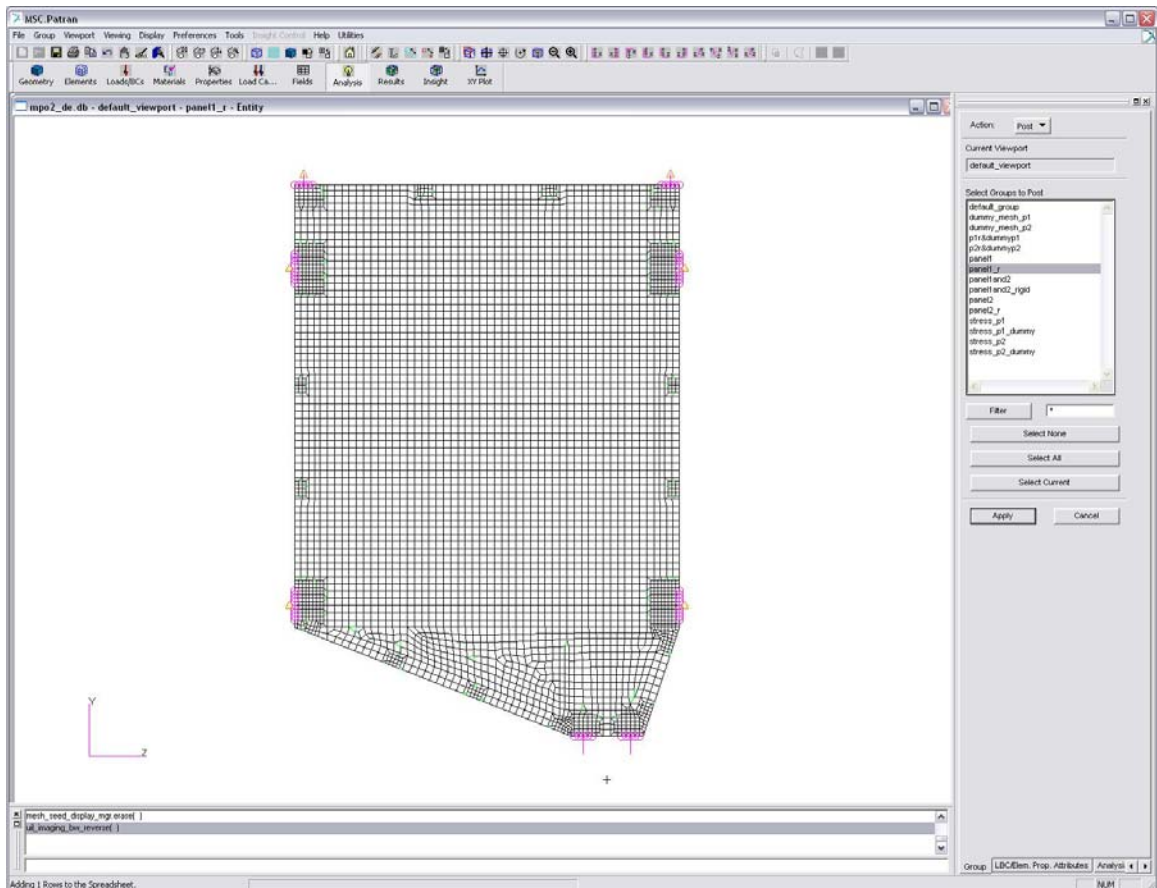


Figure C.1-1: BEPI COLOMBO MPO panel 1 FEM model

Then we have just to follow the same procedure as already described in Appendix B for generating a flexible body.

Action:

Analyze

Object:

Selected Group

Method:

Analysis Deck

Job Name

“p1r_10_SaS_1”

Select Group...

panel1_r

Translation Parameters...

...leave the default values

Solution Type...

The Solution Type window appears as shown in Figure C.1-2.

Then we have to choose the ASET/QSET. The new window that pops up enables us to choose one of the DOF list we have previously defined as AP DOF list (refer to Appendix B).

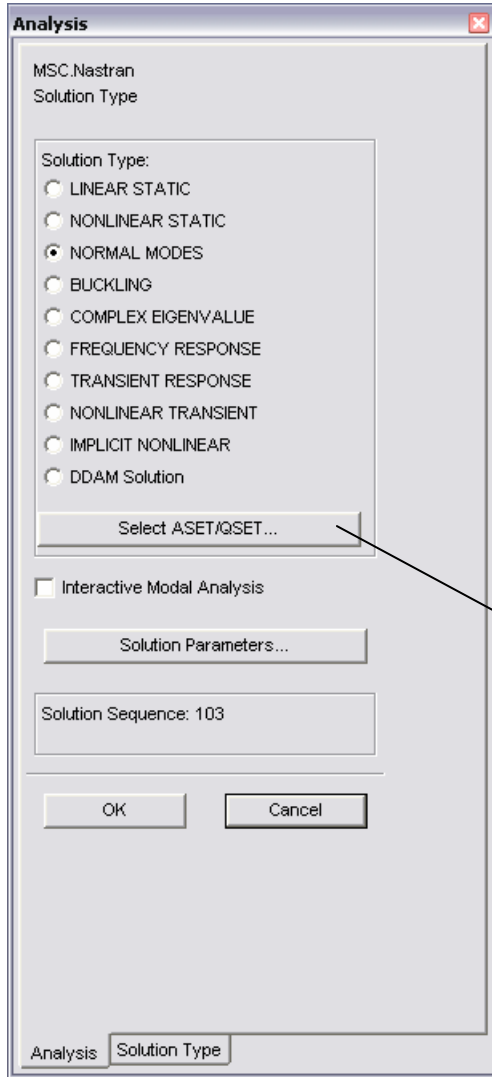


Figure C.1-2

Solution Type NORMAL MODES

Select ASET/QSET

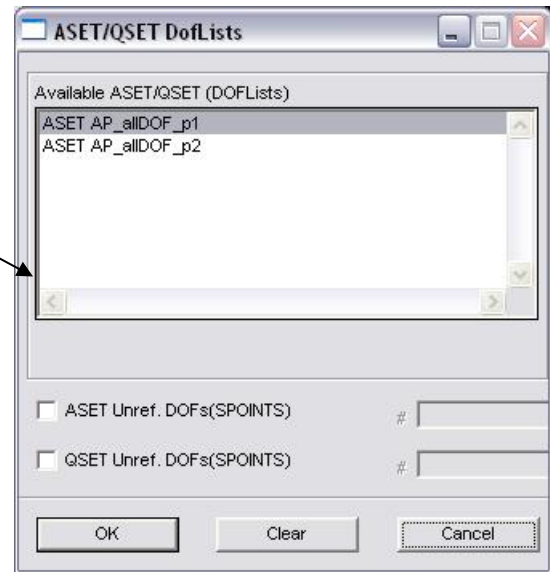


Figure C.1-3

Solution Parameters...

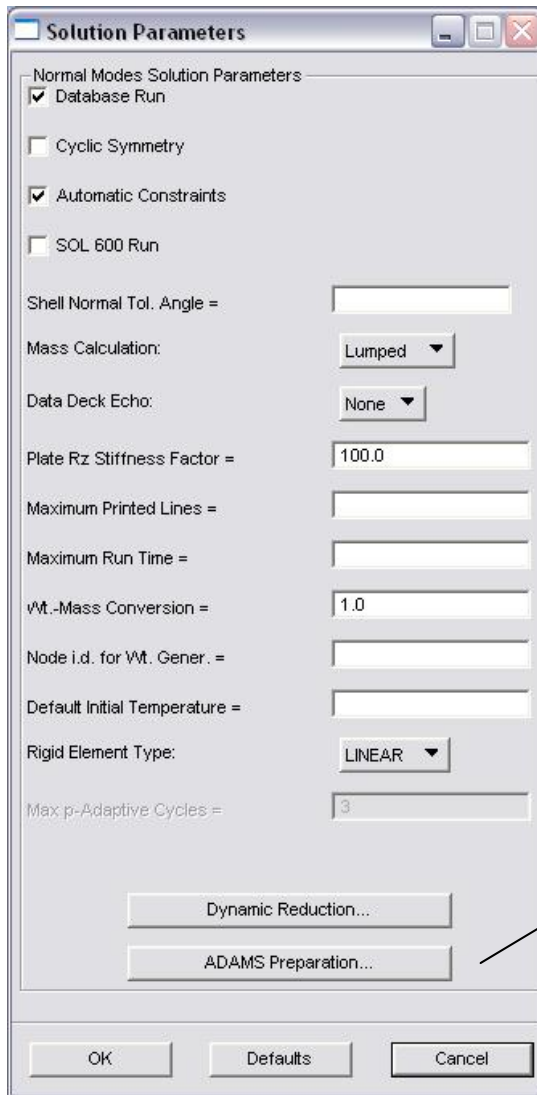


Figure C.1-4

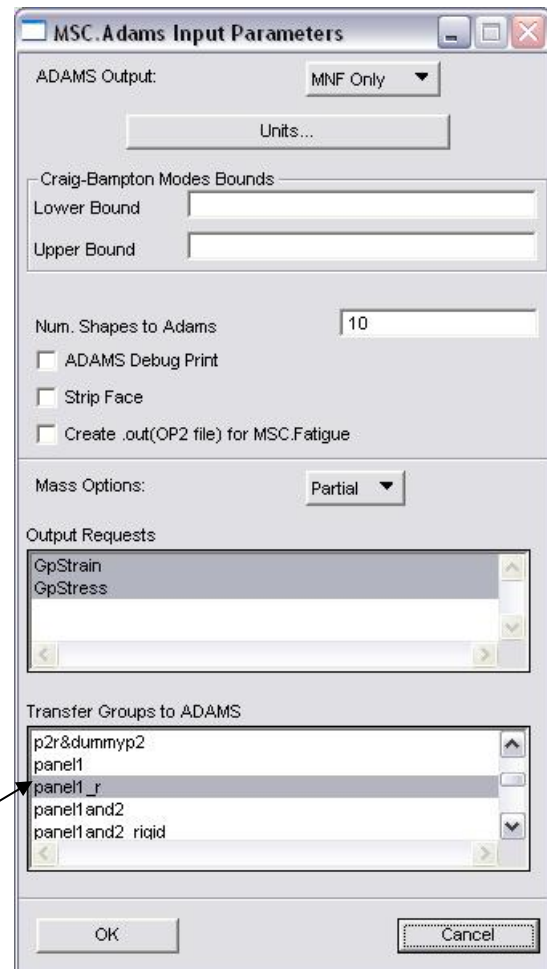


Figure C.1-5

As shown in Figure C.1-5 this time we have to highlight GpStrain and GpStress in the Output Request and select the panel1_r as target.

Remember to change the unit as desired and select a MNF Only run.

The next step is to generate a subcase, “p1r_10_SaS_1” with a free-free modal analysis. This time, we have to make NASTRAN calculate also stresses and strain, so we will have to change also the Output requests accordingly.

Subcases...

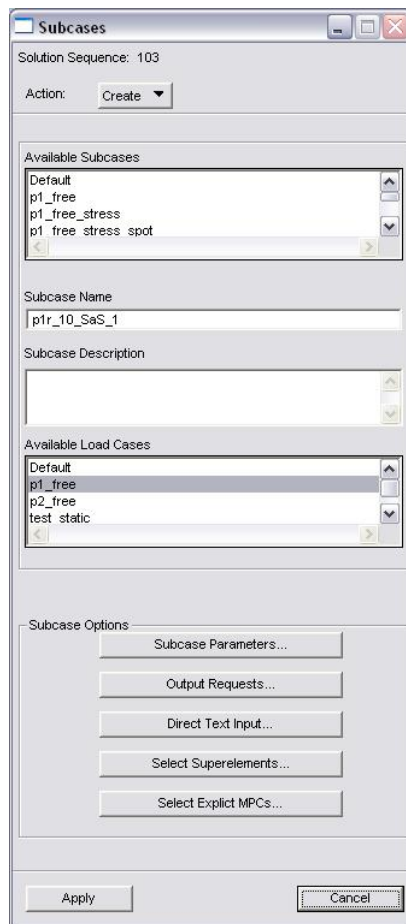


Figure C.1-6

We have to select the “free-free” load case previously created “p1_free”.

Output Request...

*Form
Type:*

Advanced

The window that appears is shown in Figure C.1-7

We have now to select in the top-left corner table the output we want and then associate this output to the “panel1_r” group present in the top-right corner table.

The outputs to select are

- Element Stresses
- Element Strains
- Grid point Stresses

We will not concentrate on the several options associated to each output and we will use the default values. Anyway, refer to the NASTRAN reference guide for detailed help with respect to the use of these options.

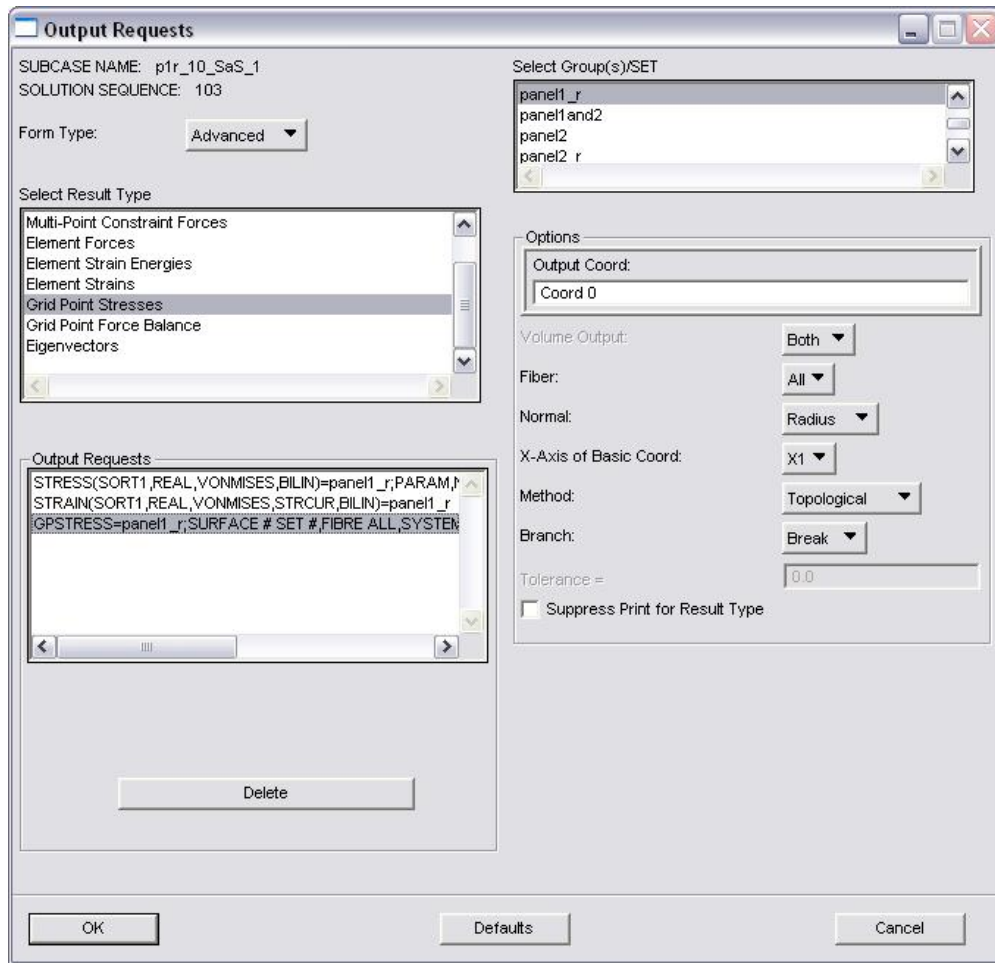


Figure C.1-7

We have to select the subcase just created and run the analysis Figure C.1-8.

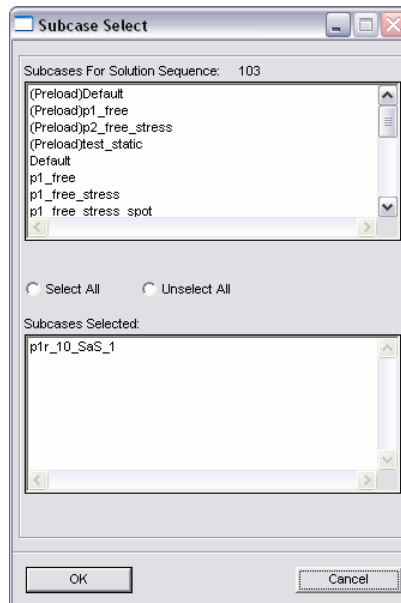


Figure C.1-8

In this case the bdf file obtained doesn't need to be modified.

C.2 Spot mesh S&S + PLOTTEL

In this second approach we will add S&S information to the MNF file only in some particular parts of the mesh. The reason for this choice is that usually we are not interested in knowledge of the stress in the whole part, but only in particular highly loaded zones.

For this reason we have to create a sub-group from panel1_r containing the mesh parts on which we are interested in calculating the S&S.

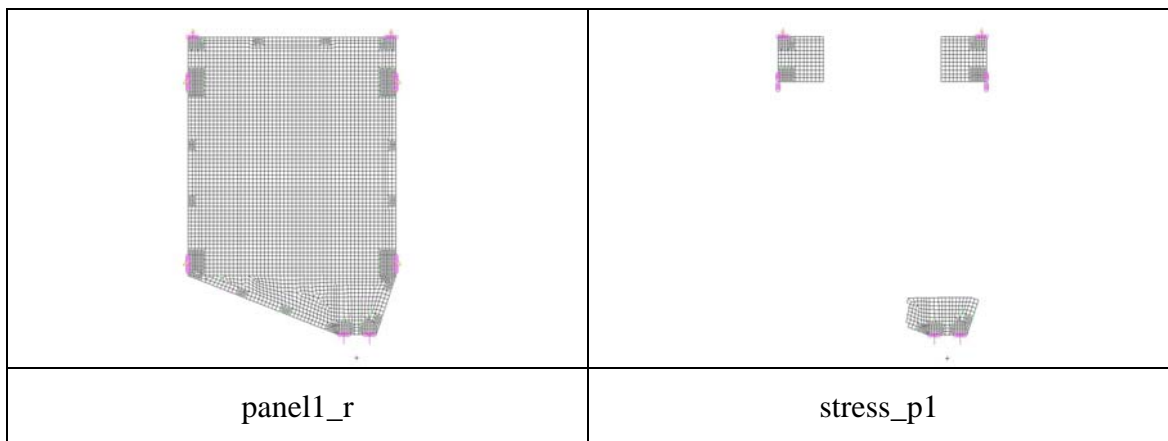


Figure C.2-1: Groups needed for generate a spot mesh stress model

Then we need a PLOTTEL grid (refer to Appendix B) to create the following groups shown in Figure C.2-2 and Figure C.2-3

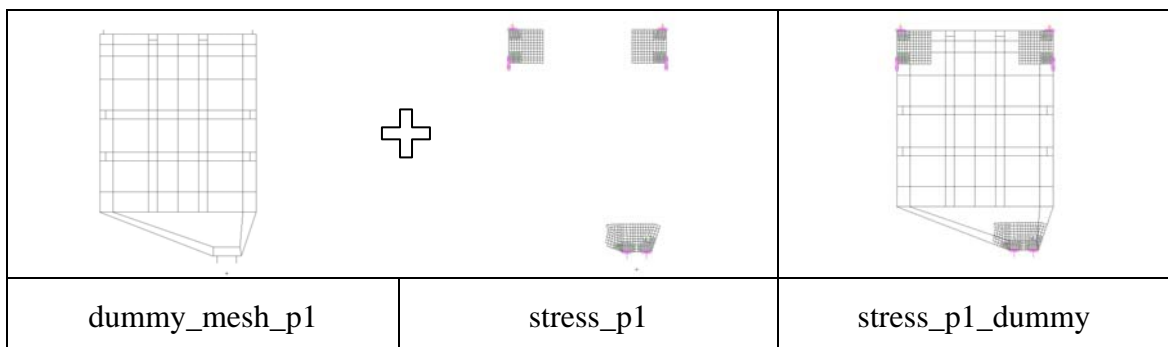


Figure C.2-2: FEM groups for graphical and stress visualization in ADAMs

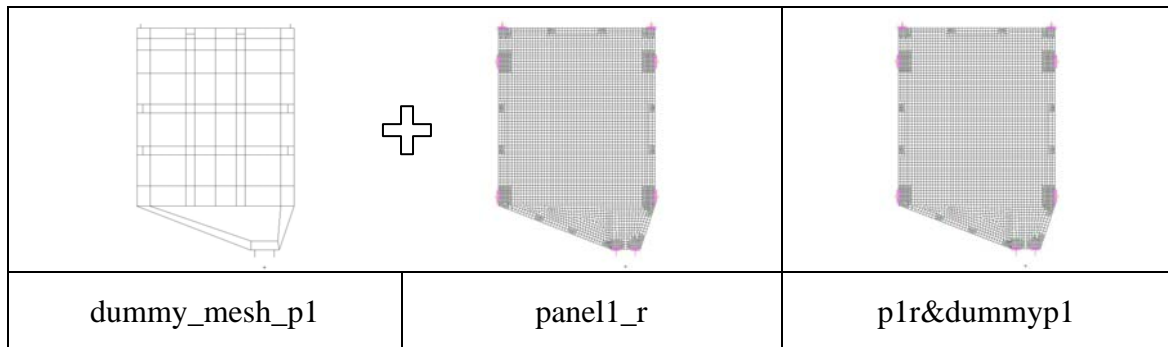


Figure C.2-3: Group containing the whole set of element

Once we have created these groups the further steps are similar to what we have seen in the first approach.

Action:

Object:

Method:

Job Name "p1r_10_SaS_2"

p1r&dummysp1

...leave the default values

We have to select other target groups in the NASTRAN-ADAMS interface and in the NASTRAN output request than in the first approach.

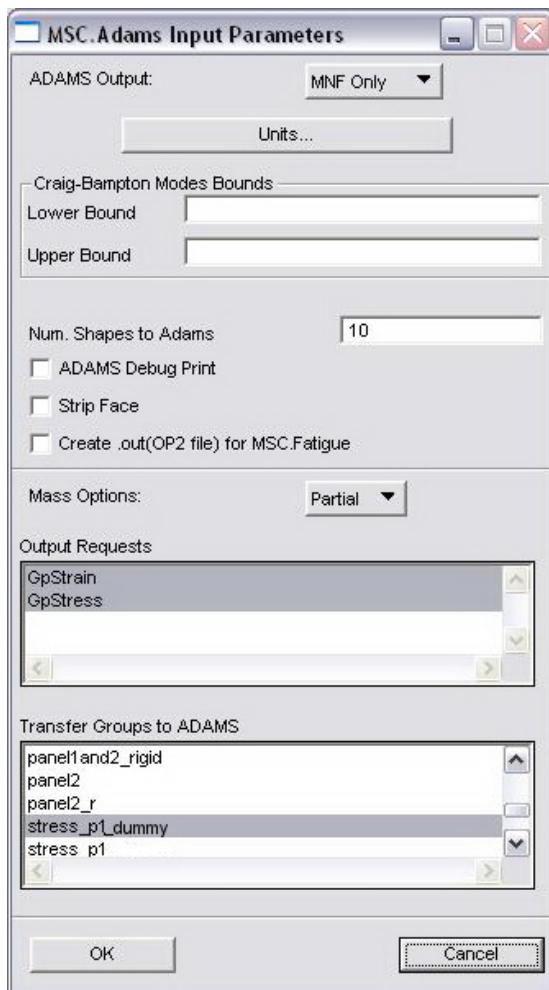


Figure C.2-4

In the NASTRAN-ADAMS interface we have to select stress_p1_dummy as “Transfer Groups to ADAMS”

Then we have to create a new subcase associated with a free-free modal analysis “p1r_10_SaS_2”

In the output request of this subcase we have to select the “stress_p1_dummy” as output request:

- Element Stresses
- Element Strains
- Grid point Stresses

And associate each of them to the “stress_p1_dummy” group.

At this point we can run the analysis and obtain the MNF file.

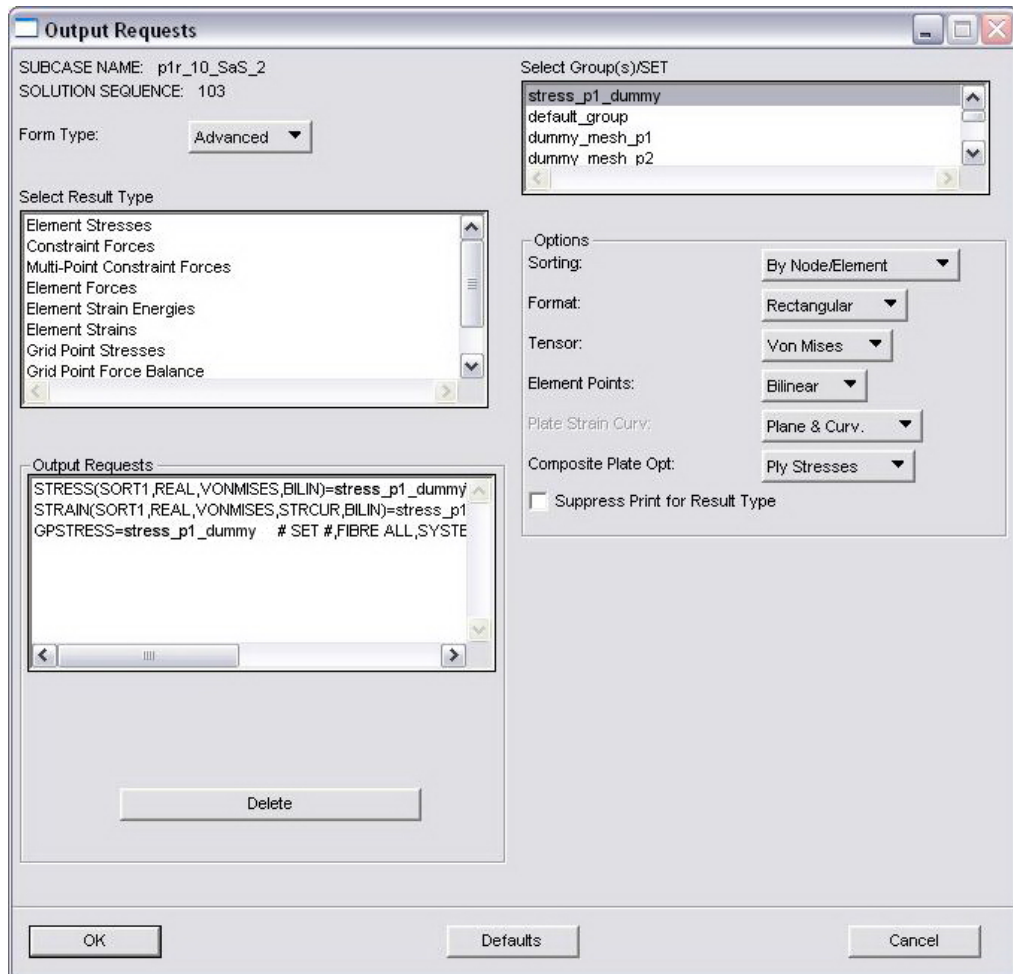


Figure C.2-5

After these changes we can run the Analysis Deck and obtain the bdf file.

In analogy of what we saw for the generation of a MNF file using the PLOTEL elements grid the bdf file that we obtain needs to be manually modified.

Figure C.2-6 shows the changes to be applied to the bdf file. Actually the change that has to be done is simply coping the OUTPUT(POST) command and his elements sets and pasting them in front and changing the argument POST with PLOT.

In this way we impose the group “stress_p1_dummy” both for graphical purpose (PLOT) and for S&S (POST) visualization in ADAMS

C.3 Checking the results in ADAMS environment

At the end we obtain 2 different MNF files. They are summarized in the following figures

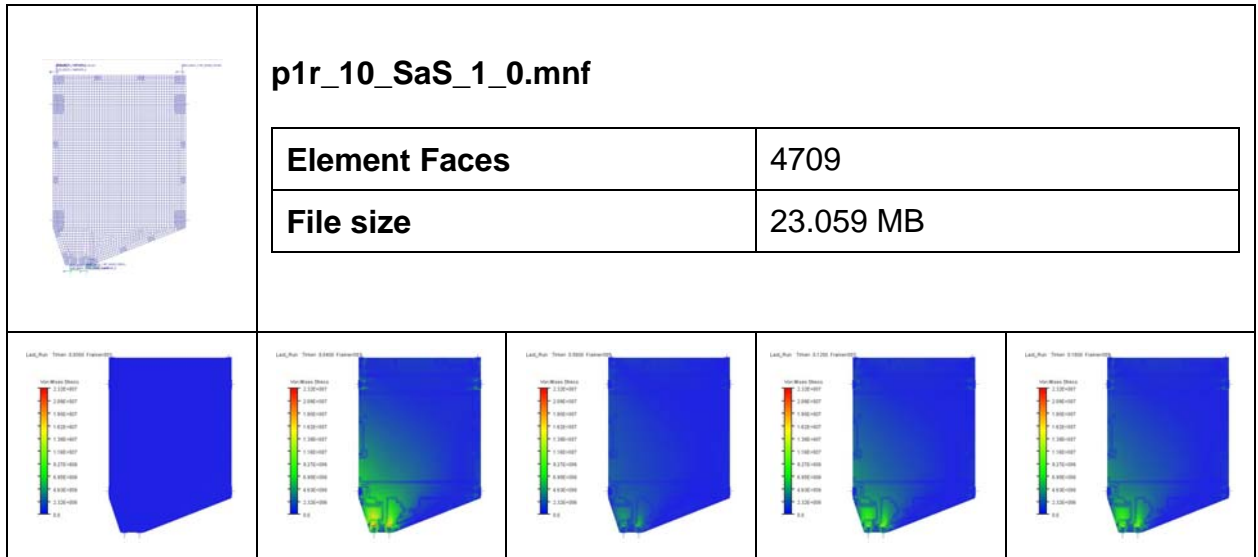


Figure C.3-1: Stresses in a Full-mesh model



Figure C.3-2: Stresses in a Spot-mesh model

The second row of each figure shows the trend of Von Mises stresses due to set of displacement and forces shown in Figure C.3-3 at different time-step.

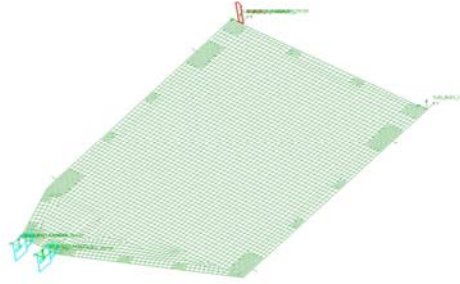


Figure C.3-3: ADAMS model used to compare the stress with NASTRAN

As we can see from picture below the results obtained with the 2 different approaches are the same.

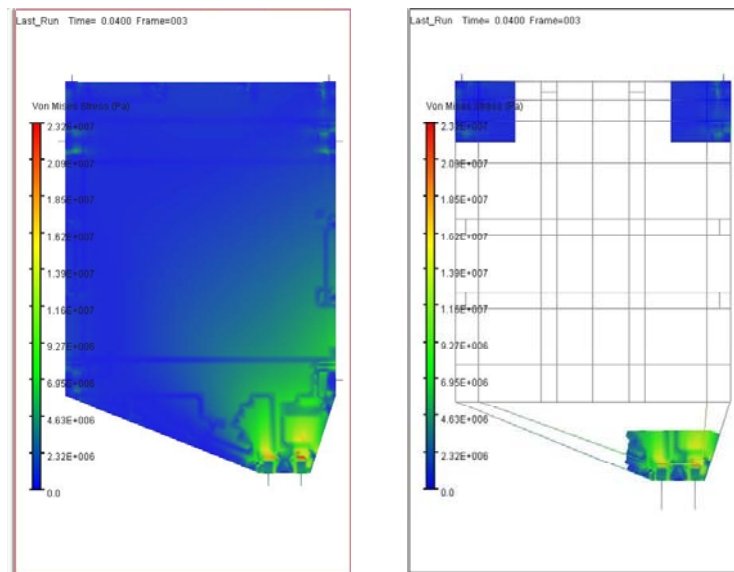


Figure C.3-4: Comparison of stress between full mesh model and PLOTEL model

We can also compare the result of the ADAMS solution after the transient with a NASTRAN static solution. The results we get are the following.

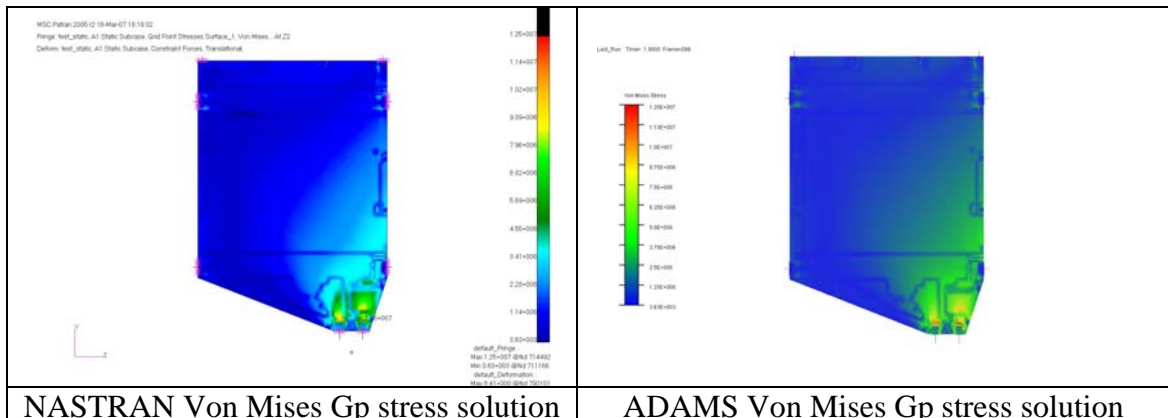


Figure C.3-5: Comparison of stress between ADAMS and NASTRAN models

The results we obtained in ADAMS are the same of the NASTRAN static analysis.

Appendix D

Flexible Bodies in ADAMS

The following tutorial will show how to import and set up a flexible body in the ADAMS environment. We will show how to substitute a rigid body with its relative flexible representation (MNF file) and how to use the main features of ADAMS/Flex.

D.1 Importing a flexible body

The model used in this tutorial is AMOS-3 on ground model. This choice is motivated by the fact that the panels are subjected to the following three kinds of loads:

- Loads on Attachment Points (hinges forces and torques)
- Loads with an offset relative to the AP (CCL forces and torques and springs forces)
- Loads on simple nodes (aerodynamic loads and torques)

We will show how to import the flexible representation of panel2. Figure D.1-1 shows the model ready for the replacement of the rigid panel2. The forces are already split and as remarked by the bottom left red square we have also added a new reference marker

that, together with the two others markers located on the hinges, will help us to define the right position and orientation of the flexible part.

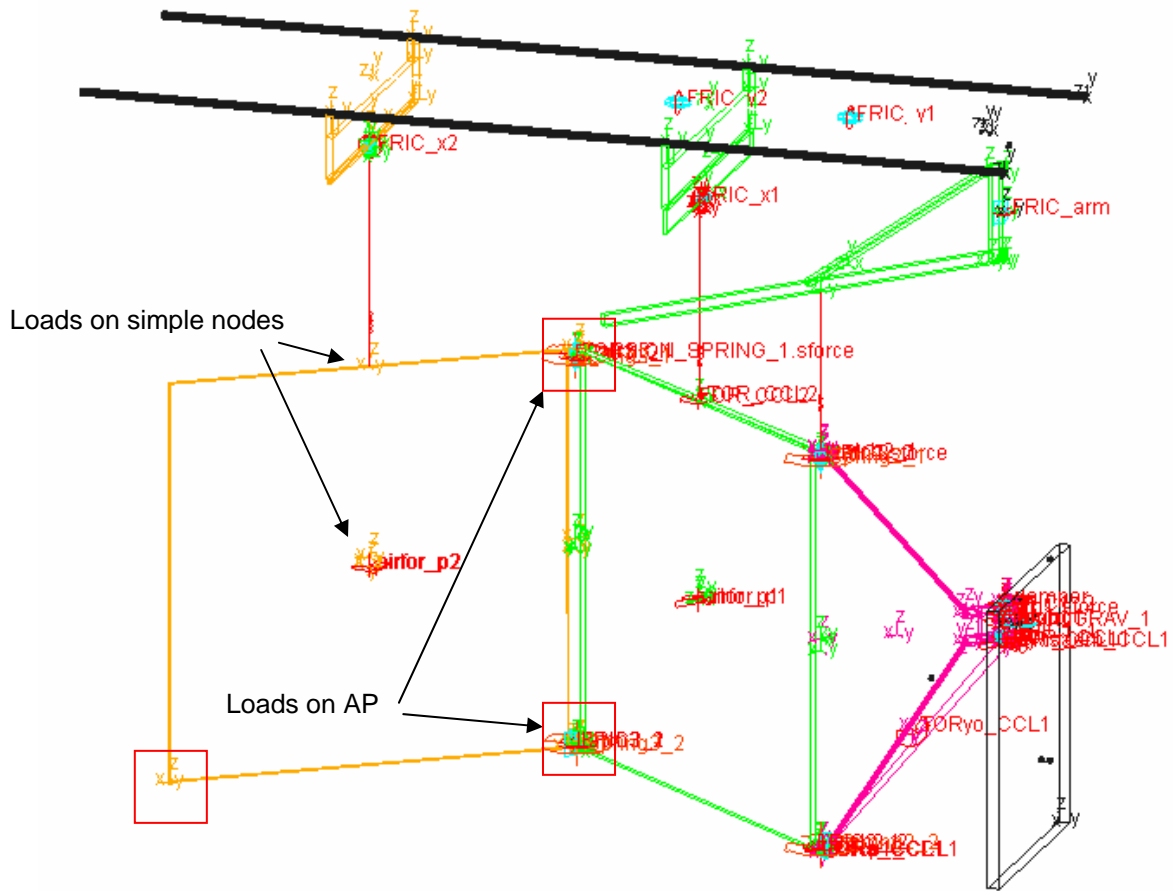


Figure D.1-1: ADAMS starting rigid model

D.1.1 Alignment

Now we are ready to replace panel2 using the ADAMS pull down menu

Build → **Flexible Bodies** → **Rigid to Flex...**

The window shown in Figure D.1-3 appears. We have to fill the “Current Part” field with the part that we want to replace and in the field below with the path to the related MNF file. It is important here to notice that ADAMS does not include the MNF file into the database but links it by following the path indicated. For this reason, to make the model compatible also on other computers, it is better to delete all the backward part of

the path and leave only the forward part of the database location. The following examples will clarify

D:\MyWorks\Patran&Adams\amos3_og\am3_p2_mnf5_rh_0.mnf

D:\MyWorks\Patran&Adams\amos3_og\MNF_files\am3_p2_mnf5_rh_0.mnf

The two paths above show two different cases. In the first path the MNF file is directly in the data base folder. In the second one we have a folder (MNF_files) that contains the MNF file.

The red part of the path is the part to delete.

Notice that for the correct working of the models, it is necessary to input the data base folder as starting folder in the entrance menu as shown in Figure D.1-2.

D:\MyWorks\Patran&Adams\amos3_og

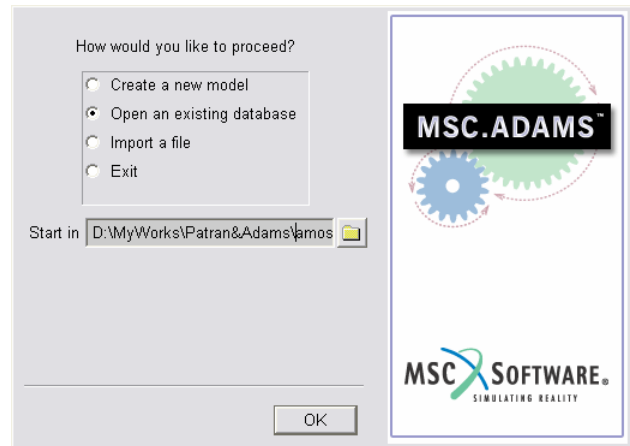


Figure D.1-2

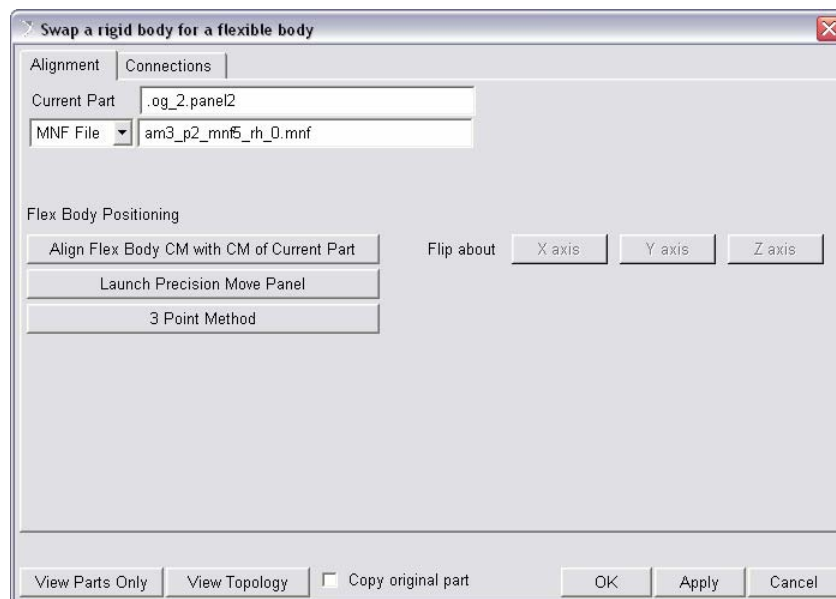


Figure D.1-3

Now we have to click on “View Part Only” and “Align Flex Body CM with CM of Current Part” to show only the two parts we need and have a first positioning.

Figure D.1-4 show the results of these two actions.

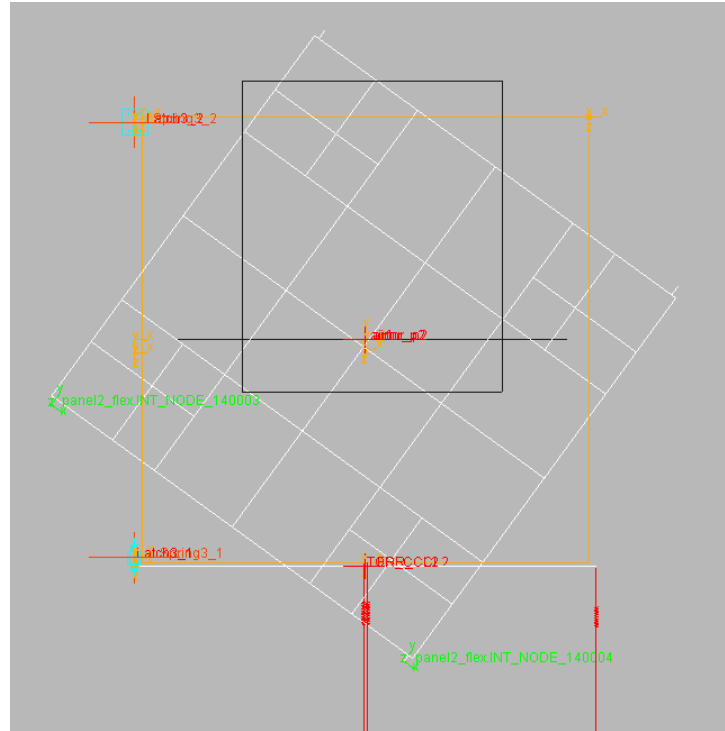


Figure D.1-4: First positioning of bodies (CM aligned)

Now we have to orient the flexible body clicking on “3 Point Method”. The user has now to select one node of the flexible body and the node of the rigid body to move it on.

Because of a bug in ADAMS the user can’t use the View Control buttons in the Main Toolbox show in Figure D.1-5 for moving the body and select the nodes. If we click on a button in the Main Toolbox ADAMS forgets the “3 Point Method” command.

To avoid this we have to use only the keyboard commands to move, zoom and so on. These commands are collected in Table D-1 but can also be visualized by right clicking on an empty background zone of ADAMS

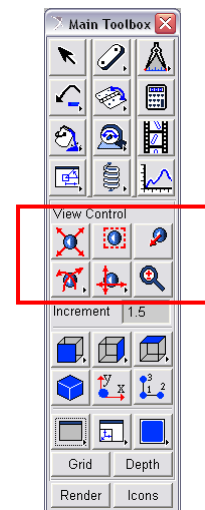


Figure D.1-5

Using this technique we are able to align all the three reference points. The process is quite tricky but if something goes wrong one has simply to click on “3 Point Method”

again and restart. When we select an AP of the flexible body and we are going to select the hinge point on which to move it we have to pay attention to select the right reference marker; that is because usually a lot of markers are present in the hinge surrounding area and not all off them are exactly located in the hinge point.

To make the choice easier one can zoom in on the hinge location and click on the right mouse button near the hinge central point. A Select window pops up that help to choose the right marker as shown in Figure D.1-6

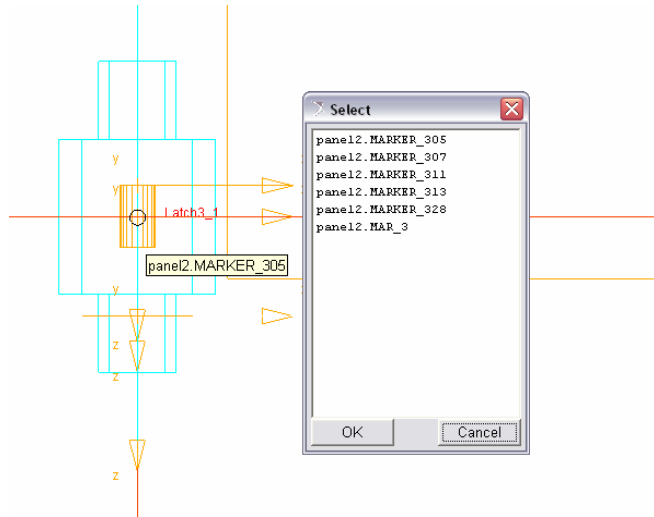


Figure D.1-6

Shift + f	Front View
Shift + t	Top View
Shift + r	Right View
Shift + i	Iso View
r	Rotate XY
t	Translate
z	Zoom In/Out
w	Zoom Box
f	Fit to View

Table D-1: Keyboard shortcuts to move the model

D.1.2 Connections

After the alignment of the three points the two parts should be superimposed as shown in Figure D.1-7. Now we have to set up the connections between the two bodies; in

other words we have to tell or confirm ADAMS on which node of the flexible body it has to move all the elements of the rigid one.

So in the “Swap a rigid body for a flexible body” window (see Figure D.1-3) we have to click on the “Connections” schedule (top left).

The new windows that appears is shown in Figure D.1-8.

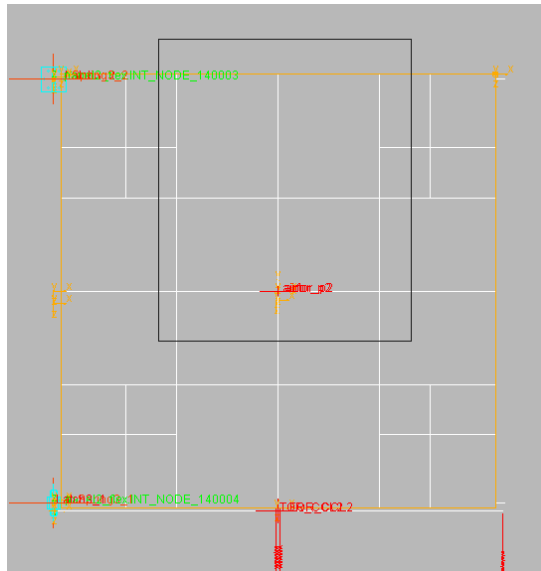


Figure D.1-7: Flexible and rigid bodies aligned

The first action is to increase the “Number of digits”. In this case we have put 8. The table shows the elements of the rigid model (Connections and their Marker), the node on to which they will be referred (Node ID) and their position (and Distance) relative to this node. The last column shows the action that we are going to apply to every connection. There are 3 options:

- **Move to node**

The Marker is moved to the node

- **Preserve expression**

If the location of the Marker that defines the connections is defined by an expression this expression is preserved.

An example of an expression that fixes the position of a marker relative to a reference node is the following

```
(LOC_RELATIVE_TO({0, -1.0E-002, 0}, .og_2.panel2.POINT_336))
```

If we preserve the expression of a marker but no expression is present ADAMS preserves the location automatically.

- **Preserve location**

The location of the marker referred to the node is preserved

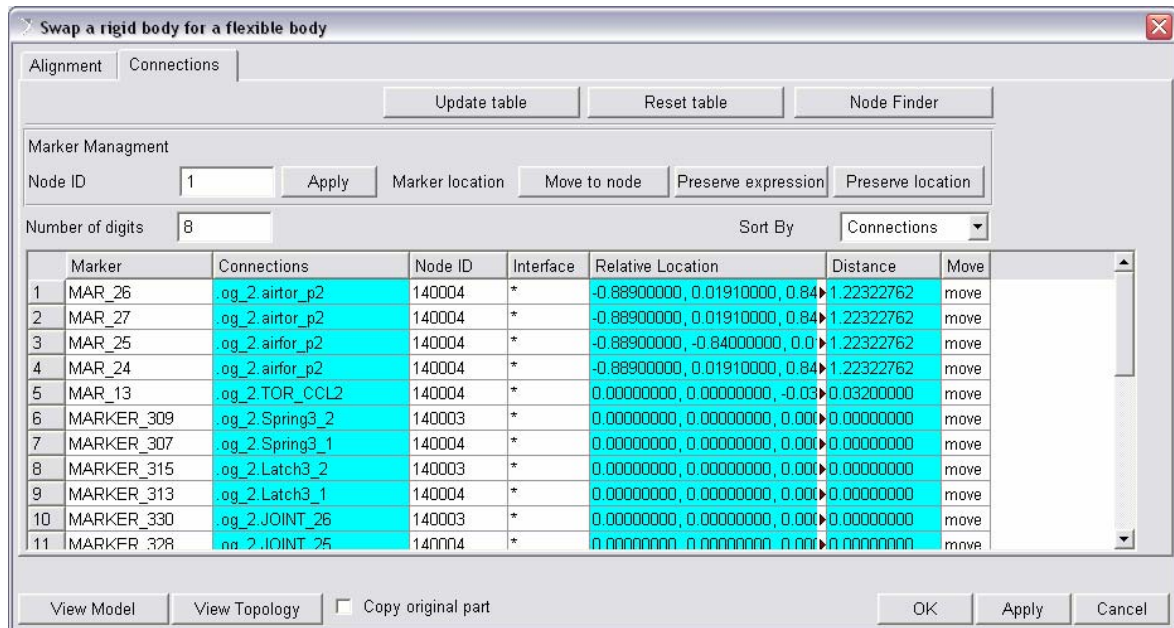


Figure D.1-8

ADAMS as default tends to move all the interface markers to the nearest AP (in this case nodes 140004 and 140003). This default setting is not good in our case so we have to manually modify the node assignment.

D.1.2.1 Load on simple nodes

The aerodynamic loads and the loads due to gravity compensation springs are examples of loads on simple nodes. To find the node of application for these loads we have to use the “Node Finder” function. If we click on this button in the Connections windows the windows of Figure D.1-9 will appear. With this utility we can pick the marker we want, in the Figure for example MAR_24 is one of the markers that define the aerodynamic loads, and find out which are the closest nodes of the flexible body. As shown in the figure we have to uncheck the “Interface Nodes Only” option because we are interested in simple nodes.

At the end we find that the reference node for aerodynamic loads will be the node number 120433. If we repeat the same procedure for the spring force we find that the node to refer it is 120545.

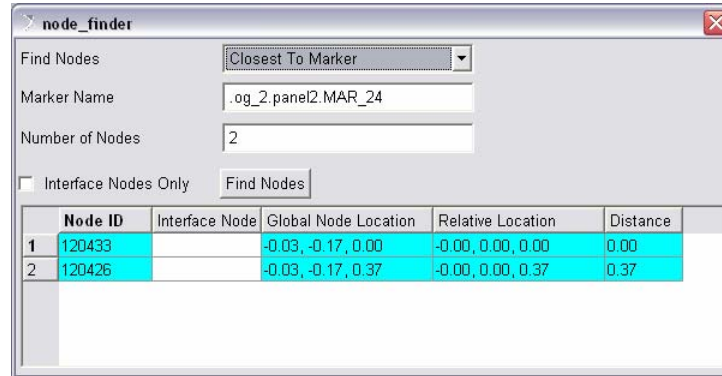


Figure D.1-9

Now we can come back to the Connections window and change the Node ID of these loads as shown in Figure D.1-10. To change the node id enter the new node in the Node ID text box and after selected the row of the table to change click Apply.

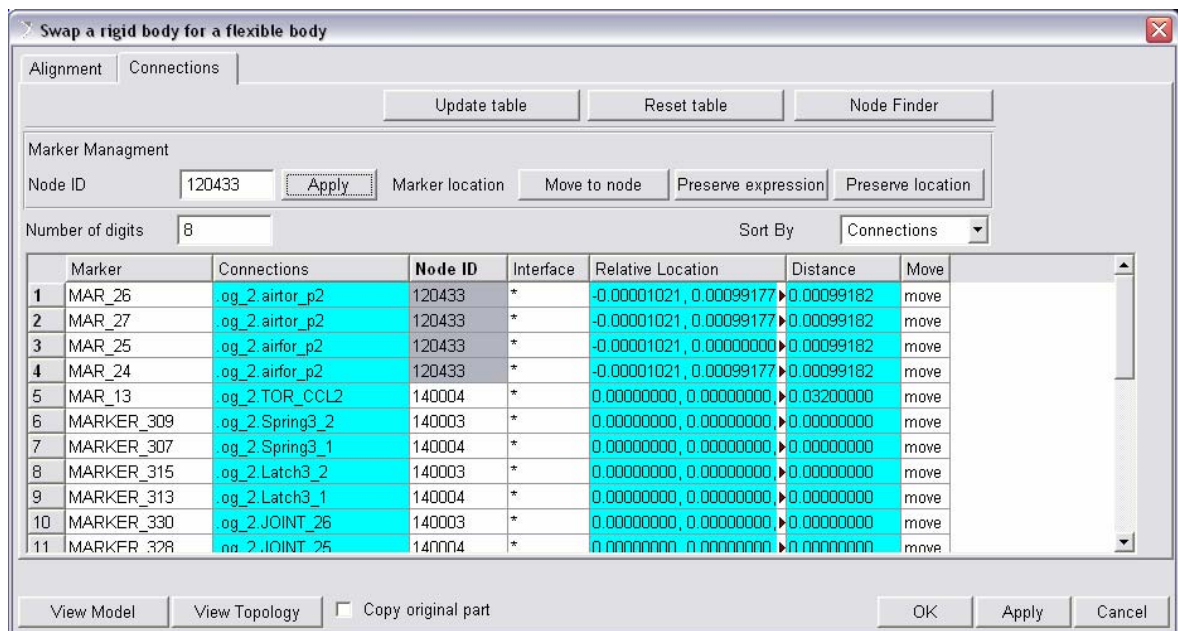


Figure D.1-10

We can see in the figure that now the distance has changed because it refers to the closest node. At this point we can decide to move the loads on the node or preserve their expressions (or location if the expression is not defined). If we decide to preserve the expression the loads will be rigidly connected from their marker location to the node. In

this case anyway there is in no difference between the two cases because the distance is already almost zero.

D.1.2.2 Loads with an offset respect to the AP

The case comes up for the application of CCL loads. These loads are automatically referred by ADAMS to the right AP (since is the closest one). What we have to do is simply to preserve their expression because ADAMS will automatically connect them to the AP with a rigid link as we want. Figure D.1-11 shows the table after the change. To modify the action select the row and then click on “Preserve expression”.

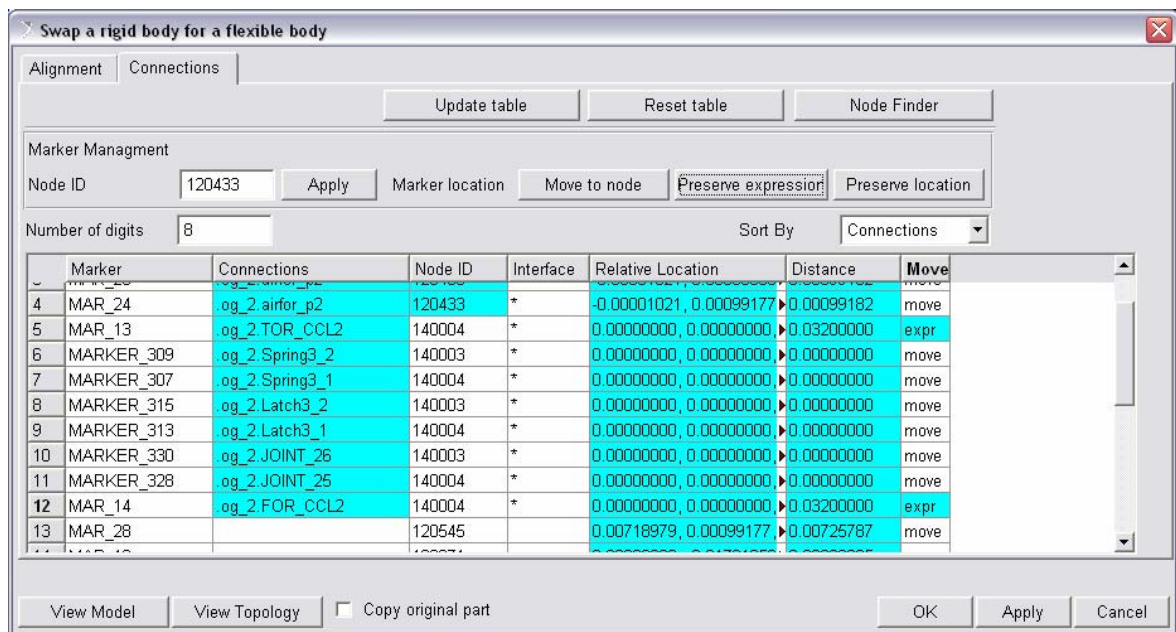


Figure D.1-11

D.1.2.3 Loads on Attachment Points

For what concern this loads we have simply to leave the table as it is. Looking at Figure D.1-11 we can see in fact that the load markers that define loads on the AP are perfectly coincident on the AP node (the distance is zero considering 8 digits).

If these markers are not perfectly aligned (error at the 4th or 5th digit), there was something wrong in the previous orientation phase or that the dimensions of the rigid panel do not match with the flexible ones. In both cases we can have some problems in the model if we go on with the replacement.

For the others markers that not belong to the three categories (so all the marker that define the geometry of the rigid panel) we can simply preserve the expression.

At the end, we can summarise the rules for the connections as shown in Table D-2

Kind of Marker	Node ID	Action
Loads on simple nodes	Change the default value with the right node number	Move (or preserve the expression)
CCL loads	Leave the default AP	Preserve the expression
Loads on AP	Leave the default AP	Move (verify if the body is correctly positioned)
Other Marker	Leave the default	Preserve the expression

Table D-2: General rules for connections

When we have finished compiling the table we can click on Apply. The flexible body now will replace the rigid one in the model.

D.2 Flexible body properties

Once we have imported the flexible body in our model we can deal with him as a normal ADAMS part. If we check it (right click and then info) for example we will able to see all its properties as shown in Figure D.2-1

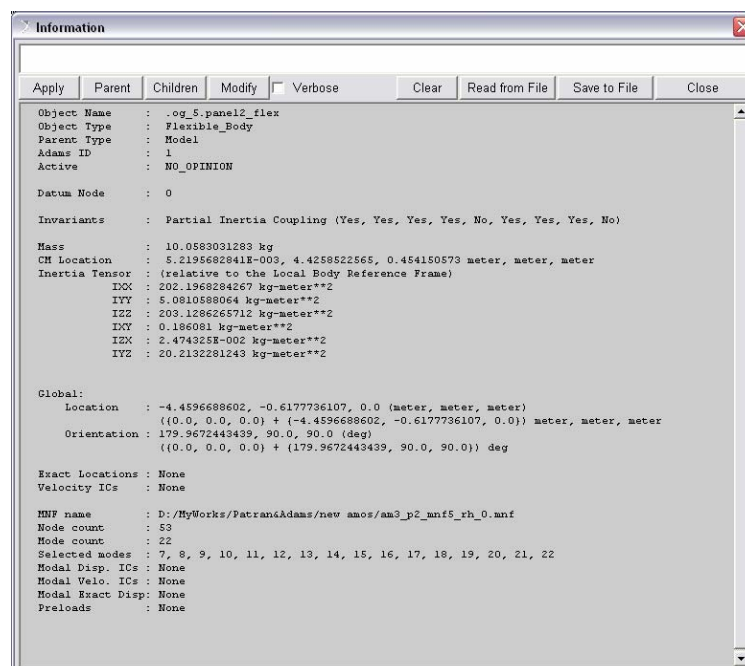


Figure D.2-1

To modify some of these properties (we can't modify mass or inertia properties) one can use the “Flexible Model Modify” panel (right click on the flexible body then modify) shown in Figure D.2-2

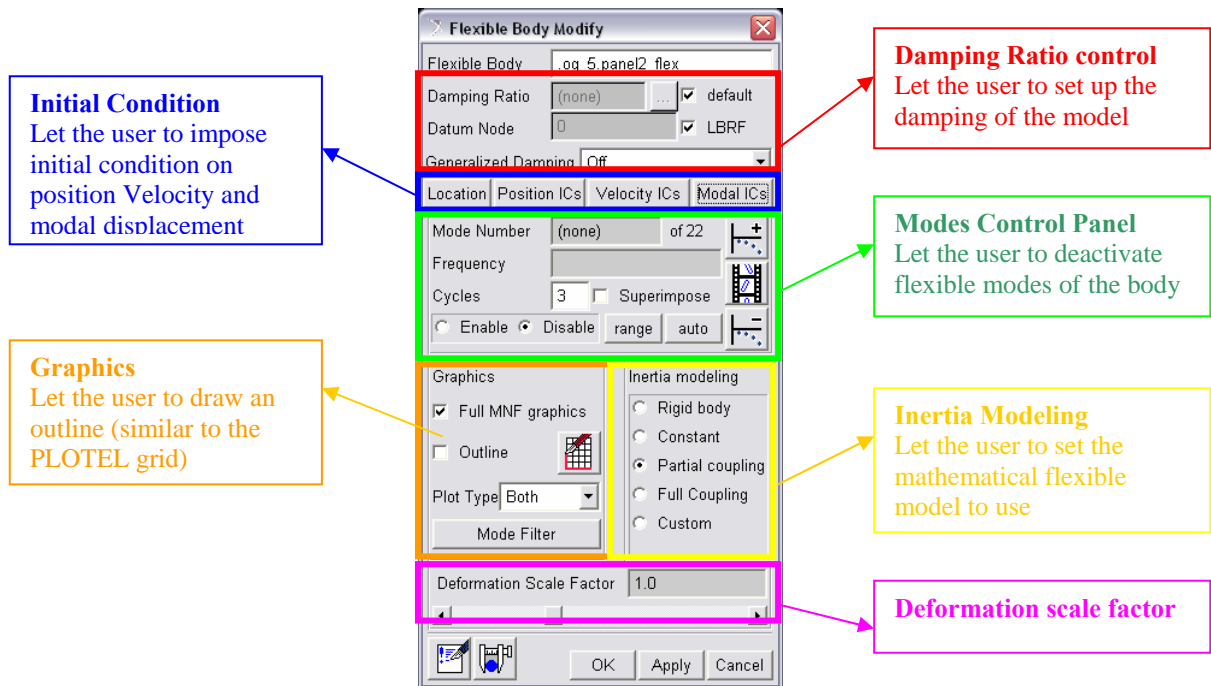


Figure D.2-2

The main features of this interface are the Damping ratio control and the Modes control panel.

D.2.1 Damping ratio

If we do not specify modal damping when we create the flexible body, ADAMS/Flex applies a default, non-zero critical damping ratio as follows:

- 1% damping for all modes with frequency lower than 100.
- 10% damping for modes with frequency in the 100 to 1000 range.
- 100% critical damping for modes with frequency above 1000.

We can change the default modal damping in three ways:

- Assign a single scalar critical damping ratio that ADAMS/Flex applies uniformly to all modes.

- Enter MSC.ADAMS run-time function expressions to create complex damping phenomena in your flexible body. In addition, function expressions, such as FXFREQ and FXMODE, allow us to apply different levels of damping to individual modes.
- Control the damping using the DMPSUB user-written subroutine. DMPSUB lets us set different levels of damping for different modes and the damping can vary over time.

For more details on how to write custom damping function please refer to the ADAMS help looking for DMPSUB, FXFREQ or FXMODE.

The generalized damping option enable the user to apply the same damping used in the FEM model (if introduced in NASTRAN and included in the MNF file).

D.2.2 Modes Control

With this interface the user can check all the modes that compose the Craig-Bampton orthogonalized basis. The user can decide to deactivate the flexible modes or the range of frequency that he considers useless.

Anyway, as we have seen in the theoretical background chapter, the high frequency modes (eigenvectors) may be important for the representation of boundary modes in the AP areas. From there, one should carefully check the changes generated in the model by such deactivation.

Bibliography

[1] *Ahmed A. Shabana*. Dynamics of Multibody System, second edition. Cambridge University Press

[2] *E. Funaioli, A. Maggiore, U. Meneghetti*. Lezioni di Meccanica Applicata alle Macchine, vol II. Patron Editore

MSC Documentation

[3] ADAMS, NASTRAN & PATRAN reference guides

[4] ADAMS/Flex Theoretical Background

[5] NASTRAN/ADAMS interface documentation

[6] MSC online support (<http://www.mscsoftware.com/support/>)

EADS ASTRIUM Internal Documentation

[7] AMOS-3 Solar array – SG Deployment Analysis Report (AMSG-ASO-TN-2000-0006)

[8] BEPI COLOMBO – Release and Deployment Analysis MPO S/A 2 (ARB4B-DNS-AN-1000-0001)